APPLICATION OF ZIRCONIUM-COATED TITANIUM WIRES AS RESTORATIVE ORTHODONTIC MATERIALS

By

KHALED ABEDELA MAHDI ALI

Thesis submitted in fulfillment of the requirements for the degree

Magister of Technology: Dental Technology

In the Faculty of Health & Wellness Sciences

At the Cape Peninsula University of Technology

Supervisor: Professor. D Gihwala

Co-supervisor: Dr J Mars

Bellville

May 2013

DECLARATION

I, Khaled Abedela Mahdi Ali, declare that the contents of this dissertation/thesis represent my own unaided work and that the dissertation/thesis has not previously been submitted for academic examination towards any qualification. Furthermore, it represents my own opinions and not necessarily those of the Cape Peninsula University of Technology.

Signed

Date

ABSTRACT

Orthodontic archwires are made from different alloys. It is now possible to match phases of treatment with orthodontic archwires according to its mechanical properties. On this basis, the titanium molybdenum alloys (TMA) in its beta phase have an excellent combination of strength and flexibility when used as archwires to apply biomechanical forces that affect tooth movement. It has recently gained increased popularity in orthodontic treatment. There are, however, disadvantages associated with the use of orthodontic archwires, such as high surface roughness, which increases friction at the archwire-brackets interface during the sliding process. The surface roughness of dental materials is of utmost importance. Properties such as desirable tensile strengths, load deflection, hardness and low modulus of elasticity and resistance against corrosion & wear determine the area of the contact surface, thereby influencing the friction.

The main object of this study was to improve the strength and surface roughness of the beta-titanium orthodontic archwires (β-Ti III) and timolium archwires (TIM), taking into account of retention of the archwires strength. The following tasks were performed. Layers of Zr were deposited on the β-Ti archwires and compared with the archwire strength before and after Zr deposition. The structure of selected archwires and its composition and surface roughness was investigated before and after Zr deposition, using scanning electron microscopy (SEM) and atomic force microscopy (AFM). The force of selected archwires before and after deposition with layers of Zr by Hounsfield deflection testing was studied.

Two commercially available orthodontic archwires were used in this study, namely, β-Ti III and TIM orthodontic archwires. The archwires were cut into 25 mm long specimens. In this study, the electron beam-physical vapour deposition (EB-PVD) technique was applied to deposit pure Zr (thicknesses of 5, 10, 25 and 50 nm) on selected archwires and the effects thereof were investigated using AFM, SEM and the Hounsfield deflection test. Results of SEM and AFM analysis and deflection tests showed significant differences between Zr-coated archwires compared with uncoated archwires. Zr-coated archwires (5, 10, 25 and 50 nm depositions) had reduced surface roughness compared with uncoated archwires. A high load deflection rate was exhibited by the coated β-Ti III archwires and a low load deflection rate was exhibited by the coated TIM archwires. There was a difference in load deflection rate between the coated and uncoated archwires. Deposition of 5, 10, 25 and 50 nm Zr on both types of β-Ti orthodontic archwires is recommended for even sliding mechanics due to resulting reduced surface roughness with a good load deflection rate compared with uncoated β-Ti orthodontic archwires.

KEYWORDS

Surface roughness

Zirconium

Titanium

Deflection test

Beta titanium orthodontic archwires

Orthodontic archwires alloys

Coated materials

Electron beam-physical vapour deposition

Scanning electron microscopy

Atomic force microscopy

ACKNOWLEDGEMENTS

I wish to thank: My supervisor Dr J.A. Mars of the Department of Biomedical Sciences for his guidance, support and always having time to help throughout this study; My supervisor Professor D. Gihwala for his insight into this study.

Furthermore, I wish to thank:

- The Libyan government for financial assistance throughout this study.
- My family for their ongoing support.
- The personnel Department of Mechanical Engineering at the Cape Peninsula University of Technology, Cape Town, South Africa for the unlimited use of their equipment and laboratories to conduct this study.
- Professor. Basil Julies, Head: Electron Microscopy Unit in the Physics Department at the University of the Western Cape for his assistance during the experiments.
- Dr. Mlungisi Nkosi. Research Scientist at iThemba LABS, Faure, South Africa, for the use of the equipment and laboratories to conduct this study.

TABLE OF CONTENTS

LIST OF FIGURES

LIST OF TABLES

ABBREVIATIONS

ε	-	Modulus of elasticity
ε_r	-	Recoverable strain
ε_s	-	Unloading
AFM	-	Atomic force microscopy
Co-Cr	-	Cobalt-chromium alloy
CVD	-	Chemical vapor deposition
EB-PVD	-	Electron beam-physical vapour deposition
EDAX	-	Energy dispersive x-ray analysis
IF-WS_2	-	Inorganic fullerene-like tungsten disulfide
ITO	-	Indium tin oxide alloy
MeV	-	Mega electron volt
F	-	Force exerted measured in miga pascal (MPa) or giga pascal (GPa)
Ni-Ti	-	Nickel-titanium alloy
PIII	-	Plasma immersion ion implantation
ppm	-	parts per million
PVD		Physical vapour deposition
SEM	-	Scanning electron microscopy
SEM-EDAX		Scanning electron microscopy-energy dispersive x-ray analysis
SS	-	Stainless steel
TiAlN	-	Titanium aluminum nitride alloy
TIM	-	Titanium alloyed with various metals for phase stabilisation
Ti-Ni	-	Titanium Nickel alloy
TMA	-	Titanium molybdenum alloy
TMAL	-	Titanium molybdenum alloy low friction
TPS	-	Thermal plasma spray
$T\alpha$, T_{β}, $T\omega$	-	Temperatures which titanium was heated for these phases to form
UTS	-	Ultimate tensile strength

WC/C	-	Tungsten carbide/carbon alloy
YS	-	Yield strength
α, β, ω	-	Description of type of microstructural phases of alloyed material according

CHAPTER ONE

INTRODUCTON

1.1 Introduction

Biomaterials based on metals and metals alloys are widely used in both medical and dental applications (Arango *et al*., 2012). These metals and alloys have specific physical properties, such as excellent electrical conductivity, thermal conductivity (Cohen, 1994) and appropriate mechanical properties, such as desirable tensile strengths, load deflection, hardness and low modulus of elasticity (Burstone & Goldberg, 1980) and, resistance against corrosion and wear (Faria *et al*., 2011). Some metals can be used as passive substitutes of hard tissues (dental implants) and fracture healing aids (bone plates, screws, orthodontic brackets and archwires) (Park *et al*., 2000). The most extensively used metallic biomaterials are pure Ti and Ti alloys, stainless steel (SS) and chromium-cobalt (Cr-Co) alloys (Geetha *et al*., 2009).

Titanium and its alloys were first introduced in medicine and dentistry in 1971 (Andreasen & Hilleman, 1971; Thompson, 2000) and different specialities within the dental field take advantage of this material. Titanium alloyed with elements such as molybdenum or copper has widespread use in orthodontics (Albrektsson *et al*., 1986). Alloys with other metals, such as Al or V, are used in oral rehabilitation and implantology (Palmquist *et al*., 2010); Park *et al*., 2000) and maxillofacial surgery (El-Zohairy *et al*., 2010).

Titanium is an allotropic material that can exist in three microstructural phases, namely the α, β- and ω-Ti phases. The α-microstructural phase is obtained by heating Ti metal to 880°C (Campbell, 2008), maintaining a pressure of more than 5 GPa and then quenching the heated product. The β-Ti microstructural phase is obtained by heating the metal to temperatures higher than 880°C and maintaining a pressure of 5 GPa. The ω phase is brittle and obtained by increasing the pressure up to 120 GPa and has as yet no medical or dental appliction when alloyed with other metals (Hennig *et al*., 2008). These microstructural phases are shown in **Figure 1.1.** The α phase is characterized by high strength and low weight (Park *et al*., 2000). The β-phase shows high corrosion resistance (Bania, 1994). These microstructural phases are not stable when quenched to room temperature. To avoid this instability, various elements such as C, Al and Mo are incorporated into the matrix, thereby forming the alloys. Al and Mo are of the most common elements used to stabilise such a phase for Ti alloys (Park *et al*., 2000).

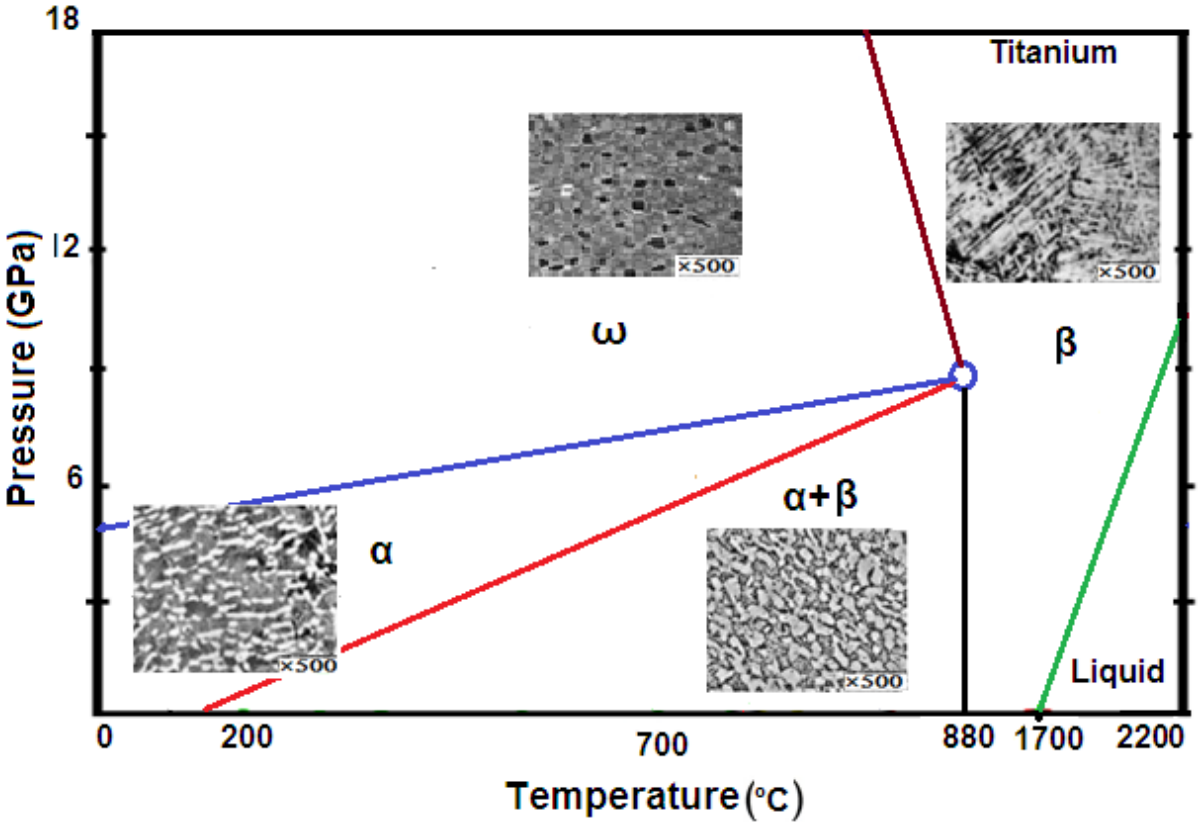

Figure 1.1: The representation of the formation of the Ti α-, β- and ω- microstructural phases as a function of temperature and pressure (Juvvadi *et al*., 2010), SEM microstructural phases for the Ti α-, β-, α-+β- and ω- (Geetha *et al*., 2009).

The α-Ti phase contain light elements such as C, O and N as phase stabilizers. The most stable phase is β-Ti and the less stable phase is α-Ti. The strength of β-Ti alloys is greater than that of α+β and α-Ti alloy (Velisavljevic *et al*., 2012). The additions of β stabilisers are required to keep the entire β-structure and prevent ω embrittlement (Bania, 1994). The amount of α stabilisers should not exceed 9% in the Al equivalent to prevent ω embrittlement. The thermal ω phase can act as a nucleation site for precipitation of the α phase, leading to homogeneously and finely dispersed α particles (Ankem & Greene, 1999). The β-stabilising (**Tables 1.1** and **1.2**) addition is required to improve the β-microstructure especially when the application of α stabilisers such as Al or Sn is made (Bania, 1994; Williams *et al*., 1972).

Tabe 1.1: The approximate wt.% of elements needed to stabilise the β-microstructure of pure Ti (Weiss *et al*., 1998).

β-Stabilisers	Fe	Cu	W	Cr	Ni	V	Ta	Co	Mo	Mn	Nb
wt. %	3.50	13.00	22.50	6.50	9.00	15.00	45.00	7.00	10.00	<0.05	36.00

The β-Ti alloys show the microstructure, including the nature of the grain size and the extent of the stability of the β phase strongly influence the deformation mechanisms and the mechanical properties of β-Ti alloys. Increasing the control of precipitation of the α phase has led to improvements in strength and fracture toughness of the metastable β-Ti alloys (Ankem & Greene, 1999).

Tabe 1.2: The approximate wt.% of an element needed to stabilise some Ti alloys (Donachie, 1988).

Element (Wt. %)	Alpha (Ti-6Al-2Sn)	Alpha+Beta (Ti-6Al-4V)	Beta (Ti-11Mo-6Zr-4.5Sn)
N	0.5	0.05	0.05
C	0.05	0.10	0.10
H	0.0125	0.0125	0.020
Fe	0.25	0.30	0.35
O	0.15	0.20	0.18
Al	6.0	6.0	<0.05
Sn	2.0	<0.05	4.5
Zr	4.0	<0.05	6.0
Mo	2.0	<0.05	11.0
V	<0.05	4.0	<0.05
Cu	<0.05	<0.05	<0.05
Mn	<0.05	<0.05	<0.05
Cr	<0.05	<0.05	<0.05
Si	0.08	<0.05	<0.05

The most common Ti alloy used for dental applications such as brakets is Ti-6Al-4V. This alloy consists of 6 wt% Al and 4 wt% of V with Al and V being the main alloying elements (Park *et al*., 2000). Other Ti alloys, such as nickel-titanium (NiTi) and copper-nickel-titanium (CuNiTi) are also used for manufacturing orthodontic archwires. At present, NiTi alloys have a composition of 50-55% nickel and 40-45% titanium (Ferreira *et al*., 2012). To this 5% Cu is added alloys with the aim of increasing its strength and reducing energy loss where the alloy's elasticity can sustain very large deflections and return to their original shape with the production of moderate and uniform forces. 0.5% Cr is added to CuNiTi alloys to reduce the stress transformation temperature to 27°C (Parvizi *et al*., 2003).

The β-Ti III archwires have a composition of 78% Ti, 11.5% Mo, 6.0% Zr and 4.5% Sn. Al, V, Mn and Cr are four elements which are common to many α and α+β alloys. Timolium (TIM) is an advanced technology titanium archwire within a smooth surface that greatly reduces friction. It contains Ti (89.9%), Al (6.1%) and V (3.2%), which confirms that this product is a mixture of α and β phases (Donachie, 1988; Kusy *et al*., 2004).

Saliva, as it contains bacteria, viruses, yeast, fungi and their products (Anandkumar & Maruthamuthu, 2008), may cause corrosion of orthodontic appliances (House *et al*., 2008). The alloys used in orthodontic appliances are formatted as a passive oxide film to resist corrosion but this layer is not ideal since it can be disrupted by chemical and mechanical attacks (House *et al*., 2008).

Elemental release of metals and ions of alloys in salivary concentration is influenced by the matrix composition of the alloy. Zn and Cu are released from stainless steel (SS) through the microstructures of the alloy (Schmalz *et al*., 2008). Cr can also be released by this alloy (Matos de Souza *et al*., 2008; Sfondrini *et al*., 2009). Gjerdet *et al*., (1991); Mikulewicz *et al.*, (2012) have indicated that N ions in salivary concentration are released and inceased in the oral environment after three weeks of insertion of fixed orthodontic appliances. The major corrosion products of alloys are Fe, Cr and Ni. Although all three elements potentially have adverse effects, Ni and Cr have receive the most attention because of their reported potential for producing toxic, allergic or carcinogenic effects (Mikulewicz *et al.*, 2012; Pereira *et al*., 1999). Insertion of Ni with the matrix infrequently leads to hypersensitivity due to the formation of rashes, swelling and pain in the oral and labial mucosae (Al-Waheidi, 1995; Mikulewicz *et al.*, 2012).

The major challenge in orthodontic biomaterials when metals are used, in the control of friction between the archwire and brackets. A percentage of the applied force is dissipated to overcome friction, while the remaining percentage is transmitted to the supporting structures to induce tooth movement (Cunha *et al*., 2011). Therefore, the total force is determined by the force to move a tooth and the force needed to overcome friction between the bracket and the archwire (Angolkar *et al*., 1990; Kapila *et al*., 1990). A high friction coefficient is needed in case of anchorage, whereas for retraction of teeth and space closure, a low friction coefficient is desirable (Burrow, 2009). Friction coefficients differ among those materials used for fabricating orthodontic archwires, which in turn, can control treatment times compatible to the bracket/archwire combination applied (Guerrero *et al*., 2010).

The ideal properties of an orthodontic archwire depend on the requirements set in mechan-otherapy at a specific treatment stage. As such, selection of the appropriate archwire is often complex. Criteria such as the force control and the need for a specified elastic or plastic zone must be taken into account in the process. Orthodontic treatment is related to the movement

of teeth to aesthetically enhance facial appearance and the enhancment of the occlusion of teeth so that they align with each other during mastication (Wyllie *et al*., 2007). In this study, a load deflection test for orthodontic archwire tests was chosen mainly because of its close simulation to clinical application, reproducible results and the ability to differentiate wires. Evaluation of the load deflection property is the most important parameter determining the biological nature of tooth movement.

β-Ti alloys form one of the most versatile classes of materials with respect to processing, microstructure and mechanical properties (Weiss *et al*., 1998). These alloys include stable β, metastable β and β-rich alloys. They offer an alternative to the α+β alloys due to their increased heat treatability, wide and unique correlation of strength to weight ratios, deep hardening potential and inherent ductility. They also possess superior fatigue resistance compared to α+β alloys. These alloys are used in aerospace, power plants, sporting goods, the automotive industry, orthopedic implants and many other applications (Weiss *et al*., 1998).

Titanium molybdenum alloy (TMA) orthodontic archwire (**Table 1.3**) produces a variation in force-deflection behaviours. Consistent with an informed description of Mo addition in the β-Ti alloy, it is aimed to the stabilization of the β-phase in Ti alloys in order to improve the formability and strenght of the archwires. Mo is considered one of strongest elements in its application (Brantley & Eliades 2000; Gurgel *et al*., 2011).

Table 1.3: Composition of Titanium molybdenum alloy archwire (Szuhanek *et al*., 2010).

Element	Ti	Mo	Zr	Sn
Wt.%	79	11	6	4

The basic phases in Ti alloys such as Ti–6Al–4V are the α and β phases. Depending on the ratio of the amounts of α and β phases, Ti alloys may be broadly classified as α, β and α+β, as shown in **Figure 1.2**. Within the latter category are the subclasses near-α and near-β, referring to alloys whose compositions place them near to α/(α+β) and near to β/(α+β) phase boundaries, respectively. It is widely considered that the mechanical properties of Ti alloys are very sensitive to the characteristics of the microstructure. The type of phases, grain size and grain shape, morphology and distribution of the fine microstructure (α+β) determine the properties and therefore the applications of Ti alloys. A classification of Ti alloys based on the amount of retained β phase at room temperature has been reported (Semiatin *et al*., 1997). The final microstructure is formed during the thermo-mechanical and heat treatment processing. It is therefore important to understand the correlation between the

processing parameters, microstructure and other properties which would allow the optimization of the processing parameters and alloy composition, in order to achieve the desired combination of properties for any particular application (Collings, 1994; Malinov *et al*., 2004). The stability of the quenched phase in β-Ti alloys is characterized by its ability to transform into martensite during the deformation or quenching process. The phase is retained in a metastable state by quenching (**Figure 1.2**) (Laheurte *et al*., 2005).

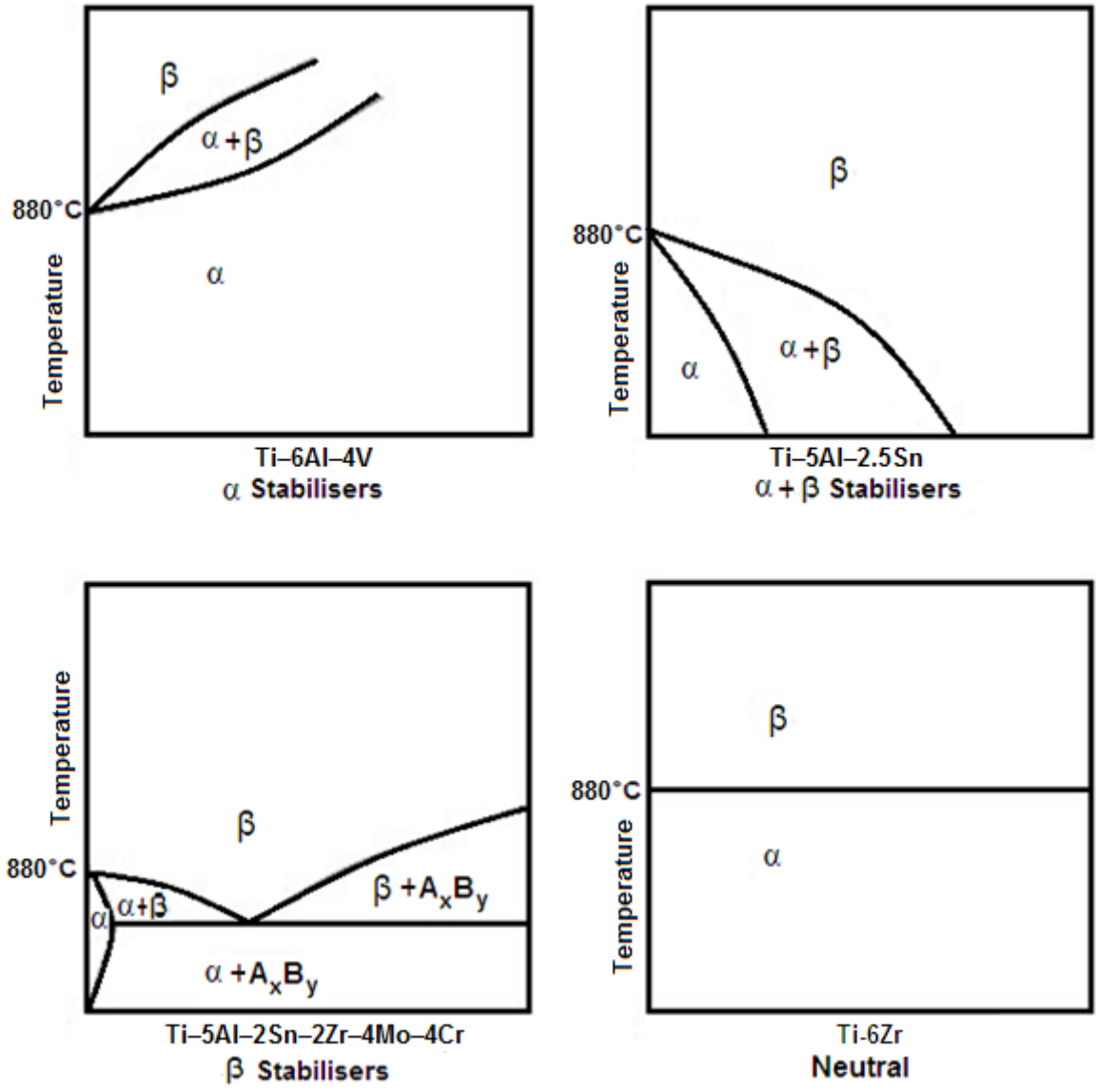

Figure 1.2: Phase diagram for Ti alloys (Campbell, 2008).

Tooth movement, during orthodontic treatment, is associated with a sliding process between the orthodontic archwires and brackets. When the two objects slide across each other at extremely slow speeds, as occurs in orthodontics, they are observed to move differently compared to faster moving objects. Extremely slow moving objects alternate between

extended periods without relative movement and periods of rapid movement. This phenomenon is observed in the movement of archwires and orthodontic brackets that contact along a fault line. Teeth move along an archwire in the same manner in what is described as the “stick-slip” phenomenon. The stick part of the cycle involves elastic loading of the system until the force within the system overcomes the static force of friction. The two objects then slip across each other until the force stored in the system diminishes below the frictional force and then they stick again (Rossouw *et al.*, 2003).

1.2 Problem statement

Many approaches have been used to overcome the aforementioned disadvantages. Coating the surface of orthodontic metallic wires using various techniques and materials, as well as modifying the surface of wires and brackets, are among those strategies developed to improve both the mechanical and biological properties of metals used in orthodontics.

TMA archwire has disadvantages such as high surface roughness, which increases the friction between the archwire interface with orthodontic brackets during the archwire sliding mechanics (Tecco *et al*., 2009). Improving the surface roughness and load deflection is the initial step and toward determining sliding archwire behaviour (Verstrynge *et al*., 2006)

TMA orthodontic archwires are used with brackets to apply biomechanical forces that affect tooth movement (Goldberg *et al*., 1979). This movement can however be resisted by frictional forces. Various surface characteristics, such as roughness of orthodontic archwires, might affect the sliding process by influencing the coefficient of friction of orthodontic brackets. Therefore the surface characteristics are important determinants of the effectiveness of archwire-guided tooth movement (Loftus *et al*., 1999)

Since TMA archwires has high surface roughness, the application of deposition of Zr should decrease surface roughness for TMA archwires and improve its strength as well.

1.3 Background to the problem

Orthodontic archwires, made from different alloys, offer alternative structures of archwire usage in all phases of orthodontic treatment (Gurgel *et al*., 2001). The archwire functions as a guide for movement of the brackets (**Figure 1.3**) (Szuhanek *et al.*, 2010). Ideally, archwires should have good balance of stability in an oral environment, stiffness, resilience and formability, with the ability to form without affecting the strength (Vijayalakshmi *et al*., 2009). Good characterization is therefore needed to ensure a good outcome (Juvvadi *et al*., 2010). It is presently possible to match the phases of orthodontic treatment with the mechanical

properties of the archwires. On this basis, the selection of orthodontic archwires should be based on an understanding of the mechanical characteristics of the archwire, required for the planning, active and retention phases of orthodontic treatment (Gurgel *et al*., 2001).

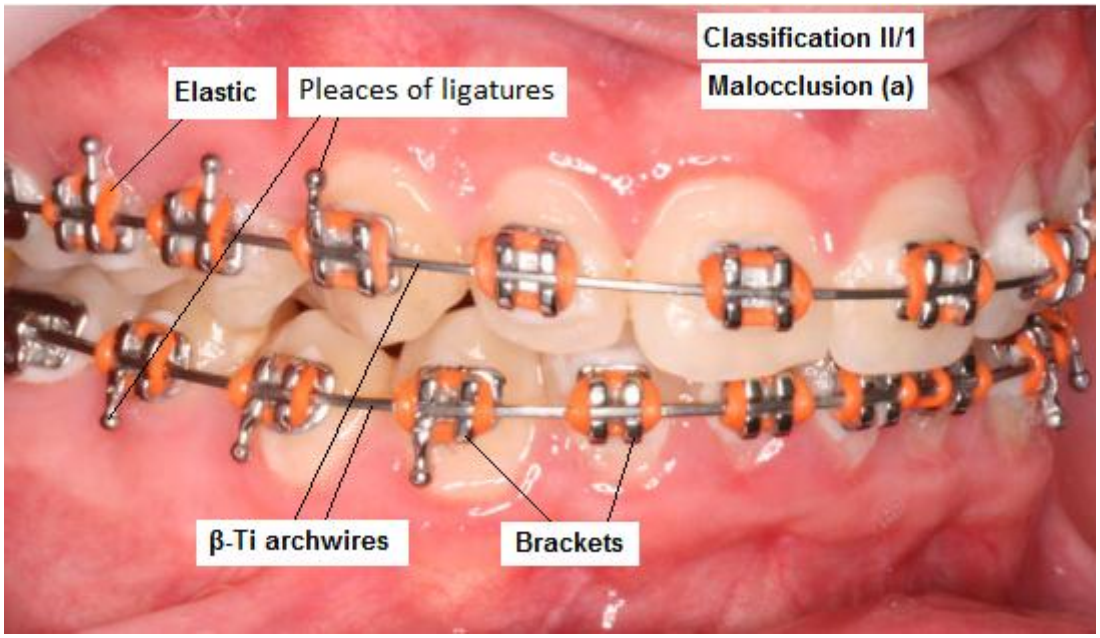

Figure 1.3: Example of the oral location of orthodontic archwires and brackets during orthodontic treatment (Szuhanek *et al*., 2010).

TMA orthodontic archwires were introduced in the latter half of the 20th century (Goldberg *et al*., 1979). These alloys were envisaged for orthodontic use after it became evident that its elastic modulus is less than that of SS and equivalent to that of nickel-titanium (Ni-Ti) alloy, which was then regarded as the conventional alloy. TMA archwires have excellent formability, flexibility and clarity of the material and have good ability to joining its parts by welding. TMA archwires have a low potential for hypersensitivity and good biocompatibility referring to the ability to reduce undesirable reactions produced by a normal immune system. This is because TMA archwires do not contain Ni in their matrix and that biocompatibility is a property or quality of being biologically compatible by not producing a toxic, injurious effects on biological systems (Kusy *et al*., 2007).

The use of TMA archwires, however, has several disadvantges. For example, high surface roughness, which increases friction at the archwire-bracket interface during the sliding process; susceptibility to fracture during bending (Tecco *et al*. 2009); and, β-Ti archwire is usually not considered the archwire of choice for close spacing because of its high frictional resistance (Kula *et al*., 1998).

The TMA archwires present low modulus of elasticity (ε) and resilience greater than that of SS. They also possess sufficient shape memory, medium stiffness, good formability, weldability and high attrition. They offer a good combination between stiffness and elasticity, which provides good characteristics for the finishing stage in orthodontic treatment (Szuhank *et al*., (2011); Vijayalakshmi *et al*., (2009) has indicated that β-Ti archwires are kinder in nature to the teeth as well as supporting tissue when compared with other archwire alloys. The TMA archwires have a great combination of strength and flexibility. These properties make them extremely useful as medium archwires between the initial alignment and finishing stages of completing the treatment of crooked teeth (Kula *et al*., 1998).

1.4 Hypothesis

The application of ion implantion on the the surface of TMA orthodontic archwires improves the surface roughness and reduces the strength of these archwires. The deposition of layers of Zr 5,10, 25 and 50 nm leads to improved surface roughness and maintains or improves the rate of deflection force. Because Zr has adequate mechanical properties, good corrosion resistance and excellent biocompatibility, it is assumed to be an ideal element for the surface modification.

1.5 Objectives

The main objective of this study was to improve the surface roughness while maintaining adequate deflection force of two types of TMA archwires. The following tasks were undertaken:

- Deposit thicknesses of Zr on the two types of Ti-alloyed archwires.
- Investigate the force of selected archwires before and after deposition with thicknesses of Zr by the method of Hounsfield deflection testing.
- Investigate the structure of selected archwires and their composition and the surface roughness, before and after Zr deposition, using scanning electron microscopy (SEM) and atomic force microscopy (AFM).

CHAPTER TWO

LITERATURE REVIEW

2.1 Introduction

During orthodontic treatment archwires play an important role because they provide the force systems necessary for tooth movement. Once an archwire is engaged into the bracket/band, it exerts forces on the tooth (**Figure 2.1**). The forces transmitted to a tooth by an archwire depend on several parameters of the archwire used and the relationship between the braces in which the archwire is engaged (Luppanapornlarp *et al*., 2010). An archwire can be used in a rectangular or round section, depending on the desired clinical result (Szuhanek *et al*., 2010).

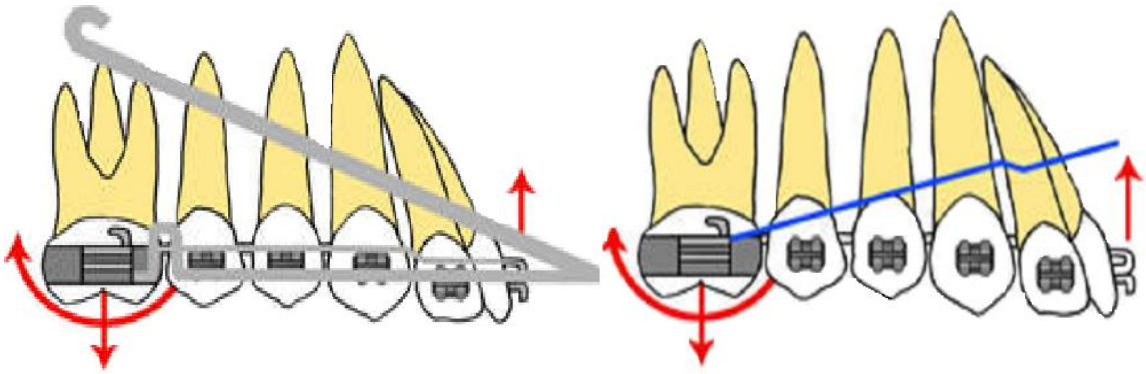

Figure. 2.1: Schematic diagram during fixed orthodontic treatment, β-Ti archwires are used in order to achieve the final settling of the dental occlusion and the force developed by a deformed archwire is transmitted to the teeth through fixed appliances (e.g. braces, molar bands and tubes) and tooth movements are achieved (Szuhanek *et al.,* 2010).

The β-Ti orthodontic archwires have been extensively used in orthodontics because of their favorable characteristics such as excellent formability, low stiffness and efficient working range for tooth movement (Gurgel *et al.*, 2011). The archwires used in fixed orthodontics should be able to slide through the brackets easily. β-Ti archwires exhibit high surface roughness that affects the sliding through brackets (Gurgel *et al*., 2011).

The β-Ti orthodontic archwires have been exploited in orthodontics because of their favourable characteristics such as excellent formability, low stiffness and efficient working range for tooth movement. β-Ti archwires have become popular in all areas of orthodontic treatment (Gurgel *et al.,* 2011). The archwires used in fixed orthodontic should be able to

slide through the brackets easily. β-Ti archwires exhibit high surface roughness that lead to effect on the sliding motion between archwire and brackets (Gurgel *et al*., 2011). To reduce surface roughness on these archwires, a nitrogen ion implantation technique has been used (Burstone *et al*., 1995; Kula *et al*., 1998; Kusy *et al*., 1992). Some authors have however questioned the effectiveness of this process in the reduction of surface roughness and they have answered questions regarding nitrogen ion implantation on the surface of archwires and its effect on archwire strength. Results of force tests of different types of β-Ti archwires showed that the force of β-Ti archwires implanted with nitrogen was less than that of unimplanted β-Ti archwires and that this process only aids in the reduction of friction (Gurgel *et al*. 2011; Kula *et al*. 1998; Verstrynge *et al.* 2006).

The β-Ti archwires were used for specific application in a segmented arch technique for making of retraction loops. Recently β-Ti archwires have been engaged in the construction of an intrusion arch (Sifakakis *et al*., 2009). β-Ti archwires are also useful in cantilevers for intrusion or extrusion of teeth. These applications make it possible to individualize tooth movement while providing a controlled force system (Gurgel *et al*., 2011). β-Ti III archwire is a type of β-Ti archwire (Burstone *&* Goldberg, 1980). TMA archwires are of the β-Ti type. Ti-Ni archwires have Ni content of 55 wt% and Ti content of approximately 45 wt%. The β-Ti archwires are also used in a strong, cold work, hardened form like Ti-Ni archwires which provide superelasticity (s_e). Ti-Ni wires present a substantial recovery strain (ε_r), as shown in **Table 2.1,** where the unloading secant modulus (ε_s) is 20 Gpa.

Ti-Ni wires are not weldable, have minimal ductility and are used in preformed arches. The presence of the high Ni concentration in Ti-Ni alloys raises some concerns about the potential of allergencity or toxicity of this archwire (Laheurte *et al*., 2007).

Table 2.1: Quantitative evaluation of Ti-Ni and β-Ti III archwires for orthodontic use (Laheurte *et al.,* 2007).

Archwire	Unloading secant modulus εs (GPa)	Recovery strain εr (%)	Workability	Weldability	Biocompatibility
Ti-Ni	12–30	4–5	No	No	Yes
β-Ti III	40	3	Yes	Yes	Yes (Ni free)

2.2 Historical overview of the use orthodontic archwires

Kusy (1981) compared the application theoretical strength, stiffness of Ti-Ni and β-Ti archwires with SS and cobalt-chromium (Co-Cr) archwires. With the apparent stiffness as criterion, equivalent force systems are established in the elastic region between the conventional and the new archwire alloys. In bending experiments, calculations show that the

Ti-Ni alloy makes a superior starting archwire and has stiffnesses similar to SS archwires. But with approximately twice the strength, the β-Ti alloy makes a particularly good intermediate archwire.

Angolkar *et al*. (1990) investigated the frictional resistance offered by ceramic brackets used in combination with archwires of different alloys and sizes during *in vitro* translatory displacement of brackets. Outcomes with ceramic brackets were also compared with findings of treatment with SS brackets. SS, Co-Cr, β-Ti and Ti-Ni archwires of different cross-sectional sizes were tested in medium-twin monocrystalline ceramic brackets with both 0.45 mm and 0.55 mm slot sizes. The archwires were ligated into the brackets with elastomeric modules. Brackets were moved along the archwire by means of an Instron universal testing machine and the frictional force was measured by a density cell and recorded graphically. Archwire friction in the ceramic brackets increased as the archwire size increased and rectangular archwires produced greater friction than round archwires. β-Ti and Ti-Ni archwires were related with higher frictional forces than SS or Co-Cr archwires.

Kusy *et al*. (1990) investigated the effect of surface roughness on the coefficients of friction for SS and β-Ti and Ti-Ni archwires. The surface roughness of different materials influence the coefficients of friction and ultimately the movement of teeth. Archwires were slid between contact flats to simulate orthodontic archwire-bracket appliances using laser specular reflectance measurements. The surface roughnesses of these archwires varied from 0.04 μm for SS to 0.23 μm for Ti-Ni. It was concluded that the β-Ti archwire had the highest coefficient of friction although the Ti-Ni archwire was the roughest.

Prososki *et al*. (1991) measured the surface roughness and static frictional force resistance of orthodontic archwires using. Ti-Ni alloy archwires were studied. One β-Ti alloy archwire, one SS alloy archwire and one Co-Cr alloy archwire were compared with the Ti-Ni archwires. The average roughness in micrometers (μm) was measured with a profilemeter. Frictional force resistance was quantified by pushing archwire segments through the SS self-ligating brackets of a four-teeth clinical model. The Co-Cr alloy and the Ti-Ni alloy archwires showed the lowest frictional resistance. The SS alloy and the β-Ti alloy archwires showed the highest frictional resistance. The SS alloy archwire was the smoothest archwire tested and the Ti-Ni was the roughest. There was no appreciable correlation between calculated average roughness and frictional force values.

Barrett *et al*. (1993) compared the corrosion rate of a standard orthodontic appliance consisting of bands, brackets and SS or Ti-Ni archwires. Analysis revealed Ni and Cr as corrosion products. Appliances immersed for four weeks in a prepared artificial saliva medium at 37°C were analyzed. Ten identical sets were used, each simulating a complete orthodontic appliance used on a maxillary arch with a full balance of teeth. Five sets were

ligated to SS archwires and the other five sets were ligated to Ti-Ni archwires. Ni and Cr release was quantified by flameless atomic absorption spectrophotometry. The analysis of variance was used to verify whether differences existed between the Ni and Cr release according to archwire type. The results indicated that orthodontic appliances release measurable amounts of Ni and Cr when placed in an artificial saliva medium and, further, that Ni release reaches a maximum after approximately one week, after which the rate of release decreases with time. On the other hand, Cr release increases during the first two weeks and levels off during the subsequent two weeks. The release rates of Cr or Ni from SS and Ti-Ni archwires are not significantly different and for both archwire types the release of Ni was, on average, seven times greater than Cr.

De Franco *et al*. (1995) compared frictional resistances between Teflon-coated SS and clear elastomeric ligatures used with various combinations of brackets and archwires. SS metal, polycrystalline ceramic and single-crystal ceramic 0.55 mm slot brackets were used with SS and Ti-Ni archwires, with dimensions of 0.45 mm and 0.40 mm×0.55 mm. Friction was measured in the dry state at bracket-archwire angulations of 0, 5, 10 and 15 degrees. Introducing by connect of the archwires into the brackets were measured for each archwire type and bracket-archwire angulation. Results showed that Teflon-coated ligatures produced less friction than elastomers for all bracket–archwire combinations. It was concluded the ceramic brackets generally produce greater frictional resistance than SS brackets. Suggestions are that Teflon-coated ligatures are useful in reducing the high friction of ceramic brackets in cases when an aesthetical appliance is imperative.

The surface roughness and irregularity of the surface of archwires are very closely related to their corrosion behaviour (Verstrynge *et al*., 2006). The characteristic of archwires is a necessary factor influencing the effectiveness of arch-guided tooth movement during clinical orthodontic treatment. It also contributes to the biocompatibility and aesthetics of orthodontic appliances (Bourauel *et al*., 1998).

Although Ti-Ni orthodontic archwires are used with brackets to apply biomechanical forces that affect tooth movement, Ti-Ni is unsuitable for long-term use. Once Ti-Ni devices are eroded by active saliva, the release of corroded material and Ni ions into oral cavities can cause significant health problems. For example, Ni may generate allergenic, toxic and carcinogenic reactions (Widu *et al*., 1999).

Loftus *et al*. (1999) reported that the frictional forces with self-ligating and conventional SS brackets and with ceramic brackets with SS clinical orthodontic treatment SS slots are similar when tested under simulated clinical conditions. However, brackets with ceramic slots generate higher friction than brackets with SS slots. Friction is higher with β-Ti archwires

than with Ti-Ni archwires but the friction associated with each of these two archwires is similar to that of SS archwires.

Kusy & Whitley (2003) investigated the influence of fluid media on the frictional coefficients in orthodontic sliding. From a controlled experiment in which the worst-case frictional couple for orthodontic sliding was used and the fluid media was varied, only human saliva can be used to quantify the magnitude or to rank the efficiency or reproducibility of orthodontic sliding. The overall outcomes seem independent of whether values of static or kinetic frictional coefficients are considered or whether methods including regression lines or conventional averaging are employed. If artificial saliva is to emulate the frictional characteristics that human saliva possesses, then artificial saliva must be engineered that varies greatly from those products that currently are marketed for very different purposes.

Cacciafesta *et al.* (2003) demonstrated that metal-insert ceramic brackets generate appreciably lower frictional forces than traditional ceramic brackets but higher forces than SS brackets. β-Ti archwires have higher frictional resistance than SS and Ti-Ni archwires, although no significant differences were found between SS and Ti-Ni archwires. All brackets showed higher static and kinetic frictional forces as the archwire size increased. Metal-insert ceramic brackets are visually satisfying, but a costly alternative to conventional SS brackets in patients with aesthetic demands.

Cheng *et al.* (2004) demonstrated a new technique for modifying Ti-Ni alloy surfaces with tantalum (Ta) by means of plasma immersion ion implantation (PIII). Ti-Ni alloys implanted with Ta modified the surface morphology and chemical composition. When implanted Ti-Ni alloys were immersed in 0.9% NaCl solution at 37°C, the altered surface of Ti-Ni alloys increased the open-circuit corrosion potential and decreased the corrosion current density. The pitting potential for the Ta-implanted Ti-Ni alloy is approximately 810 mV, more than 200 mV higher than that of the unimplanted specimens. Indications are that the PIII technique is an efficient technique to enhance the corrosion resistance of Ti-Ni alloys.

Cash *et al.*, (2004) demonstrated that SS self-ligating brackets generated significantly lower static and kinetic frictional forces than both conventional SS and polycarbonate self-ligating brackets, which showed no significant differences between them. TMA archwires had higher frictional resistances than SS and NiTi archwires. No significant differences were found between SS and NiTi archwires. All brackets showed higher static and kinetic frictional forces as the wire size increased. In patients with esthetic demands, polycarbonate self-ligating brackets are a appropriate substitute to conventional SS and ceramic brackets.

Kusy *et al*., (2004) compared and discussed the surface roughnesses and sliding resistances of six types of β-Ti archwires, namely (β-Ti III, RES, CNA, TMA, TMAL and TIM). They were

studied as functions of composition, morphology, surface roughness and sliding mechanics by using scanning electron microscopy (SEM) and a frictional testing machine. In the latter test, all archwires were coupled with 0.55 mm SS brackets in which normal forces were applied by 0.25 mm SS ligatures. With regard to composition, five archwires were true β-Ti alloys having nominal compositions of 80% Ti, 10% Mo, 6% Zr and 4% tin and one were an α-β alloy having a nominal composition of 90%Ti, 6%Al, 3%V and 1% other elements. Morphologies varied from surfaces with striations, scale, or layers of drawn material that suggested surface steps or fissures. Specular reflectance and optical roughness measurements divided the archwires into two groups of three: β-Ti III, RES and CNA had an overall mean value of 0.148 μm; and TMA, TMAL and TIM had a mean overall value of 0.195 μm. These roughness measurements and its accompanying details of the compositional analyses suggested that there could be as few as two vendors manufacturing the five β-Ti products. For six different values of angulations that embraced the passive and active regions of sliding, the coefficients of friction varied rather narrowly from 0.17 to 0.27 and were independent of surface roughnesses. Although these contemporary products are better than their predecessors for over a decade ago, other issues might be more important than surface finishes or frictional resistances because all products appear fairly comparable (Kusy *et al*., 2004).

Kaneko *et al.* (2004) investigated the performance decline of four major alloys of orthodontic archwires (Ti-Ni, β-Ti, SS and Co-Cr-Ni), caused by hydrogen absorption during short-term immersion in an acid fluoride solution. The hydrogen-related degradation of orthodontic archwires after immersion in 2.0% acidulated phosphate fluoride solution at 37°C for 60 min was evaluated by a tensile test, scanning electron microscope examination and hydrogen thermal desorption analysis. The tensile strengths of the Ti-Ni and β-Ti archwires decreased. In particular, the Ti-Ni archwire fractured before yielding and the fracture mode changed from ductile to brittle. The amounts of absorbed hydrogen in the Ti-Ni and β-Ti archwires were 200 and 100 mass parts per million (ppm) respectively. On the other hand, the tensile strengths of the SS and Co-Cr-Ni archwires were only minimally affected by immersion. The conclusion to this study was that decreased performance of orthodontic archwires of Ti alloys occurs due to hydrogen absorption even after short-term immersion in fluoride solutions.

Verstrynge *et al*. (2006) investigated the material characteristics of SS and β-Ti archwires and concluded that there are several differences between β-Ti and SS archwires. Archwires were tested blindly for archwire dimensions, bending and tensile properties and chemical compositions this is indicated in **Table 2.2** and **2.3**. β-Ti archwires showed the highest surface roughness values and SS significantly showed the lowest hardness values.

Table 2.2: Composition different types of β-Ti and SS alloys (Verstrynge *et al*., 2006).

Ti–11.5Mo–6Zr–4.5Sn	5Al–2Sn–2Zr–4Mo–4Cr	Ti–6Al–4V	Ti-13Nb–13Zr	18 Cr-8 Ni-2 Mn-1 Si	23 Mn-21Cr-1 Mo- 0.10Ni	18 Cr-12 Ni-2Mo-2 Mn-1 Si
β-alloy	β-alloy	α-β-alloy	β-alloy	SS-alloy	Ni-free SS-alloy	SS-alloy

Table 2.3: Chemical composition of β-Ti and SS alloys (wt%) (Verstrynge *et al*., 2006).

	Fe	Nb	Al	Cr	Ni	V	Ti	Si	Mo	Mn	Zr	Sn	Sum
Ti–11.5Mo–6Zr–4.5Sn	<0.05	<0.05	<0.05	<0.05	<0.05	<0.05	78.00	<0.05	11.50	<0.05	6.00	4.50	100.00
Ti–5Al–2Sn–2Zr–4Mo–4Cr	<0.05	<0.05	5.00	4.00	<0.05	<0.05	89.00	<0.05	4.00	<0.05	2.00	2.00	100.00
Ti–6Al–4V	<0.05	<0.05	6.00	<0.05	<0.05	4.00	90.00	<0.05	<0.05	<0.05	<0.05	<0.05	100.00
Ti–13Nb–13Zr	<0.05	13.00	<0.05	<0.05	<0.05	<0.05	74.00	<0.05	<0.05	<0.05	13.00	<0.05	100.00
18 Cr-8 Ni-2 Mn-1 Si	71.00	<0.05	<0.05	18.00	8.00	<0.05	<0.05	1.00	<0.05	2.00	<0.05	<0.05	100.00
23 Mn-21Cr-1 Mo-0.10Ni	65.90	<0.05	<0.05	21.00	0.10	<0.05	<0.05	<0.05	1.00	23.00	<0.05	<0.05	100.00
18 Cr-12 Ni-2Mo-2 Mn-1 Si	65.00	<0.05	<0.05	18.00	12.00	<0.05	<0.05	1.00	2.00	2.00	<0.05	<0.05	100.00

Walker *et al*. (2007) investigated the effect of fluoride prophylactic agents on the loading and unloading mechanical characteristics and surface roughness values of β-Ti and SS orthodontic archwires. Rectangular β-Ti and SS archwires were immersed in either an acidulated fluoride agent, a neutral fluoride agent, or distilled water (control) for 1.5 hr at 37°C. After immersion, the loading and unloading elastic modulus and yield strength of the archwires were measured using a three-point bend test in a water bath at 37°C. A one-way analysis of difference was used to evaluate the mechanical testing data. SEM was also used to qualitatively evaluate the archwire topography as a function of the fluoride treatments.

Results showed that using topical fluoride agents with β-Ti and SS orthodontic archwires could reduce the functional unloading mechanical characteristics of the archwires and potentially contribute to extending orthodontic treatment. It was concluded that using topical

fluorides with SS or β-Ti orthodontic archwire might be a factor in prolonged orthodontic treatment time. Furthermore, both β-Ti and SS orthodontic archwires exhibited qualitative surface topography changes following exposure to neutral or acidulated phosphate fluoride agents. After exposure to either neutral or acidulated prophylactic fluoride gels, β-Ti and SS archwires showed a statistically significant decrease in unloading mechanical characteristics. Because unloading forces produce tooth movement, this decrease may be clinically related.

Development of new biomaterials typically takes a long time due to extensive tests and lengthy approval procedures. Plasma surface modification offers an exciting alternative by modifying selective surface mechanical and biological properties of conventional biomaterials to suit particular requests. Hence, materials that possess favourable bulk properties can have its surfaces redesigned to cater to biomedical applications (Chu, 2007). Plasma surface modification is a popular method to enhance the multi-functionality and mechanical properties, as well as biocompatibility of artificial biomaterials and medical devices. Research work on plasma modification of NiTi alloys and cardiovascular materials, namely diamond-like carbon is described. The shape memory effect and super-elasticity of NiTi alloys allow for a novel surgical technique for gradual correction of spinal deformity (Chu, 2007). From this study concluded that plasma surface modification is a versatile technique and has many advantages in the field of biomaterials engineering. For example, individual surface biological properties can be altered without changing the desirable bulk properties of the biomaterials such as strength and inertness. The applications of PIII to the surface modification of NiTi orthopedic materials as well as the synthesis and biocompatibility of Ni and phosphorus doped diamond-like carbon films is described. The results showed that PIII produces an effective surface barrier to mitigate Ni out-diffusion and using the proper conditions, the PIII treated NiTi rods retain the shape recovery properties.

Silva *et al.*, (2007) concluded that the improvements of surface properties achieved by PIII nitrogen implantation in a Ti_6Al_4V sample at high temperatures are confirmed by an increase in surface hardness due to a significant enrichment of nitrogen in the structure. The process becomes more efficient with increases in temperature. The experimental results show that at 800°C the diffusion process is substantially greater than at 550°C. They could confirm this result by comparing the layer thicknesses measured by Glow Discharge Optical Spectroscopy (GDOS) and Auger Electron Spectroscopy (AES) techniques. The wear resistance is improved because the fretting wear decreases for both conditions of high and low plasma potentials (PP). These results confirm the improvement of the surface mechanical properties of the Ti_6Al_4V alloy treated by both of the low and high PP. However, with low PP, deeper layers and higher wear resistance could be analysed.

Redlich *et al*. (2008) investigated a new type of composite metal-nanoparticle coating that significantly reduces the friction force of various surfaces, particularly archwires in orthodontic applications. The coating is based on an electrodeposited Ni film impregnated with inorganic fullerene-like nanospheres of tungsten disulphide (WS_2). Results of their tests showed a reduction of up to 60% of the friction force between coated rectangular archwires and self-ligating brackets, in comparison to uncoated archwires. They concluded that coating not only significantly reduces friction of commercial archwires but also maintains this low value of friction for the duration of the tests in comparison to archwires coated with Ni film without the nanoparticles. The coated surfaces of the archwires were tested by SEM equipped with an energy dispersive analyser and by x-ray powder diffraction, before and after the friction tests. Using the results of these analyses, it was possible to qualitatively estimate the state of the Ni and inorganic fullerene-like tungsten disulfide (IF-WS_2) coating before and after the friction test compared to Ni coated archwires without the IF-WS_2.

Tantalum (Ta) coatings were successfully deposited on the surface of TiNi alloy samples by the multi arc ion-plating technique. The Ta coating effectively suppresses the release of Ni ion. The amount of released Ni ion from the coated NiTi alloy sample is about 1/30 times that from the uncoated NiTi alloy sample after immersing in the 0.9% NaCl solution for forty nine days. The compatibility of the NiTi alloy coated with tantalum is better than that of the uncoated one and following annealing treatment, the compatibility of the Ta-coated sample behaves the best. The Ta coating can efficiently improve the radiopacity of the NiTi alloy (Cheng *et al*., 2006)

Enhanced corrosion resistance of Zr coating on biomedical TiNi alloy was prepared by PIIID. Zr film was prepared on TiNi alloy by the PIIID technique to enhance its corrosion resistance and prolong its working lifetime (Zheng *et al*., 2008). The AFM results show that the film was relatively smooth. The X-ray photoelectron spectroscopy (XPS) and X-ray diffraction (XRD) results indicate that the implant element of Zr was partial to oxidation. The potentiodynamic polarization measurements in the Hank's solution at 37°C show that the corrosion resistance of the alloy was improved by the Zr coating film. The atomic absorption spectrometry (AAS) tests also indicated that the Ni ion concentration released from the substrate in the Hank's solution after the polarization test was greatly reduced, in comparison to the unmodified TiNi alloy sample. The study concluded that Zr film deposited on TiNi alloy by PIIID was successful, with a relatively smooth surface morphology. The open circuit potential for Zr film coated sample keeps a steadier and higher value than the uncoated substrate. The current density in the anodic region for Zr film coated sample is very low at the scanned potential range and the current density is almost unchanged with the increase

of the anodic potential, exhibiting significant corrosion resistance. The Zr film can also effectively reduce the Ni ion concentration released from the substrate in the Hank's solution.

Lee *et al*. (2010) investigated atomic force microscopy (AFM) images depicting changes in the surface roughness of bracket surfaces that were contacted and altered by archwires before and after *in vitro* and *in vivo* sliding movement. Atomic force microscopy measurements provided detailed information on surface roughness variance before and after the sliding test *in vitro* and intra oral location. Results of this study showed that the ceramic bracket has good biocompatibility and experiences less friction which supports in the effectiveness of arch-guided tooth movement.

AFM can be useful to a wide variation of samples (conductors, insulators) and may be operated in different environments (vacuum, air and liquid), which make it possible to examine biological systems (biomolecules, cells) under physiological conditions. A major advantage of the AFM over classical microscopy techniques is that it can simultaneously provide information on local physical properties, such as mechanical properties and interaction forces. In particular, force-distance curves, made by recording the deflection of the cantilever while the sample is moved up and down, allow one to directly measure surface forces in aqueous environments, such as van der Waals and electrostatic forces, solvation forces, steric forces and intermolecular forces between complementary molecules (Binnig *et al*., 1986).

Ushiki *et al*., (1996) declared that, the advantage of the AFM for biologists is that AFM can visualize non-conductive materials. AFM images of plasmid DNA are comparable to those recorded by transmission electron microscopy using a rotary shadowing technique and have the advantage of being able to directly examine the molecule without staining or coating.

AFM is a device designed to exploit the level of sensitivity. It is used to investigate both conductors and insulators on an atomic scale and envision a general-purpose device that will measure any type of force; not only the interatomic forces, but electromagnetic forces as well (Binnig *et al*., 1986). They proposed a new system where the scanning tunneling microscope (STM) is used to measure the motion of a cantilever beam with an ultrasmall mass. The force required to move this beam through measurable distances (4-10 Å) can be as small as 10-18N. The masses included in the other techniques are too large to reach this rate. This level of sensitivity noticeably penetrates the regime of interatomic forces between single atoms and opens the door to a range of applications (Binnig *et al*., 1986).

AFM images are obtained by measurement of the force on a sharp tip (insulating or not) shaped by the proximity to the surface of the specimen. The cantilever with the stylus is inserted between the AFM specimen and the tunneling tip. It is fixed to a small piezoelectric

element called the modulating piezo, which is used to drive the cantilever beam at its resonant frequency. The STM tip is also mounted on a piezoelectric element and this serves to maintain the tunneling current at a constant level. The AFM specimen is connected to a three-dimensional piezoelectric drive, as the x, y, z scanner. A feedback loop is used to preserve the force acting on the stylus at a constant level. Viton pieces are used to damp the mechanical vibrations at high frequencies (Binnig *et al*., 1986).

The potential use of an AFM for study of surface properties of orthodontic materials, including the surface roughness of orthodontic archwires, has been evaluated (D'Antò *et al.*, 2012). As mentioned, AFM has many advantages, such as the production of topographical three-dimensional images in real space with a very high resolution (10 Å); the samples do not require any special treatment; and, quantitative values for the investigated parameters can be obtained. The most important drawback of this analytical technique is, however, the small scan size, which, in conjunction with the slow velocity of scanning often impedes a complete analysis of the sample (Braga & Ricci, 2004). Therefore, there may be some unselected regions with surface defects and therefore with much greater roughness, that would be of clinical importance (D'Antò *et al.*, 2012).

Chemical vapor deposition (CVD) diamond is a new potential biomedical material which has the advantage of chemical inertness, extreme hardness and low coefficient of friction, among others. In orthopaedics and maxillofacial surgery, these properties could improve implant performance, reducing metallic corrosion and particle wear. In a study, two types of CVD diamonds were analysed: microcrystalline diamonds (MD) and nanocrystalline diamonds (ND), both produced by hot-filament CVD. The diamond tubes were previously characterized by SEM, AFM and Raman scattering spectroscopy (RSS). Its results showed nanocrystalline CVD diamond had an average surface roughness less than microcrystalline diamonds CVD diamond (Rodrigues *et al*., 2010).

Jian-hong *et al*. (2011) evaluated the static and kinetic frictional forces produced by different combinations of orthodontic archwires and brackets. They tested three types of archwires (SS, Ni-Ti, TMA alloys) and two types of brackets (SS and self-ligating) **Table 2.4**. Both static and kinetic frictional forces of each archwire-bracket combination were measured 25 times using a custom-designed apparatus. They also evaluated surface topography and hardness of the archwires. All outcomes were statistically analyzed using two-way analysis of variance and Tukey's test. Results indicated that the static frictional force was significantly higher than the kinetic frictional force in all archwire-bracket combinations not involving TMA archwire. TMA archwire had the highest friction, followed by Ni-Ti archwire and then SS archwire when using the SS bracket. Furthermore, there was no difference between Ni-Ti and SS archwires when using the self-ligating bracket. For TMA archwires, the friction was higher when using

the SS bracket than when using the self-ligating bracket. The SEM results indicated that SS archwire exhibited the smoothest surface topography. The hardness decreased in the following order: SS archwire < TMA archwire < Ni-Ti archwire. This study demonstrated that the frictional forces of brackets are influenced by different combinations of bracket and archwire.

Table 2.4: Chemical composition of SS,TMA,Ni-Ti orthodontic archwires (wt%) (Juvvadi *et al*., 2010).

	Fe	Cr	Ni	Ti	Mo	Zirconium	Sn	Sum
SS	72.39	18.17	9.02	<0.05	<0.050	<0.05	<0.05	99.58
TMA	<0.05	<0.05	<0.05	78.4	11.33	6.28	4.05	100.06
Ni-Ti	<0.05	<0.05	55	<0.05	<0.05	<0.05	<0.05	100.00

Amini *et al*. (2012) found that Ti-Ni archwire made by All-Star Orthodontics (USA) and the SS archwire made by American Orthodontics (USA) have a significant number of porosities and defects and do not differ appreciably in terms of their surface roughness. Furthermore, the SEM was used at 1000 times magnification to revaluate the micromorphological characteristics of the TI-NI and SS archwires. Surface characteristics were determined on the basis of a visual evaluation of the surface irregularities. The SEM system was equipped with an energy dispersive x-ray analysis (EDAX), to analyze the chemical composition of the archwire The spectrophotometer received and analyzed the x-ray energy spectrum from the archwire surface to differentiate between the compositions of the orthodontic archwire materials (**Table 2.5**).

Amini *et al*. (2012) evaluated the surface roughness of two types of orthodontic archwires made by four different manufacturers. Tests were conducted on 35 specimens of seven different orthodontic archwires, namely, Ti-Ni archwires from the following manufacturers American Orthodontics, OrthoTechnology, All-Star Orthodontics and Smart Technology and one SS archwire from the manufacturers American Orthodontics, OrthoTechnology and All-Star Orthodontics. SEM-EDX was used to determine the composition of each archwire. SEM and surface profilometry were used to determine the surface roughness of each archwire.

Table 2.5: Chemical composition of orthodontic archwires (wt%) measured by scanning electron microscopy energy-dispersive x-ray analysis (SEM-EDXA) (Amini *et al*., 2012).

Manufacturer	Alloy	Si	Ti	Cr	Fe	Co	Ni
American Orthodontics Sheboygan,USA	Ti-Ni	0.31	38.66	0.17	0.25	0.25	60.35
	SS	1.05	0.32	19.07	70.54	<0.05	9.01
Orthodontic Technology Tampa, USA	Ti-Ni	0.67	42.02	0.19	0.19	0.18	56.76
	SS	1.14	0.26	18.97	70.83	<0.05	8.80
All-Star Orthodontics Columbus, USA	Ti-Ni	0.51	41.89	0.24	0.31	0.24	56.81
	SS	1.23	0.18	19.01	70.57	<0.05	9.02
Smart Technology Beijing, China	Ti-Ni	0.97	41.33	0.08	0.20	<0.05	57.42

No other elements were detected and the detected fractions in each archwire added up to 100%.

The results showed more defects and cracks were on the SS archwire made by American Orthodontics and the Ti-Ni archwire made by All-Star Orthodontics than the others. It was found that the Ti-Ni archwire manufactured by All-Star Orthodontics and the SS archwire made by American Orthodontics were the roughest archwires.

Arango *et al*. (2012) conducted research on different approaches, such as coating and surface treatment of archwires. The purpose of that study was to provide an overview of the coating and surface treatment methods performed on metallic biomaterials used in orthodontics. Its finding was that orthodontic surface treatment is an important area of active research. Many materials and techniques were applied to modify the surfaces of dental materials.

Sterilization methods may affect the properties of orthodontic archwires (Alavi & Sinaee, 2013). They evaluated the effect of dry heat and steam sterilization on the load deflection properties of five types of β-Ti alloy archwires. The specimens comprised 30 straight lengths of five types of β-Ti alloy archwires: Titanium molybdenum alloy low friction (TMAL), coloured TMAL, resolve (RES), beta-titanium molybdenum alloy (BETA) and Connecticut new archwire (CAN). Thirty archwires segments were divided into three groups of ten samples. Group 1 was the control group. Group 2 specimens were sterilized by dry heat in an oven (60 min at 160°C). Group 3 specimens were sterilized by steam in an autoclave (15 min at 121°C). All the archwires specimens were then subjected to a 3-point bending test machine to evaluate the load deflection properties.

Results showed that dry heat sterilization significantly increased the force levels for both loading and unloading of CNA, BETA and RES and during a loading. Steam sterilization significantly increased force levels for both loading and unloading, of BETA and during an unloading with no effects on the load-deflection characteristics of TMAL, CNA and RES. It was concluded that dry heat sterilization increases the stiffness of RES, BETA and CNA, but autoclave sterilization does not have any effect on load-deflection properties of most of the β-Ti archwires tested, indicating that clinicians who want to offer maximum safety for the patients can autoclave TMAL, RES and CNA before applying them (Alavi & Sinaee, 2013).

Alavi & Sinaee (2013) evaluated the effect of steam and dry heat sterilization techniques on load deflection behavior of six types of β-Ti alloy archwires: TMA, TMAL, TMAL Coloured, RES, BETA and CNA. Thirty archwires segments were divided into three groups of 10. Group 1 was the control group and the group 2 samples were sterilized by dry heat in an oven (60 minutes at 160°C) and group 3 by steam in an autoclave (15 minutes at 121°C). All the archwires samples then underwent a three-point bending test to evaluate load deflection properties.

The results showed that dry heat sterilization significantly increased force levels during both loading and unloading of CNA, BETA and RES and during loading of TMAL Coloured ($P < 0.05$). Steam sterilization significantly increased force levels during both loading and unloading of BETA and during unloading of TMAL Coloured ($P < 0.05$), with no effects on the load-deflection characteristics of TMAL, CNA and RES ($P > 0.05$).

2.3 Surface characteristics of orthodontic brackets

There are significant differences between the friction of β-Ti orthodontic archwires and SS and Ti-Ni orthodontic archwires with SS brackets. β-Ti archwires have higher frictional resistance than SS and Ti-Ni orthodontic archwires. Frictional forces of all orthodonic brackets increased as the archwire size increased (Cacciafesta *et al*., 2003). Rectangular archwires produced greater friction than round archwires. β-Ti and Ti-Ni orthodontic archwires are associated with higher frictional forces than Co-Cr or SS orthodontic archwires. Archwires in ceramic brackets produced appreciably stronger frictional force than archwires in SS brackets (Angolkar *et al*., 1990).

In another study Cacciafesta *et al*. (2003) demonstrated that metal-insert ceramic brackets generate significantly lower frictional forces than conventional ceramic brackets but higher forces than SS brackets. Metal-insert ceramic brackets are not only visually pleasing, but also an appropriate alternative to conventional SS brackets in patients with aesthetic demands.

2.4 Deactivation of β-Ti archwires

The mechanical properties of orthodontic β-Ti archwires are important in order to accomplish the desired treatment results. β-Ti alloys offer good use of orthodontic appliances design and good thermal treatment which can modify the strength/elasticity ratio and can improve clinical therapeutical properties (Szuhanek *et al*., 2010).

The mechanical properties of SS and CAN archwires were compared and evaluated (Juvvadi *et al.* 2010). SS was the smoothest archwire. It had the lowest friction and spring-back values and high values for stiffness, modulus of elasticity (ε), yield strength (YS) and ultimate tensile strength (UTS). The TMA alloy was the roughest archwire. It had high friction and intermediate springback, stiffness and UTS values. The β-Ti archwire was intermediate in terms of smoothness, friction and UTS but had the highest spring-back. The β-Ti archwire with increased UTS and yield strength (YS) had a low ε value, suggesting that it would have greater resistance to fracture, thereby overcoming a major disadvantage of β-Ti archwires. The β-Ti archwire would also deliver gentler forces.

The β-Ti III archwire type of β-Ti archwires do not contain Ni. It has good weldability, its performance for recoverable deformation is inferior and it has a higher unloading ε_s compared with Ti-Ni (Laheurte *et al*., 2005). For orthodontic applications, a significant recoverable deformation and a low unloading ε_s are desirable (Laheurte *et al*., 2007). The presence of α or ω phases in the isothermal second phase, resulting from isothermal treatment or an insufficient cooling rate, decreases the ductility and pseudoelastic behaviour of β-Ti alloys. For an alloy quenched at a temperature higher than the temperature of the beta phase (T_β), the plastic deformation and grain size growth result in an increase in the ε_r and a decrease in the unloading ε_s, leading to a significant improvement in the mechanical properties of the alloy (Laheurte *et al*., 2007).

The main reason for the application of β-Ti archwires alloys is because the maximum elastic deflection increases with the yield strength/modulus of elasticity ratio of the material, β-Ti alloys possess one of the highest such ratios. The β-Ti alloys can achieve yield strengths in excess of 1.38×10^{10} N/m^2 while maintaining an elastic modulus of between 5.5 and 11×10^{10} N/m^2, compared to the 17×10^{8} N/m^2 yield strength and 19.3×10^{10} N/m^2 modulus of elasticity of SS. These Ti alloys have good formability, even after considerable cold working and good environmental stability (Williams *et al*., 1973).

All orthodontic archwires presently available have specific disadvantages of surface roughness or release of Ni ions, so no ideal orthodontic archwire is currently available. It is therefore important that the orthodontist understands the specific characteristics of each orthodontic archwire and be aware of the appropriate uses of each type of

alloy (Gurgel *et al*., 2011). Because of the multi-stage processing required for β-Ti archwires, few companies in the world manufacture this type of Ti alloy (**Table 2.6**). It is important that the quality control process of β-Ti archwires and other orthodontic archwires be strictly maintained. All companies that market these archwires should provide their activation-deactivation force range (Gurgel *et al*., 2011). Despite the inherent significant formability of β-Ti archwires, its processing can be problematic because of the reactivity of Ti that can result in some batches of β-Ti archwires being susceptible to fracture during clinical manipulation (Brantley & Eliades, 2000). Laboratory tests do not necessarily reflect the clinical situation, although they do provide a basis for comparison of different archwires (Gurgel *et al*., 2001; Kapila *et al*., 1989; Kusy *et al*., 2007).

The desirable properties of an orthodontic archwire depend on the requirements set by mechanotherapy at a specific treatment stage (Laheurte *et al*., 2007). Consequently, selection of the appropriate archwire is often complex. Criteria such as the degree of torque control, the desired load-deflection rate and the need for a specified elastic or plastic zone must be taken into account. In general, three factors determine the rigidity of the archwire: the length, the cross-section and the elastic modulus of the alloy.

The traditional method to modify the rigidity involves varying the dimensions of the archwire by using incrementally larger cross-section archwires in the slot or adjusting the configuration of the loops. The use of materials with a low elastic modulus, such as Ti alloys, was introduced as an alternative way to improve strength, namely, variable modulus orthodontics (Burstone, 1980; Goldberg *et al*., 1979).

Table 2.6: Chemical composition (wt%) of β-Ti archwires (Kusy *et al*., 2004).

β-Ti archwire	Elements								Manufacturer
	Ti	Mo	Zr	Sn	Al	V	Mn	Cr	
β-Ti III	80.60	9.50	5.90	3.90	0	<0.05	0.20	0.10	3M Unitek, Monrovia, USA
RES	79.60	9.90	5.80	4.00	0.20	<0.05	0.30	0.40	GAC, Islip, USA
TMA	78.20	11.03	6.30	3.70	0.20	<0.05	0.30	0.30	Ormco, Glendora, USA
TMAL β-Ti low friction archwire	79.00	11.00	6.00	3.30	0.30	<0.05	0.30	0.20	Ormco, Glendora, USA
timolium (TIM)	89.90	0.30	0.30	0.40	6.10	3.20	<0.05	<0.05	TP Orthodontics, Lodi, USA

According to Burstone & Goldberg, 1980), the ε of a β-Ti archwire is approximately twice that of a Ti-Ni archwire and less than half that of a SS archwire. Its stiffness makes it ideal in applications where less force than steel is required, but the lower modulus would be inadequate to develop the required force magnitudes.

Furthermore, Kapila *et al*. (1989) stated that the relatively low forces generated by β-Ti archwires implies that smaller forces are needed than that required for SS archwires. This counteracts the counterproductive forces generated by β-Ti archwires. Although various archwire alloys are available for retraction of teeth, SS archwires have always been the mainstay for this phase of treatment. The β-Ti archwire has an great balance of properties, including high springback, low stiffness, high formability and the ability of direct welding. However, a major drawback is its high coefficient of friction. Some batches of β-Ti archwires are susceptible to fracture during clinical manipulation (Brantley & Eliades, 2000). The β-Ti archwires demonstrate higher levels of bracket archwires friction than SS or Co-Cr archwires (Garner *et al*., 1986).

Ormco Corporation Calif (USA) has the exclusive patent on β-Ti archwires (Hilgers *et al*., 1992). However, since 2000 other companies have introduced new β-Ti archwires (Kusy *et al*., 2004). A major concern now is the activation-deactivation behaviour of each of the new β-Ti archwires being marketed. The mechanical properties of β-Ti archwires from different alloys have been investigated in several studies (Gurgel *et al.*, 2001; Gurgel *et al*., 2011). The mechanical properties of β-Ti archwires are an important parameter in achieving optimal tooth movement (Kusy *et al*., 2004). Surface treatment with ion-implantations of nitrogen into β-Ti archwires reduced the static and kinetic coefficients from 0.50 and 0.44% respectively, before implantation, to 0.20 and 0.25% respectively, after implantation (Kula *et al*., 1998). It is important for orthodontists to have reliable information about the mechanical properties of the different commercial β-Ti archwires (Gurgel *et al*., 2011).

Gurgel *et al.* (2011) carried out *in-vitro* tests to simulate a deflection inducing tooth movement. β-Ti archwires showed plastic deformation during activation. The force-deflection curves distinguished wires that exhibited more plastic deformation than others (**Figures 2.2** and **2.3**). The timolium (TIM) archwires and β-Ti archwires required a greater force to deflect and had more plastic deformation at the end of the deactivation curve. Therefore, it is advisable that β-Ti archwires be selected for clinical cases that require bends, like a T loop or cantilever. β-Ti archwire tests exhibited statistical differences indicating the existence of different forces for the same amount of deflection. Among the six types of wires analyzed in both activation and deactivation phases, only the TIM archwire exhibited forces different from the others. The TIM archwire exhibits the highest force on activation, indicating that it has higher stiffness during deflection. However, in the deactivation phase, it showed inadequate force necessary to promote dental movement after deflection of 2 mm. At a deactivation deflection of 1 mm, the TIM archwire produced a force of 27g (Gurgel *et al*., 2011). This force is insufficient to induce the biological response needed to produce dental movement in most patients (Proffit *et al*., 1993).

The TIM archwires did not exhibit favourable properties in deflection at 2 mm for levelling and alignment (Gurgel *et al*., 2011). The β-Ti low friction archwire (TMAL) type of β-Ti archwires also showed forces different from those of the other archwires tested. With activation of 1 mm, TMAL archwires showed low forces, statistically equal to forces of TMA and the RES type of β-Ti archwires. In the deactivation curve, TMAL wire had a 74g force (the lowest unloading force of the group. This finding explains the nitrogen ion implantation on the surface of the archwire and its influence on archwire strength (Gurgel *et al*., 2011).

The low deactivation force (74g) suggests that TiN on the surface of TMAL archwires only aid in the reduction of friction. TIM archwires produced a variation in force-deflection behaviours, consistent with a reported description of Mo addition in the Mo alloy (Brantley & Eliades, 2000). Additions of β-stabilisers such as Mo and V to titanium alloy aim to improve the formability toward enhance to the strength (Gurgel *et al*., 2011). In addition, Gurgel *et al.* (2011) reported that even if significant statistical differences ($p < 0.05$) were noted for TIM archwires in activation and for TIM and TMAL archwires in deactivation, other archwires had similar activation and deactivation curves. A comparison of force-deflection curves of the RES, TMA, TMAL archwires shows that the curves are similar (**Figures 2.2** and **2.3**. It is possible to recognize a near fit among the curves of archwires of Orthodontic Organizers (ORG) and TIM types of β-Ti archwires. With a force activation for deflection of 1 mm, ORG archwires exhibited a force equal to 141g. With force deactivation for deflection of 1 mm, ORG archwire exhibited a force equal to 40g. With a force activation for deflection TIM archwire exhibited a force equal to 168g. With a force deactivation for deflection of 1 mm, TIM archwire exhibited a force equal to 27g (**Figure 2.2**).

This fit indicates that perhaps two distinct types of β-Ti archwires are being produced, with different specifications or it is the result of two different manufacturers processing this alloy for orthodontic use. The hysteresis curves of TMAL, TMA and RES archwires (**Figure 2.3**) show intervals between activation and deactivation segments. This represents more flexibility. TMA archwires and TIM archwires represent a group of more rigid wires. These archwires show hysteresis curves with a larger interval between activation and deactivation phases (**Figures 2.2** and **2.3**). These archwires may be more suitable than other orthodontic archwires in any phase of orthodontic treatment that requires loops or other bends (Gurgel *et al*., 2011).

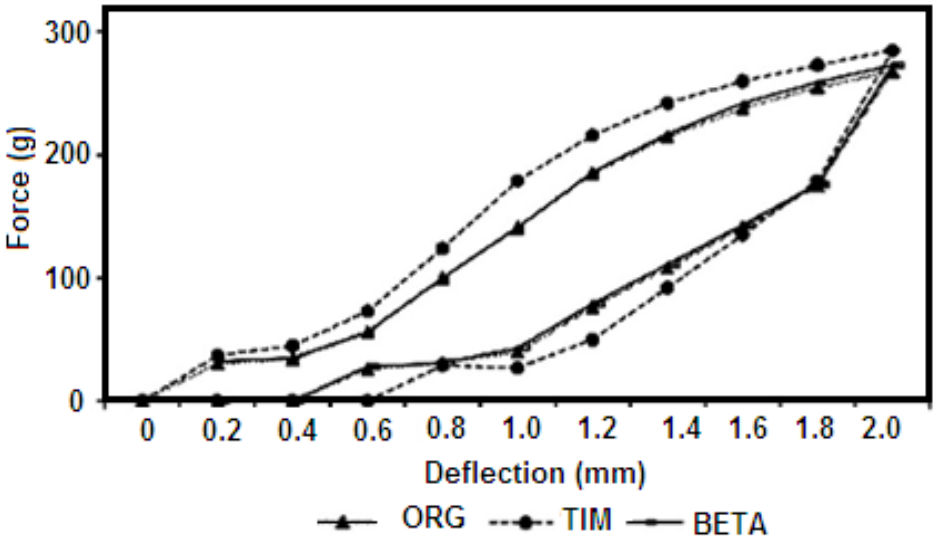

Figure 2.2: Load/Unload deflection graph for organizers (ORG) orthodontic archwire type of β-Ti orthodontic archwires and Timolium (TIM) archwire type of β-Ti orthodontic archwires and BETA (β-Ti III) orthodontic archwires type of β-Ti orthodontic archwires exhibited statistical differences, indicating the existence of different forces for the same amount of deflection (Gurgel *et al*., 2011).

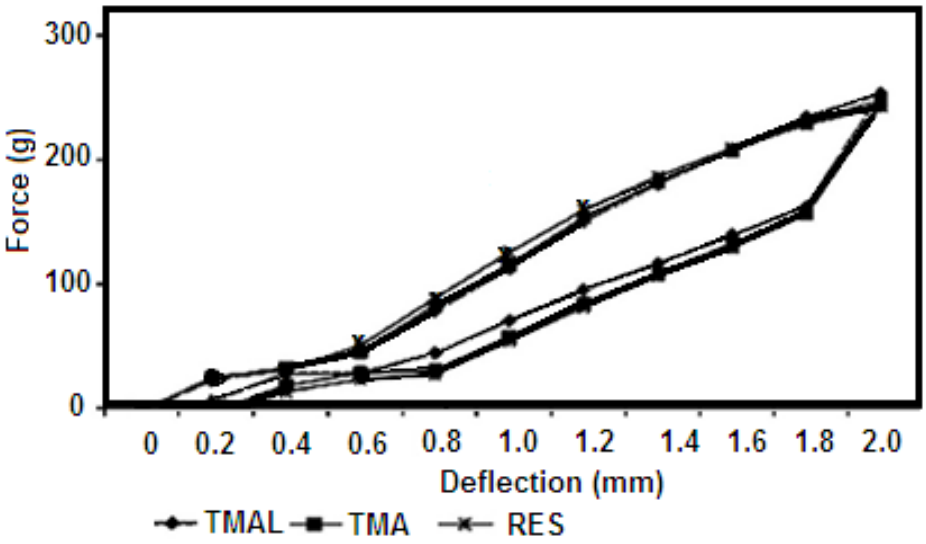

Figure 2.3: Load/Unload deflection graph for β-Ti low friction (TMAL) orthodontic archwire type of β-Ti orthodontic archwires and titanium molybdenum (TMA) orthodontic archwire type of β-Ti orthodontic archwirses and resolve (RES) orthodontic archwire type of β-Ti orthodontic archwires exhibited statistical differences, indicating the existence of different forces for the same amount of deflection (Gurgel *et al*., 2011).

2.5 Coating techniques to improve the surface roughness of β-Ti archwires

The application of coatings is one of the approaches available for modifing the surface of materials. Various coating techniques and materials have been used with the objective of improving surface characteristics (**Figure 2.4**) (Arango *et al*., 2012).

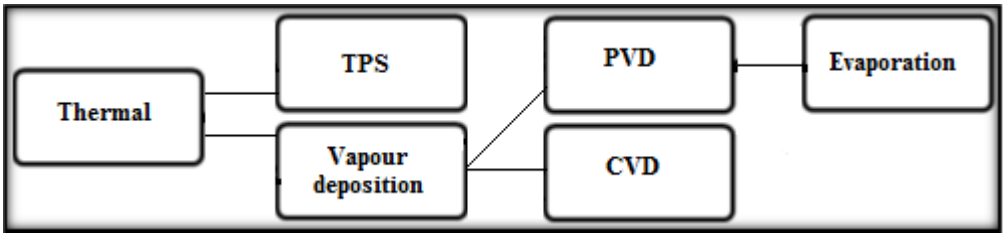

Figure 2.4: Classification of processes used for coating at industrial level (Arango *et al*., 2012).

2.5.1 Thermal plasma spray

Thermal plasma spray (TPS) is a process in which finely ground metallic and non-metallic materials are deposited on a substrate in a molten or semi-molten state. This technology is based on direct-current arc or radiofrequency inductively coupled plasma discharge, which provides high temperatures that, in turn, allow melting of any material (Fridman, 2008). Investigations into the use of this technique on metallic substrates, some of which can be used in implant dentistry, are reported (Junker *et al.*, 2010).

2.5.2 Chemical vapour deposition

Chemical vapour deposition (CVD) involves the flow of a precursor gas into a chamber that contains one or more heated objects to be coated. Chemical reactions take place on and near the hot surfaces, resulting in the deposition of a thin film on the surface. The production of chemical by-products and their further exhaustion from the chamber, along with unreacted precursor gasses, accompanies the process (Park *et al*., 2001).

CVD has some unique advantages namely the films obtained with this technique are conformal (film thickness on the side walls is comparable to thickness on the top); a wide variety of materials can be applied and they can be deposited with a high level of purity; and, high deposition rates can be achieved. Its main disadvantage lies in the required characteristics of the precursors. They need to be volatile at or near room temperature, which is insignificant for a large number of elements. Other drawbacks involve the fact that precursors can be toxic, explosive, expensive and corrosive; the by-products can be hazardous; and, films need to be deposited at elevated temperatures, which restricts the

types of materials that can be coated (Park *et al*., 2001). CVD has been used in the coating of burs used in dentistry (Borges *et al.*, 1999).

2.5.3 Physical vapour deposition

Physical vapour deposition (PVD) processes, often simply called thin-film processes, are atomistic deposition processes in which the material is vaporised from a solid or liquid source in the form of atoms or molecules and transported in the form of a vapour through a vacuum or low-pressure gaseous or plasma environment to the substrate where it condenses. Typically, PVD processes are used to deposit films with thicknesses in the range of a few nanometers to thousands of nanometers. However, PVD processes can also be used to form multilayer coatings, graded composition deposits, very thick deposits and freestanding structures. The substrates can vary in size from very small to very large and in shape from flat to complex geometries (such as watchbands and tool bits). PVD deposition rates are typically 10–100 Å (1–10 nm) per second (Mattox, 2010).

The PVD with metals technique has been introduced for the surface modification of Ti alloys Liu *et al*., (2004) and was applied to β-Ti archwires to develop surface coatings on the archwires capable of protection against fluoride-induced corrosion (Krishnan, 2011).

PVD uses reactive deposition processes. In the reactive deposition processes, compounds are formed by the reaction of the deposited material with the ambient gas environment, such as nitrogen, or with a co-depositing material. Quasi-reactive deposition is the deposition of films of a compound material from a compound source, where loss of the more volatile species or less reactive species during the transport and condensation process is compensated for by having a partial pressure of reactive gas in the deposition environment. For example, the quasi-reactive sputter deposition of the indium tin oxide (ITO) from an ITO sputtering target using a partial pressure of oxygen in the plasma. The main categories of PVD processing are vacuum deposition (evaporation), sputter deposition, vapour deposition and ion plating (Mattox, 2010).

Krishnan *et al.* (2012) coated β-Ti orthodontic archwires with titanium aluminum nitride (TiAlN) and tungsten carbide/carbon (WC/C) using PVD and evaluated the frictional properties, surface morphology and load deflection rates. They found that WC/C archwires demonstrated reduced frictional properties, better surface characteristics and low load deflection rates compared with TiAlN and uncoated archwires. Krishnan *et al.* (2011) also performed electrochemical corrosion behaviour and surface analyses, mechanical testing, elemental release and toxicology evaluations of WC/W and TiAlN coatings on β-Ti orthodontic archwires and concluded that TiAlN exhibits better resistance to fluoride corrosive effects on this type of archwire.

2.5.4 Evaporation

Evaporation is the simplest PVD method and has been proven useful for the deposition of elemental films. This process is carried out in a vacuum system in which a material is heated to temperatures near its fusion or sublimation point (Cao, 2004). Tripi *et al*. (2003) used this technique for coating Ni-Ti alloy.

2.5.5 Electrodeposition

Electrodeposition is an electrochemical process by which metal is deposited on a substrate by passing a current through on electrolyte bath. During electrodeposition, the substrate to be coated is prepared with the negative electrode or cathode in a cell that contains an electrolyte which allows the passage of an electrical current. The electrolyte is usually an aqueous salt solution of the metal to be deposited and is maintained at a controlled temperature. The electrical circuit is finished by the anode, which is usually prepared from the metal to be deposited and is located a short distance from the cathode. When a direct, low voltage current is applied, positively-charged ions in the electrolyte move toward the cathode where they undergo conversion to metal atoms and deposit on the cathode (Grainger *et al*. 1998).

Redlich *et al*. (2008) used electrodepositing to coat orthodontic archwires to reduce friction. The coating was based on a Ni film impregnated with inorganic fullerene-like (IF) nanospheres of tungsten disulfide (WS_2). Their results showed a significant reduction in friction in coated archwires and uncoated archwires. Samorodnitzky-Naveh *et al.* (2009) tested inorganic fullerene-like tungsten disulfide (IF-WS_2) nanoparticles, *in vitro*, using electrodeposition to coat Ti-Ni substrates in order to reduce friction. A substantial reduction in friction can lead to multiple applications.

Zein El Abedin *et al.* (2005) electroplated Ta on Ti-Ni alloys and evaluated corrosion behavior in a 3.5% NaCl solution. Coated samples showed better corrosion resistance than uncoated alloys. Qiu *et al*. (2010) used electrodepositing to apply hydroxyapatite and hydroxyapatite/Zr composite coatings on Ti-Ni alloys with the goal of assessing corrosion resistance. It was found that corrosion resistance significantly improved in a simulated body fluid after application of such a coating.

Arango *et al.* (2012) provided an overview of the coating and surface treatment methods performed on metallic biomaterials used in orthodontics. They concluded that orthodontic surface treatment is an important area of research. Numerous materials and techniques have been implemented to modify the surfaces of dental materials. However, a few are being used in clinical orthodontics, especially in areas such as friction control and decrease of bacterial

adhesion. In previous years, multidisciplinary research has contributed to closing the gap that has existed between material surface engineering and clinical practice.

2.5.6 Ion implantations

To reduce the surface roughness of β-Ti archwires, a nitrogen ion implantation technique was introduced. Implantation of nitrogen ions into the surface of orthodontic archwires causes surface hardening and can decrease frictional force by as much as 70% (Kusy *et al*., 1992). The effectiveness of this process in the reduction of friction was recently investigated (Gurgel *et al*., 2011). The surface of archwires and its effect on archwires strength produced a variation in force-deflection behaviour and the low deactivation force suggests that TiN on the surface of β-Ti archwires only aids in the reduction of friction. Implantation of TMA archwires with nitrogen ion does not significantly enhance space closure compared with unimplanted TMA archwires when unimplanted SS brackets are used. However, the rate of closing on TMA archwires is similar to the reported rate of sliding closure on steel wire (Kula *et al*., 1998). The disadvantage of the ion implantation process is the limited depth of penetration into the substrate (< 5 μm) (Singh *et al*., 2005).

Kobayashi et al. (2005) investigated deposition of carbon on Ti-Ni orthodontic archwires by an ion beam plating process in comparison with exposed Ti-Ni wires. The carbon deposited showed excellent mechanical and adhesion properties when used with a toothbrush machine. The carbon film does not only improve wear performance of the substrate but it can also enhance the corrosion resistance of Ti-Ni. In addition, depositions of carbon significantly protected Ni release from Ti-Ni. Due to this good corrosion, carbon films will prevent degradation of the material in the oral cavity and, moreover, will improve biocompatibility.

CHAPTER THREE

MATERIALS AND METHODS

3.1 Materials

Two orthodontic archwires were procured. Rectangular β-Ti III orthodontic archwires 0.48×0.64 mm were purchased from 3M Unitek® (USA) and TIM orthodontic archwires 3M (0.40×0.55 mm) were purchased from TP Orthodontics® (USA). Pure Zr was obtained from Good Fellow® of the United Kingdom through local agencies in Cape Town, South Africa.

3.2 Methods

3.2.1 Specimen preparation

Coatings produced by the Electron beam-physical vapor deposition (EB-PVD) process usually have a good surface finish and a uniform microstructure. The microstructure and composition of the coating can be altered by manipulating the process parameters and ingot compositions (Singh *et al*., 2005). The β-Ti III and TIM orthodontic archwires were cut into 25-mm-long specimens. Specimens were cut from the straight ends of the archwire. In this study, the EB-PVD technique was applied to deposite pure Zr (thicknesses of 5,10,25 and 50 nm) on selected archwires and then the effects thereof were investigated using AFM, SEM and the Hounsfield deflection test.

3.2.2 Coating/Deposition methods

3.2.2.1 Physical vapour deposition

Use of PVD with metals technique were used for the surface modification of Ti alloys (Liu *et al*., 2004). An EB-PVD instrument made in Pennsylvania, USA was used. It offers various possibilities for controlling variations in the structure and composition of condensed materials, for example, deposition compositions can be varied continuously (Singh *et al*., 2005).

3.2.2.1.1 Electron beam–physical vapour deposition

EB-PVD is a simple process in which a focused high-energy electron beam is directed to melt the evaporated material or materials in a vacuum chamber. The evaporating material condenses on the surface of the substrates or components, resulting in the formation of the

deposit. During deposition, external heating is often applied to the substrate for enhancing metallurgical bonding between the deposition and the substrate (Singh *et al*., 2005).

The EB-PVD process offers extensive possibilities for controlling variations in the structure and composition of condensed materials. The EB-PVD process offers many desirable characteristics such as relatively high deposition rates (up to 150 µm/min with an evaporation rate of app. 10–15 kg/hr), dense coatings, controlled composition, control the microstructure, physical and mechanical properties (Singh *et al*., 2005). EB-PVD is preferred over the plasma spray process due to smooth surface finish, better strain tolerance, better erosion-resistance properties and improved metallurgical bonding with the substrate (Singh *et al.*, 2005).

EB-PVD unit components consists of an EB-gun assembly, a water-cooled copper crucible that contains the material to be evaporated, the substrate (part to be coated) and the vacuum chamber unit with enhanced flexibility for a variety of deposition applications. The EB gun can be self-accelerated and directed or electromagnetic deflected through 180 or 270°C (**Figure 3.1**). The material to be evaporated is placed in a water-cooled copper crucible which can also serve as a pocket-type for applications involving small amounts of material to be evaporated (Singh *et al*., 2005).

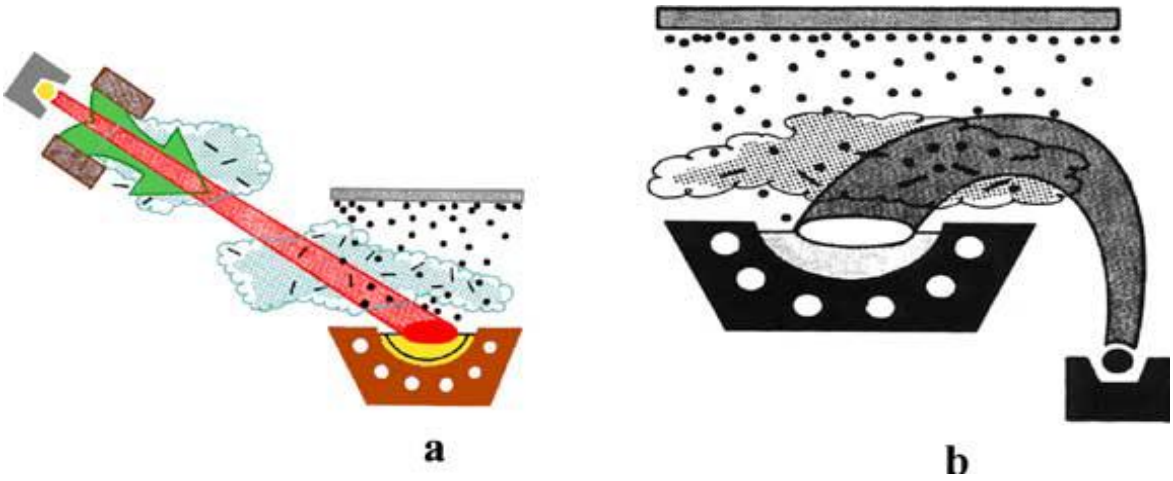

Figure 3.1: Schematic diagram showing EB-PVD: (a) straight and (b) electromagnetic deflected electron beam guns (Singh *et al*., 2005).

The apparatus and materials used included the e-beam machine (**Figure 3.2** and **3.3**). β-Ti III and TIM orthodontic archwires were substrates, the target material in this case was pure Zr. The Zr was placed into the crucible and the β-Ti orthodontic archwires substrates were mounted into the e-beam evaporator (**Figure 3.3**. The machine was closed and evacuated for 24hr. Thereafter, the e-beam deposition of Zr onto the β-Ti orthodontic archwires substrates was completed.

One Zr deposition of the same duration was done on β-Ti III and TIM orthodontic archwire substrates. This experiment was repeated under different deposition rate of 5, 10, 25 and 50 nm Zr, within the ranges from 0.6 Å/sec to 1.2 Å/sec. The vacuum pressure was approximately 2×10^{-6} mbar and the current 180 mA.

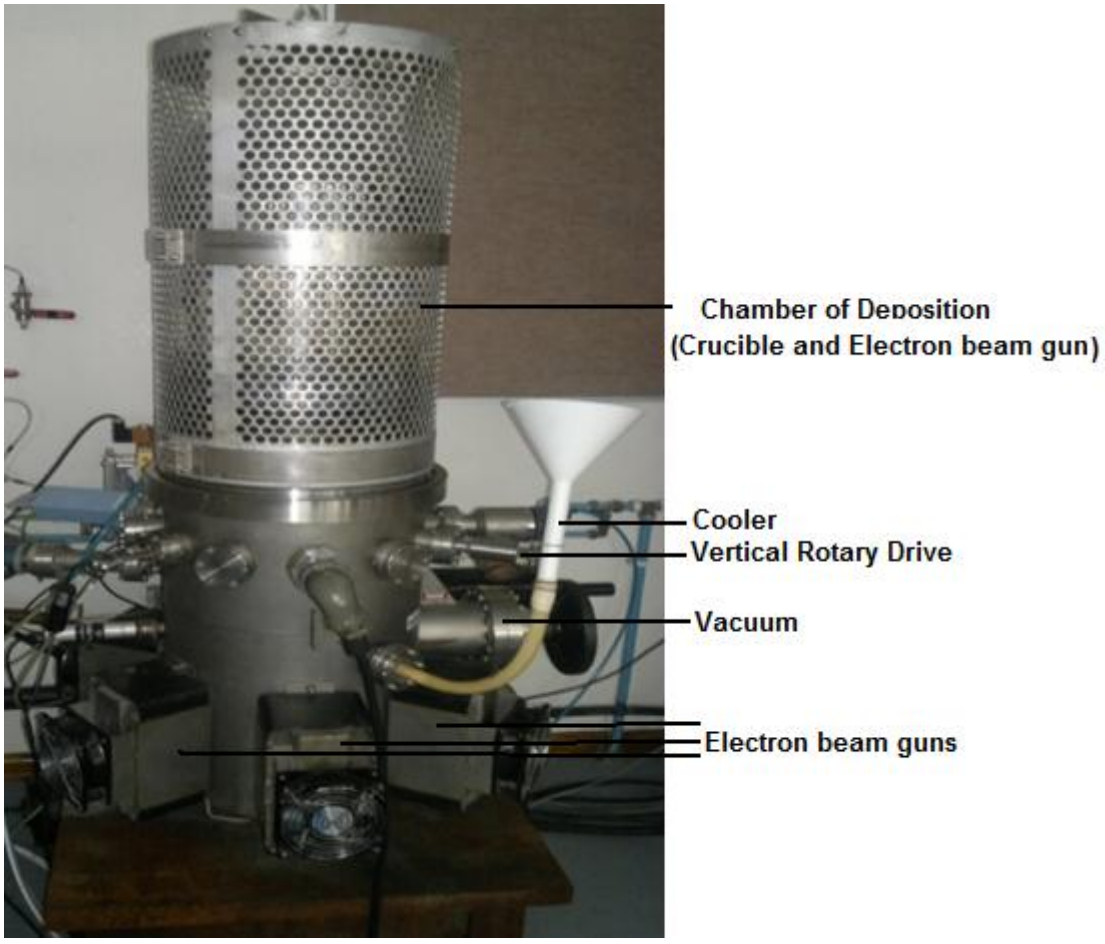

Figure 3.2: Electron beam-physical vapour (EB-PVD) Pennsylvania, American United states, used to despite 5, 10, 25 and 50 nm thicknesses of pure Zr on β-Ti III/TIM orthodontic archwires

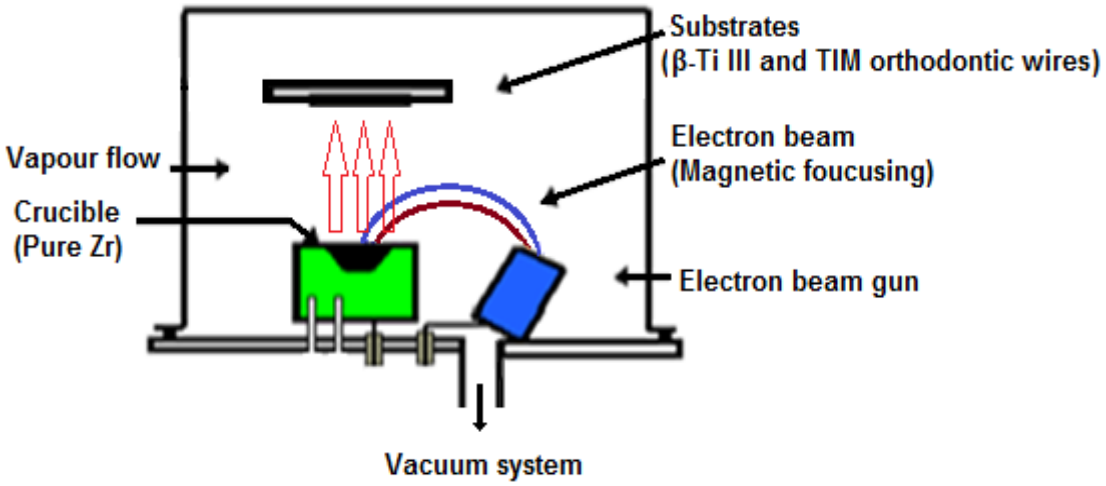

Figure 3.3: Diagram of electron beam-physical vapour (EB-PVD) shown pleases of β-Ti III and TIM archwires and pure Zr

3.2.3 Immersion in artificial saliva

In order to better simulate the oral cavity environment, archwire samples were immersed in artificial saliva (pH 5) at 37°C for 7 days. The composition of artificial saliva used is given in the **Table 3.1** (McKnight-Hanes & Whitford, 1992).

Table 3.1: Composition of artificial saliva (McKnight-Hanes & Whitford, 1992).

Components	(g/L)
Methyl-hydroxybenzoate	2.00
Sodium Carboxymethyl Cellulose	10. 00
KCl	0.625
CaCl2·2H2O	0.166
MgCl2.2H2O	0.059
K2HP4	0.804
KH2PO4	0.326

3.2.3.1Preparation of artificial saliva

Dissolve 2g of methyl-hydroxybenzoate in 800 mm of distilled water, solve 1g of methyl-hydroxybenzoate in 400 ml of water, 20 ml of the solution is keeping in a cold place for other chemical agent solvent. Boil 200 ml of distilled water then sprinkled of sodium carboxymethyl cellulose boiling water and stirring until total of sodium carboxymethyl cellulose is dissolved. Pour prepared methyl-hydroxybenzoate solution from first prepared solution into sodium

carboxymethyl cellulose then mixing them together until changing to gel form. Dissolve 0.625g of KCL in methyl-hydroxybenzoate solution from first prepared solution then pouring the solution into the solution in previous prepared solution and mixing them together. Dissolve 0.059g of $MgCl_2$. $6H_2O$ in methyl-hydroxybenzoate solution from first prepared solution then pouring the solution into the solution in previous prepared solution and mixing them together. Dissolve 0.166g of $CaCl_2$. $2H_2O$ in methyl-hydroxybenzoate solution from first prepared solution then pouring the solution into the solution in previous prepared solution and mixing them together. Dissolve 0.059g of K_2OHPO_4 in methyl-hydroxybenzoate solution from first prepared solution then pouring the solution into the solution previous prepared solution and mixing them together. Dissolve 0.326g of KH_2PO_4 in methyl-hydroxybenzoate solution from item first prepared solution pouring the solution into the solution in previous prepared solution and mixing them together. Adjust the of artificial saliva to (pH5).

3.2.4 Analytical techniques

3.2.4.1 Atomic force microscopy

The AFM was obtained from Surface imaging Systems, Veeco, Germany (**Figure 3.4**). The AFM, is an instrument that traces the surface topography of a sample with a sharp probe, while monitoring the interaction forces working between the probe and sample surface. Therefore, the AFM provides three-dimensional surface images of the sample with high resolution. AFM is a high-resolution surface imaging technique which works by scanning a sharp probe over the surface of a specimen, while measuring the forces experienced by the probe. In the most commonly used imaging mode, the probe and sample are brought in contact and the probe is scanned over the surface while the interaction force is kept constant. Otherwise, the deflection of the cantilever can be measured while the probe scans at constant height. These provide images of the surface topography with (sub) nanometer scale resolution (Binnig *et al*., 1986).

Figure 3.4: Atomic force microscopy (AFM) (Surface imaging systems, Veeco, Germany) used for determining the influence of deposited pure Zr on the surfaces of on β-Ti III/TIM orthodontic archwires

AFM has many advantages, such as the production of topographical three-dimensional profiles of the surface on a nanoscale by measuring forces between a sharp probe (<10 nm) and surface at very short distance (0.2-10 nm). The samples do not require any special treatment, such as metallization and the AFM can provide quantitative values for the investigated parameters. AFM was studied further to see the shape of the crystals and determine the influence of deposited Zr on the selected archwires surfaces. AFM was used to study the surface morphology of the layers on the β-Ti/TIM treated and non-treated archwires. The specimens for analysis by AFM did not need any special treatment. It was at into 14 mm lengths with a probe from the instrument in order to provide the required data. Use was made of the east-AFM software to translate the data of the high resolution 3-D surface images of the archwires.

3.2.4.2 Scanning electron microscopy

3.2.4.2.1 Experimental details

A FEI Nova Nano SEM 230 instrument, (Eindhoven, The Netherlands), at the Electron Microscopy Unit at the University of Cape Town, was used to analyse samples (**Figure 3.5**).

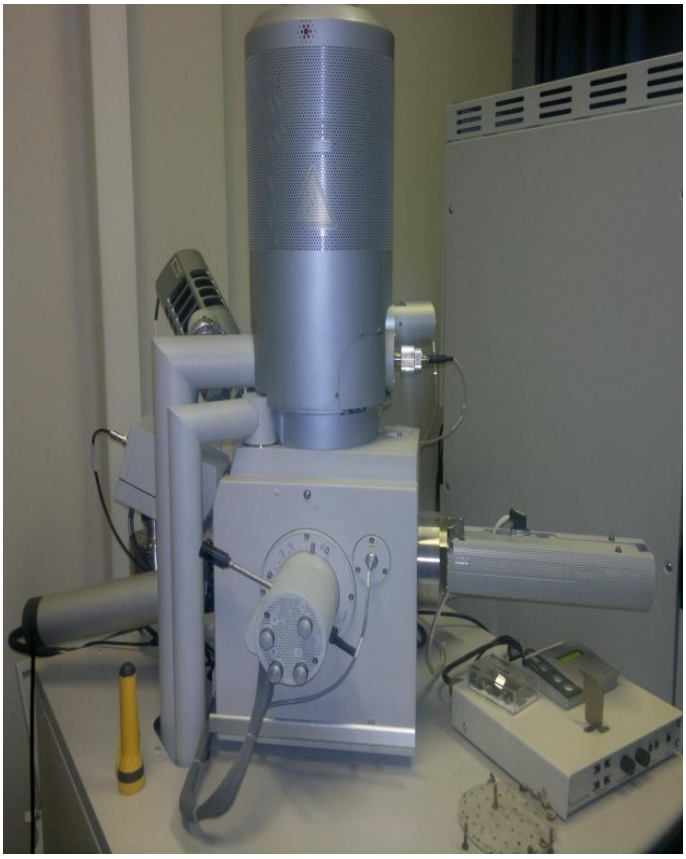

Figure 3.5: Scanning electronic microscopy (SEM) (A FEI Nova Nano SEM 230, Eindhoven, Netherlands) used fo determining elemental composition of uncoated and coated β-Ti III/TIM orthodontic archwires with 5, 10, 25 and 50nm thicknesses of pure Zr

The images were recorded at a 34° angle and the working height 5 mm. The particle sizes and distributions from SEM were determined using the Origin 8.0 software associated with the instrument.

SEM is a close relative of the electron microprobe but it is designed primarily for imaging rather than analysis. Images are produced by scanning the beam while displaying the signal from an electron mode. In many applications, the large depth of field in SEM images, typically at least 100 times greater than for a comparable optical microscope, is more relevant than the high resolution. An important factor in the success of SEM is that images of three-dimensional can be generated. The range of applications of SEM can be extended by adding other types of detectors (Reed, 2005).

In SEM a fine probe of electrons with energies typically up to 40 keV is focused on a specimen and scanned along a pattern of parallel lines. Various signals are generated as a result of the impact of the incident electrons which are collected to form an image or to analyze the sample surface. These are mainly secondary electrons with energies of a few tens of eV, high-energy electrons backscattered from the primary beam and characteristic x-rays. SEM is specifically configured to get the most information out of the largest selection

of samples, down to the nanometer level. The scanning electron microscope is as the appropriate analytical instrument in use today in materials and life-science research (Bogner *et al*., 2007).

SEM commonly have a x-ray spectrometer attached, enabling the characteristic x-rays of selected the elements to be used to produce an image. Also, with a stationary beam, point analysis can be obtained using electron microprobe probe analysis (EMPA). The spatial resolution with respect to analysis is, however, still limited to about 1 µm by beam spreading, despite the higher resolution obtainable in scanning images.

SEM uses a focused electron beam to image the surface. The image is obtained by scanning the focused electron probe across the specimen surface and collecting the results image signal from the surface. The indicator is scattering from the specimen surface and the electron beam loses energy by inelastic scattering as the electrons penetrate beneath the specimen surface. Most of the electron current from an excited specimen is due to the release of secondary electrons from the specimen surface (Brandon & Kaplan, 2008). Changes in the confined curve will change the possibility that a secondary electron can escape. An area with a positive radius of curvature increases the chances of a secondary electron escaping and vice versa, while regions with negative radius of curvature reduces the secondary electron current. Since the intensity of the image depends upon the number of secondary electrons reaching the detector, secondary electron imaging provides topographic images of rough surfaces (Brandon & Kaplan, 2008).

3.2.5 Determination of mechanical properties

3.2.5.1 Deflection test: Experimental deails

A materials testing machine, Model H25KS, Hounsfield Test Equipment Ltd. (Redhill, Surrey, United Kingdom (**Figure 3.6**) was used to determine the force by testing archwires deflection.

A selection of two orthodontic archwires, Rectangular β-Ti III orthodontic archwires (0.48×0.64 mm) and TIM orthodontic archwires (0.40×0.55 mm) were tested to compare their deflection ranges. The samples comprised uncoated and coated β-Ti III/TIM orthodontic archwires with 5, 10, 25 and 50 nm thicknesses of pure Zr.

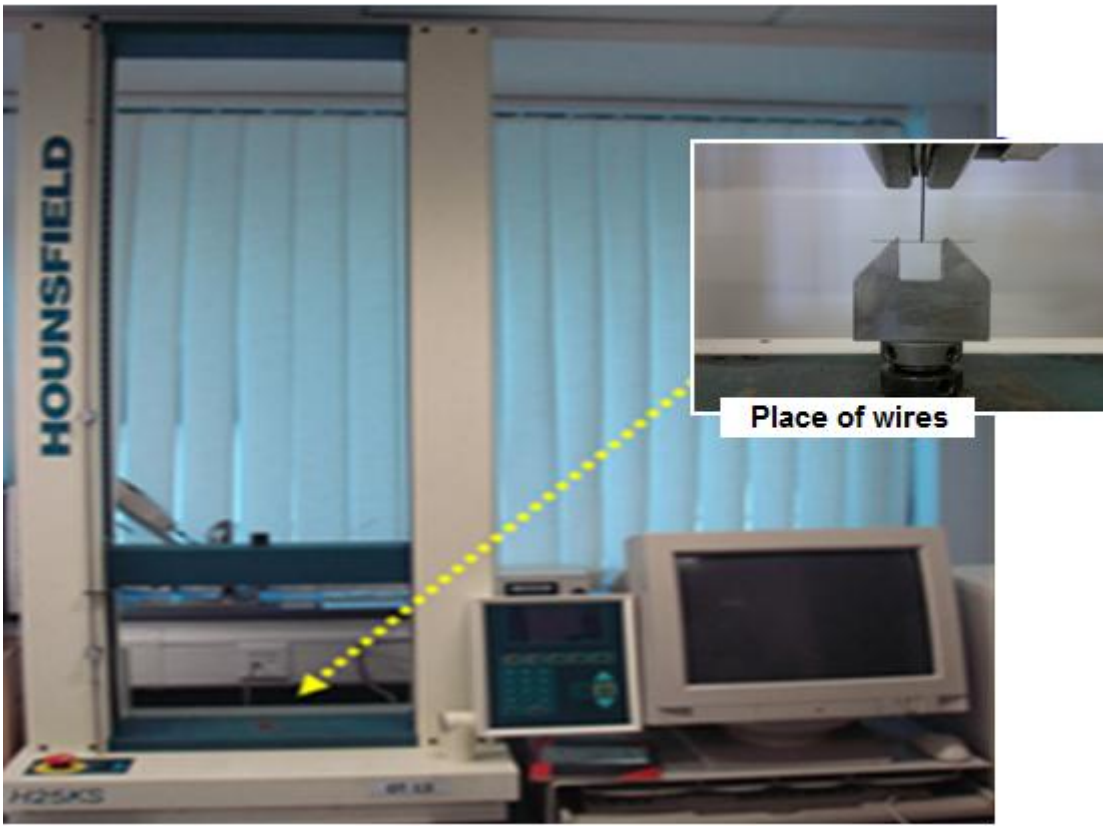

Figure 3.6: Hounsfield (Model H25KS, Redhill, England) machine used for determining load deflection characteristics for uncoated and coated β-Ti III/TIM orthodontic archwires with 5, 10, 25 and 50 nm thicknesses of pure Zr

3.2.5.1.1 Model designs

For the three-point bend design (**Figure 3.7**) the wire sample was held in slots with supports 10 mm apart and displaced at the midpoint. The wires were prepared as straight of lengths of 14 mm. A modified bending test was carried out on the wires with a Hounsfield test equipment testing machine fitted with a 5 kg and a deflecting rod tip formed from 1.6 mm diameter polished SS (**Figure 3.7**).

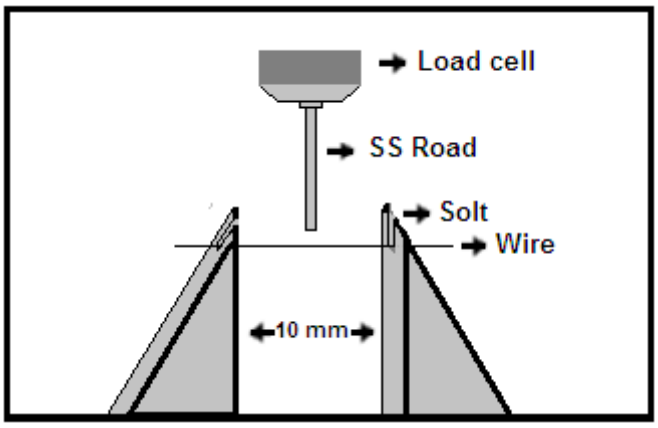

Figure 3.7: Schematic diagram showing Three-point bending apparatus for deflection test

3.2.5.1.2 Bending method

The wires were subjected to 3-point bending tests. A 5N load cell and the testing machine were operated at a crosshead speed of 2.0 mm per minute were used for the deflection tests to examine the 14 mm lengths of selected wires, its strength before and after Zr deposition treatment. The wires were positioned on the supports of the 3-point bending apparatus with a fixed span width of 10 mm. A mechanical load was applied on the centre of each wire at 90° to the wire axis, through a SS rod. By movement of the crosshead, at a speed of 0.2 mm/min, using a loading cell of 5 Kg, the load was increased in the curving until 2.0 mm of the wire of achieved.

Measurements of load deflection test are made using the computer program TexMAT® which measures the value-deflection curve. Load value measurements from the loading phase were measured digitally by selecting a deflection point as a plot on the computer screen. This point was chosen to represent a standardized portion of the unloading phase level in the load-deflection curve. The deflection points chosen were 1.0 mm less than the maximum deflection of each bend up to 2.0 mm. The force/activation curves were measured from the passive position to an activation of 2 mm. The load was applied in intervals of 0.2 mm, from 0 to 2.0 mm, during loading, to obtain representative load deflection characteristics for each wire.

CHAPTER FOUR

RESULTS AND DISCUSSION

4.1 Results

4.1.1 Introduction

Results of tests indicate that there are differences in the properties of the two commercial orthodontic archwires used in this study.

4.1.2 Deflection tests of β-Ti III archwires and TIM archwires

Deviations of deactivation forces of the wires measured at a deflection of 1 mm are shown (**Figures 4.1** and **4.2** and **Table 4.1**). Deactivation deflections of 1 mm were selected to establish a comparison parameter at the midpoint of the loading and deflection used in this study. Analysis of variance of activation forces showed significant differences between β-Ti III and TIM archwires with the same amount of activation (1 mm), TIM wires exhibited the lowest range of values, with forces of 164-176g. Uncoated β-Ti III archwires and those coated with 5 nm Zr had similar forces of 250g and coated archwires with 10 nm Zr had a force 254g. Archwires with 25 nm Zr coats had a force 257g and with 50 nm Zr coats had a force of 261g. TIM uncoated archwires had a force 164g and those coated with 5 nm Zr had a force of 170g. These coated with 10 nm Zr had a force 172g and with 25 nm Zr had a force 173g. Those with 50 nm Zr coats had a force of 176g.

Table 4.1: Results of deflection tests of various archwires: uncoated β-Ti III and timolium archwires and coated β-Ti III and TIM archwires with 5, 10, 25 and 50 nm Zr

Archwires	Deflection, 1 mm (deactivation force×g)	Deflection, 2 mm (deactivation force×g)
Uncoated β-Ti III	250	404
Coated β-Ti III with 5 nm Zr	250	407
Uoated β-Ti III with 10 nm Zr	254	409
Coated β-Ti IIIwith 25 nm Zr	257	412
Coated β-Ti III with 50 nm Zr	261	413
Uncoated TIM	164	291
Coated TIM with 5 nm Zr	170	293
Coated TIM with 10 nm Zr	172	295
Coated TIM with 25 nm Zr	173	298
Coated TIM with 50 nm Zr	176	301

4.1.3 Analysis of surface roughness (application of AFM)

Topographic irregularities were observed in all the archwires tested **Figures 4.3** and **4.4** show three-dimensional AFM topography images (5×5 nm) of all archwires analyzed. The surface morphologies of the archwires differed from one another, based on their composition. The three-dimension roughness parameter was used to quantitatively evaluate the surface topography of each archwire. There were significant differences between the different types of archwires (**Table 4.2**).

Table 4.2: Results of AFM measuremnents of surfaces roughness of various archwires: uncoated β-Ti archwire and β-Ti archwire coated with 5, 10, 25 and 50 nm Zr, uncoated TIM archwire and timolium archwire coated with 5 nm and 50 Zr

Archwires	Surface roughness (nm)
Uncoated β-Ti	35.5
Coated β-Ti III with 5 nm Zr	28.7
Coated β-Ti III with 10 nm Zr	27.3
Coated β-Ti III with 25 nm Zr	24.9
Coated β-Ti III with 50 nm Zr	20.3
Uncoated TIM	27.0
Coated TIM with 5 nm Zr	18.1
Coated TIM with 10 nm Zr	17.8
Coated TIM with 25 nm Zr	17.3
Coated TIM with 50 nm Zr	16.9

4.1.4 Surface morphology and elemental analysis (application of SEM)

Determination of the surface topography of the archwires using SEM photomicrographs showed that the uncoated β-Ti III archwires (**Figure 4.5 a**) had the highest surface roughness of all the tested archwires tested. β-Ti III archwires coated with 5, 10, 25 and 50 nm Zr had significantly reduced suface roughness (**Figures 4.6 b, c, d and e**). Uncoated β-Ti TIM archwires (**Figure 4.6 a**) had a surface roughness higher than coated β-Ti TIM archwires with 5, 10, 25 and 50 nm Zr (**Figure 4.7 b, c, d** and **c**).

The results of analysis using SEM and AFM showed that the TIM archwires exhibited less roughness than the β-Ti archwires. Deposition of 5,10, 25 and 50 nm Zr on both β-Ti III and TIM archwires led to reduced surface roughness of these archwires. Uncoated β-Ti III archwires showed the greatest surface roughness of the tested archwires which led the archwires undergoing stress making them more brittle.

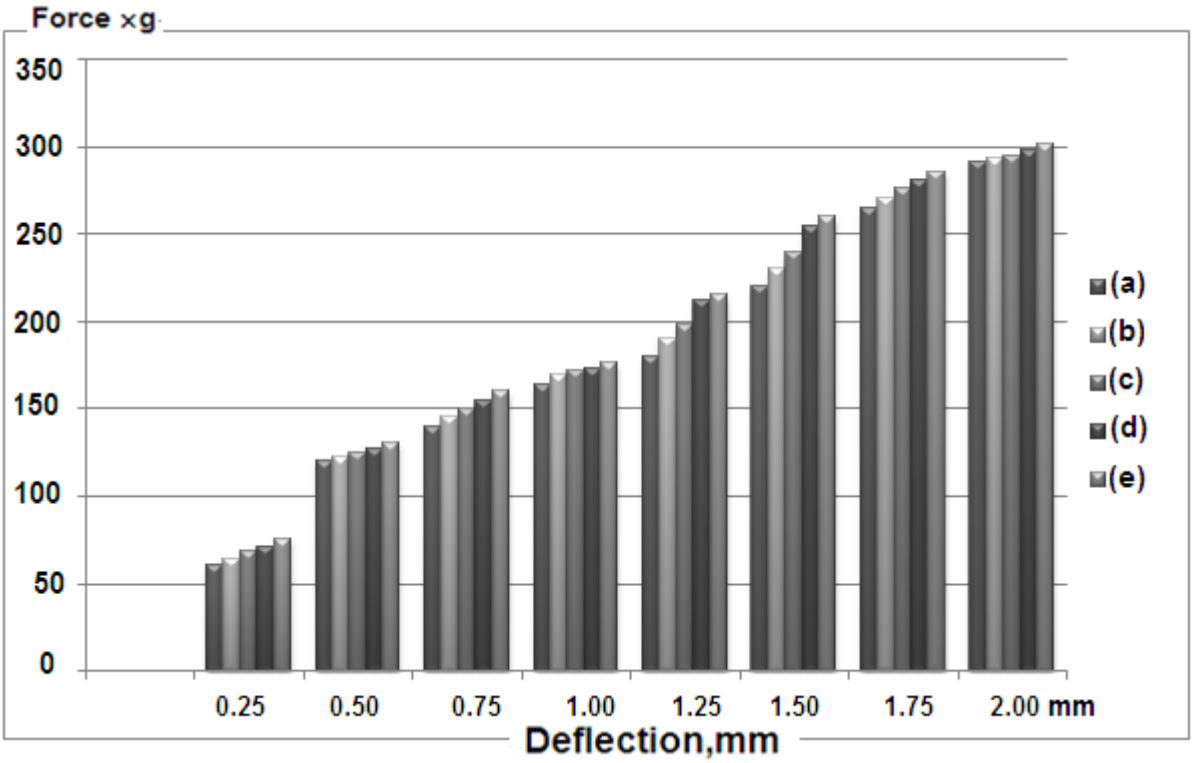

Figure 4.1: Load deflection graph for (a) Uncoated TIM archwire (b) Coated TIM archwire with 5 nm of Zr (c) Coated TIM archwire with10 nm of Zr (d) Coated TIM archwire with 25 nm of Zr (e) Coated TIM archwire with 50 nm of Zr

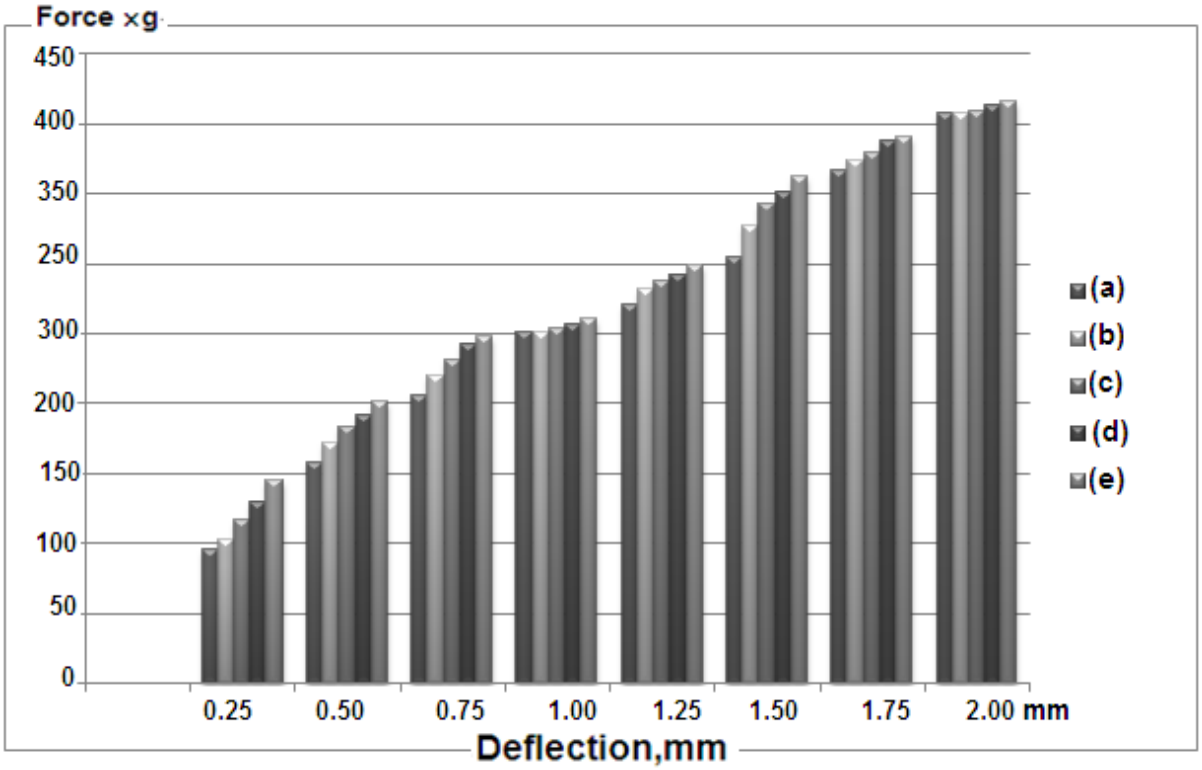

Figure 4.2: Load deflection graph for (a) Uncoated β-Ti archwire (b) Coated β-Ti III archwire with 5 nm of Zr (c) Coated β-Ti archwire with 10 nm of Zr (d) Coated β-Ti archwire with 25 nm of Zr (e) Coated β-Ti archwire with 50 nm of Zr

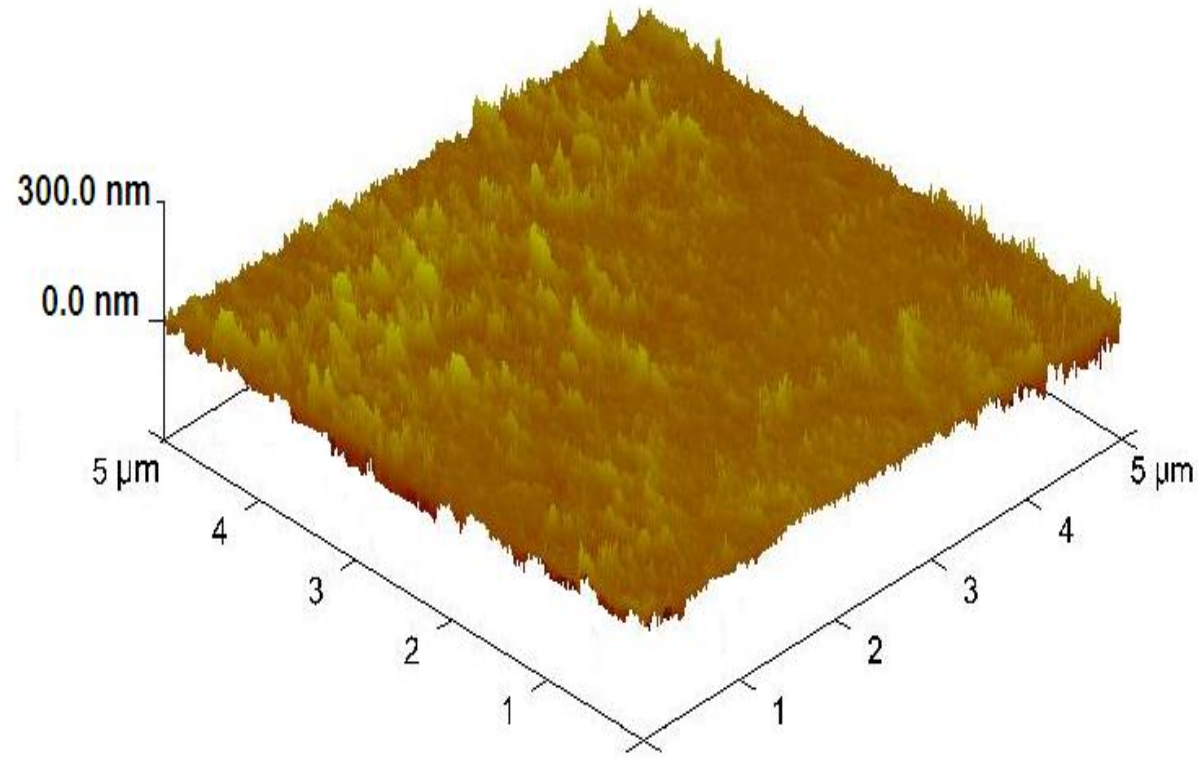

Figure 4.3: Results of AFM shown surfaces roughness (a) Uncoated β-Ti III archwire

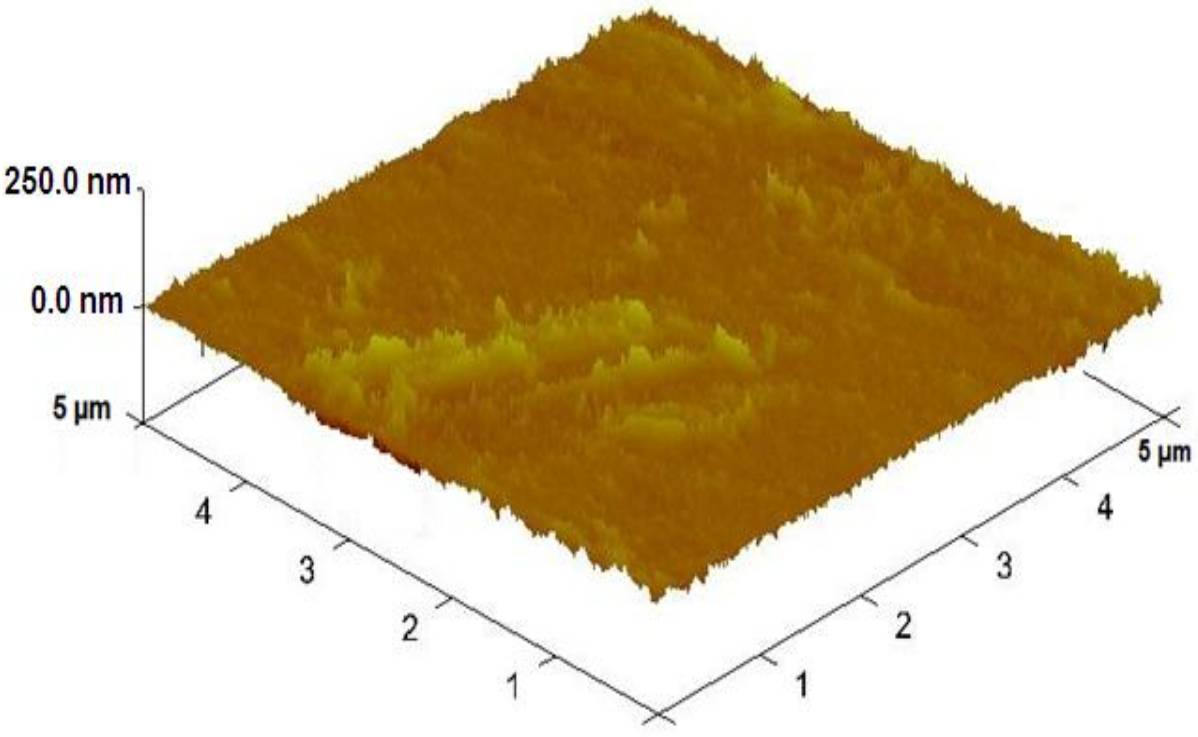

Figure 4.3: Results of AFM shown surfaces roughness (b) Coated β-Ti III archwire with 5 nm of Zr

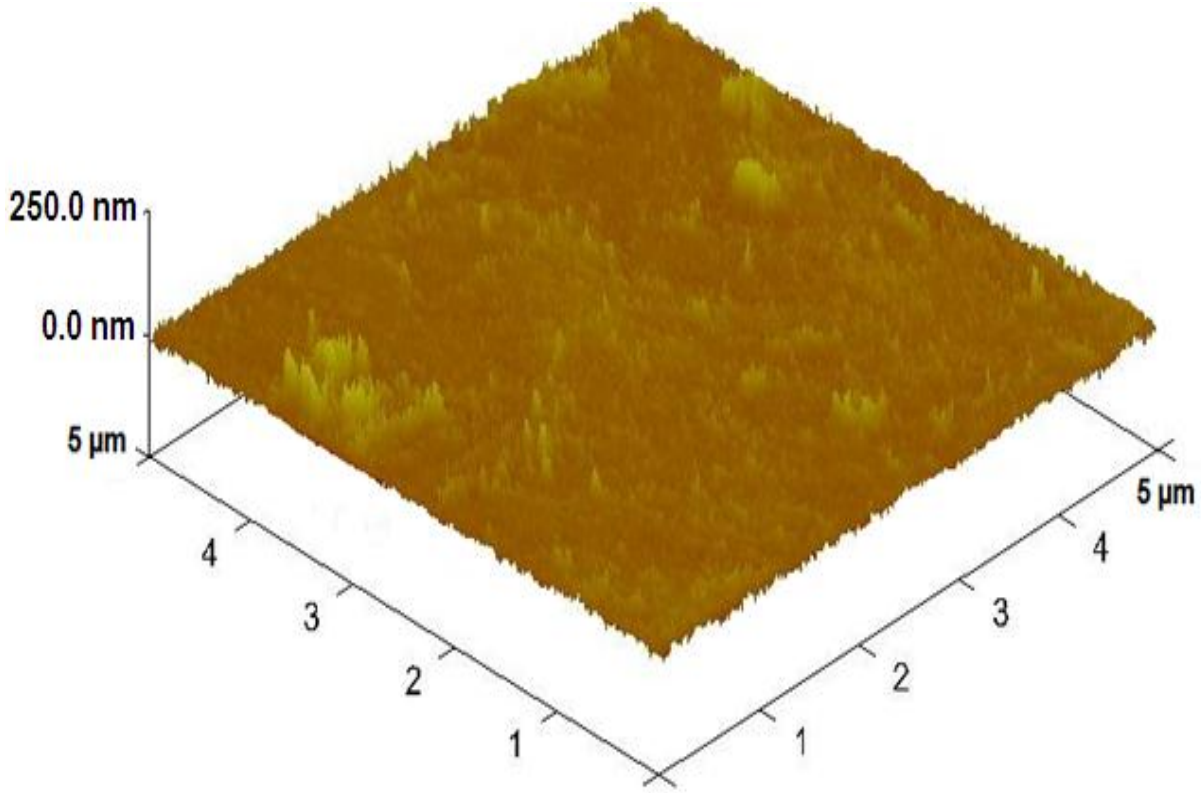

Figure 4.3: Results of AFM shown surfaces roughness of (c) Coated β-Ti III archwire with 10 nm of Zr

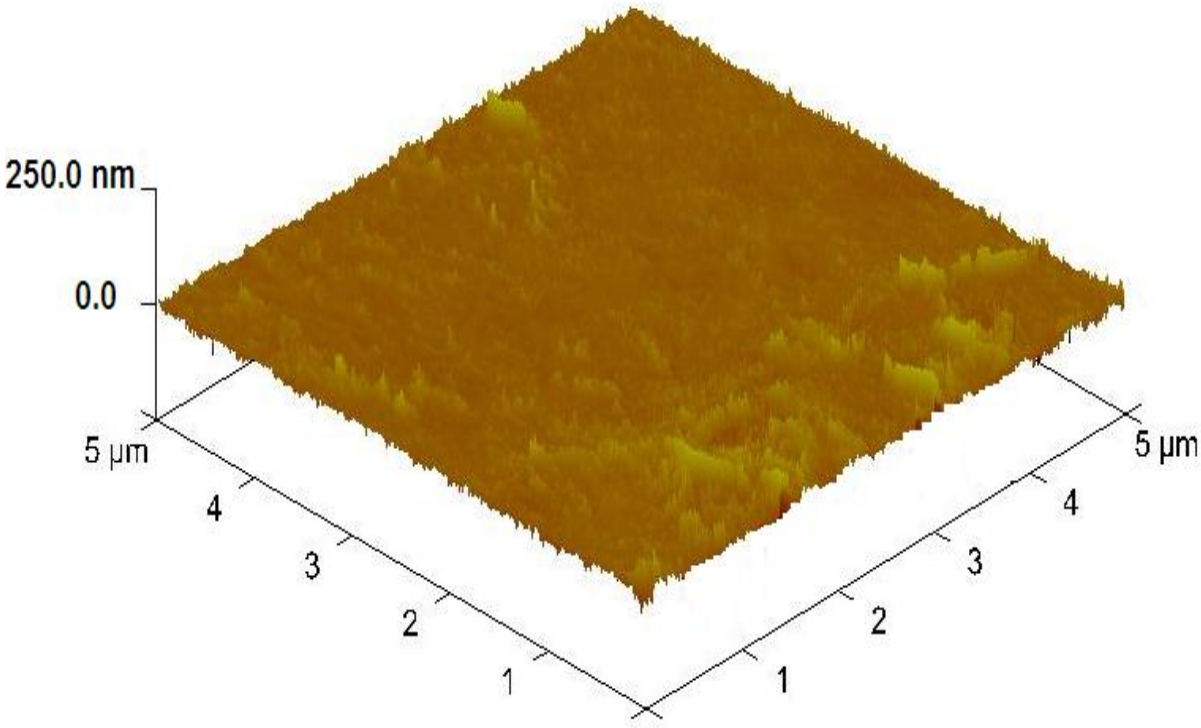

Figure 4.3: Results of AFM shown surfaces roughness (d) Coated β-Ti III archwire with 25 nm of Zr

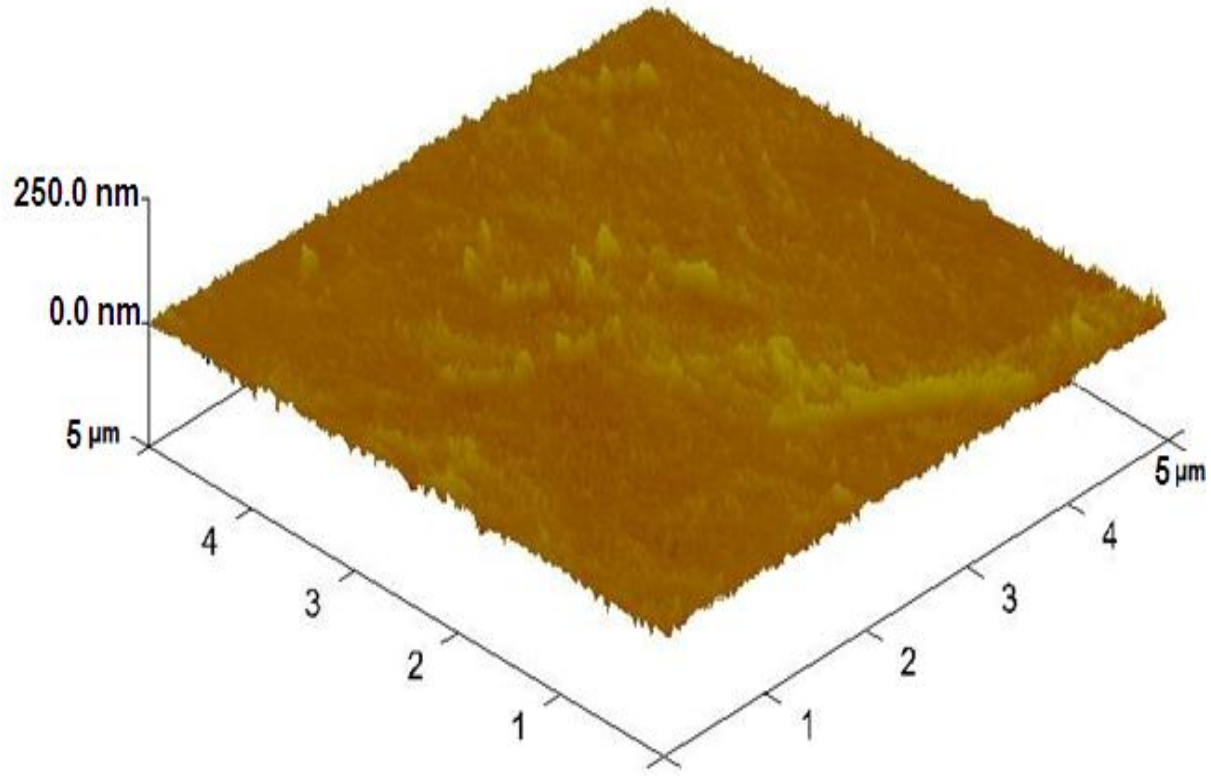

Figure 4.3: Results of AFM shown surfaces roughness of (e) Coated β-Ti III archwire with 50 nm of Zr

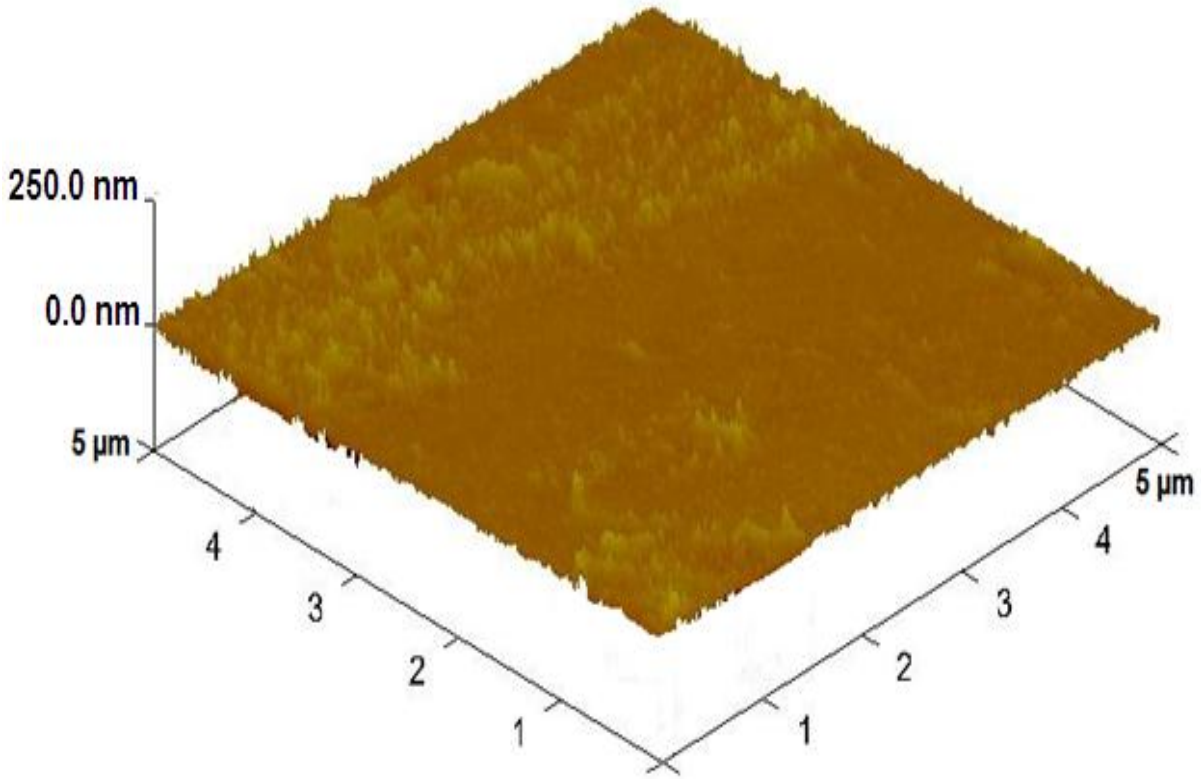

Figure 4.4: Results of AFM shown surfaces roughness of (a) Uncoated TIM archwire

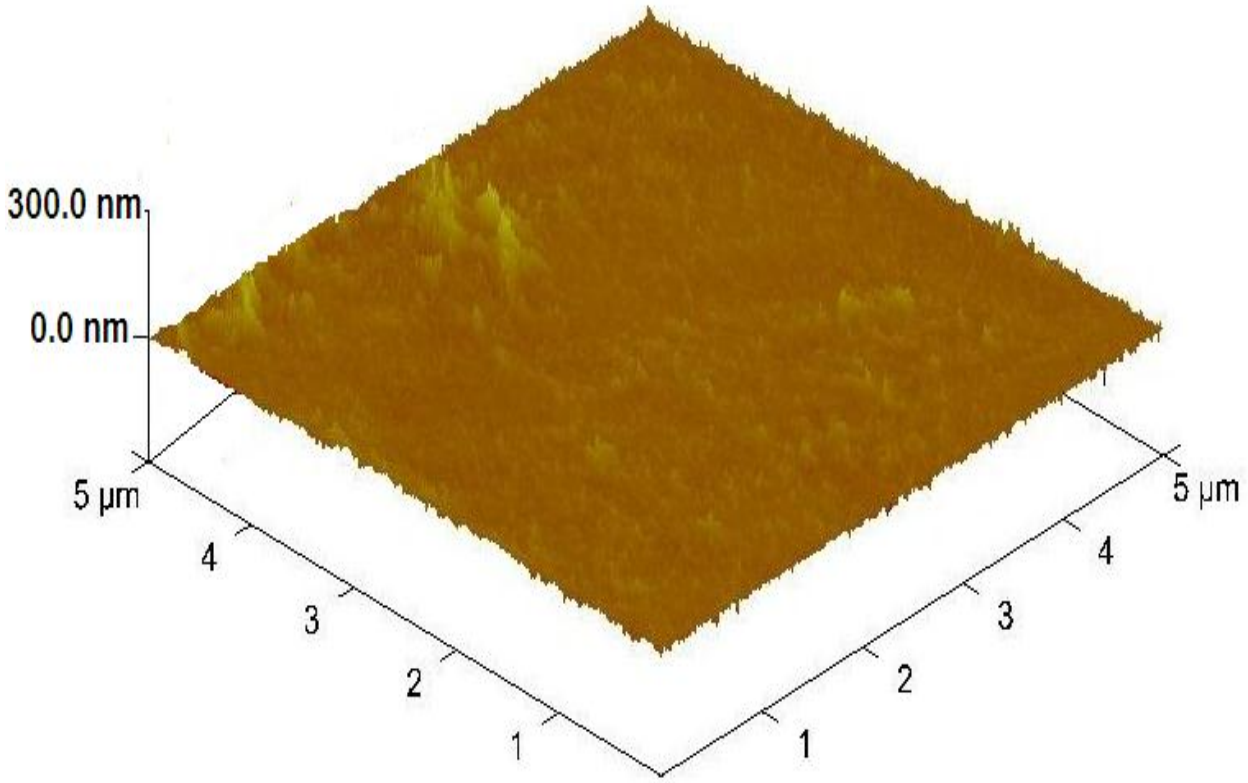

Figure 4.4: Results of AFM shown surfaces roughness of (b) Coated TIM archwire with 5 nm of Zr

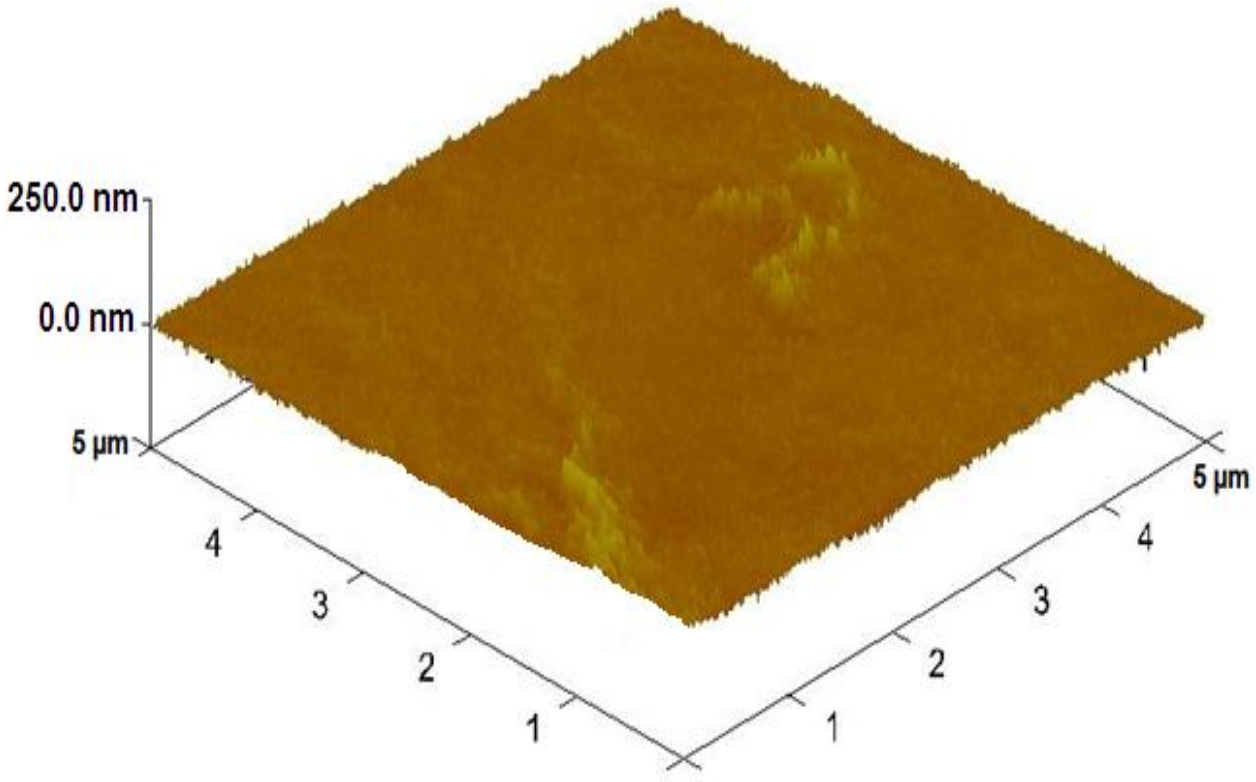

Figure 4.4: Results of AFM shown surfaces roughness of (c) Coated TIM archwire with 10 nm of Zr

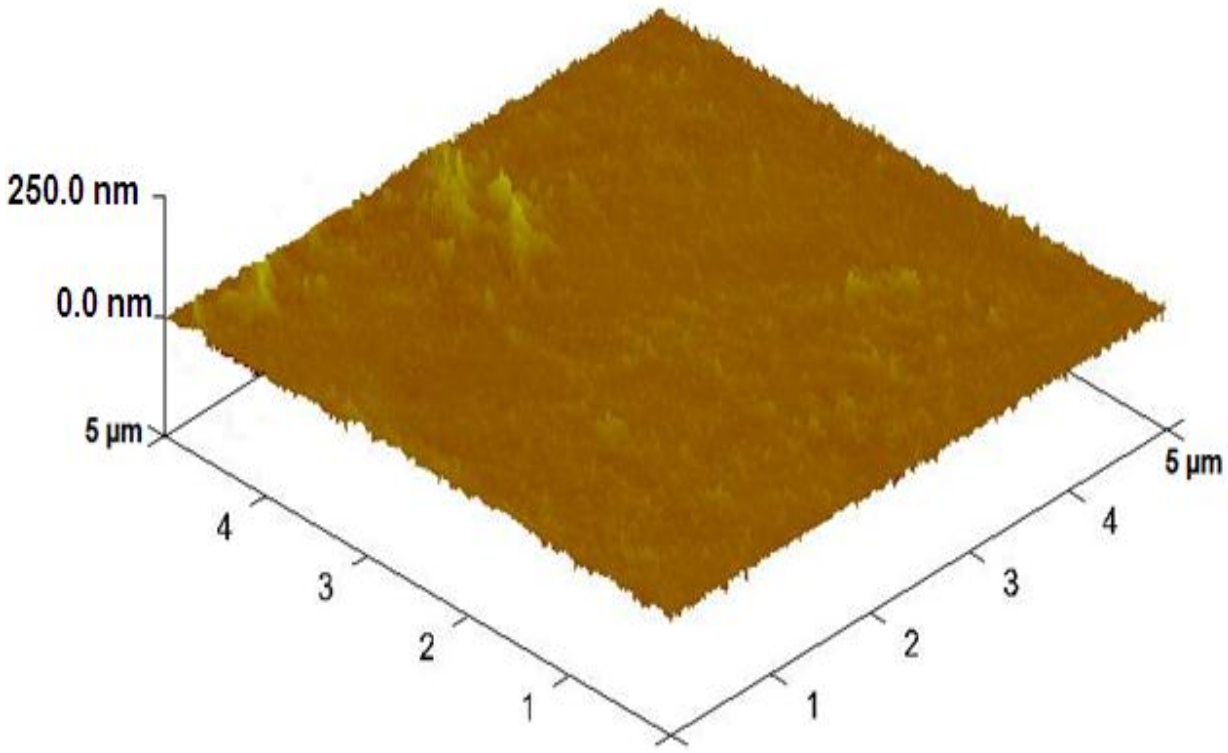

Figure 4.4: Results of AFM shown surfaces roughness of (d) Coated TIM archwire with 25 nm of Zr

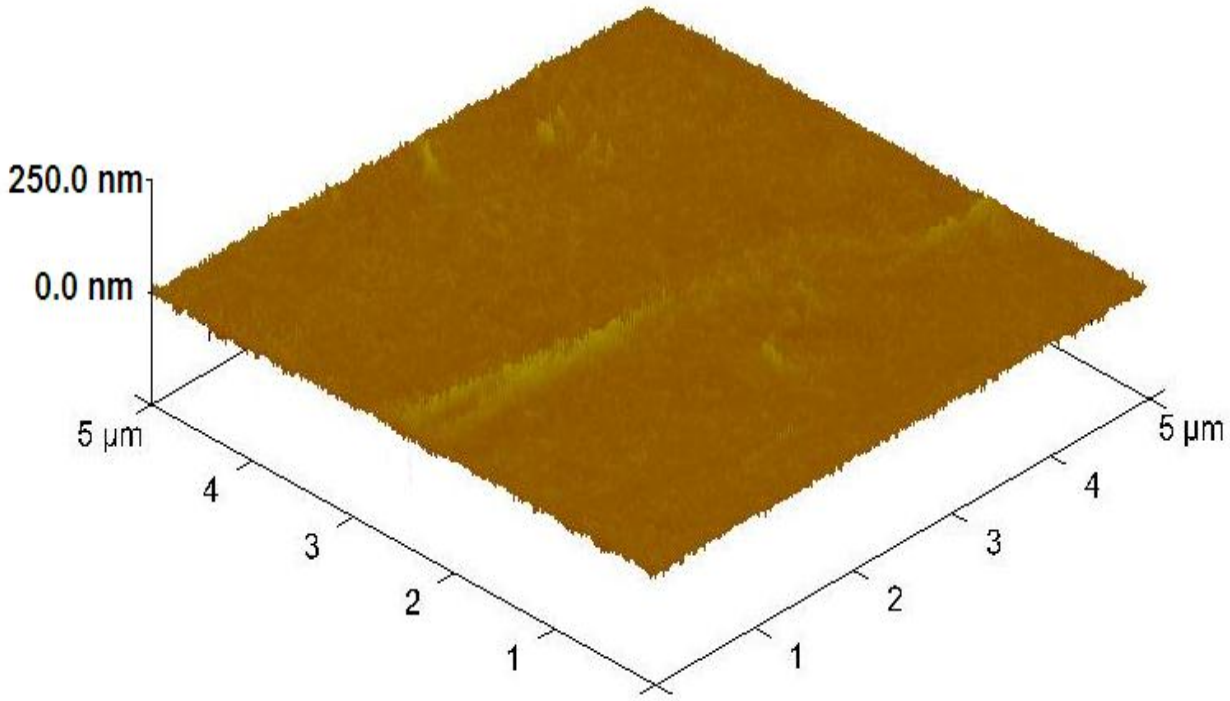

Figure 4.4: Results of AFM shown surfaces roughness of (e) Coated TIM archwire with 50 nm of Zr

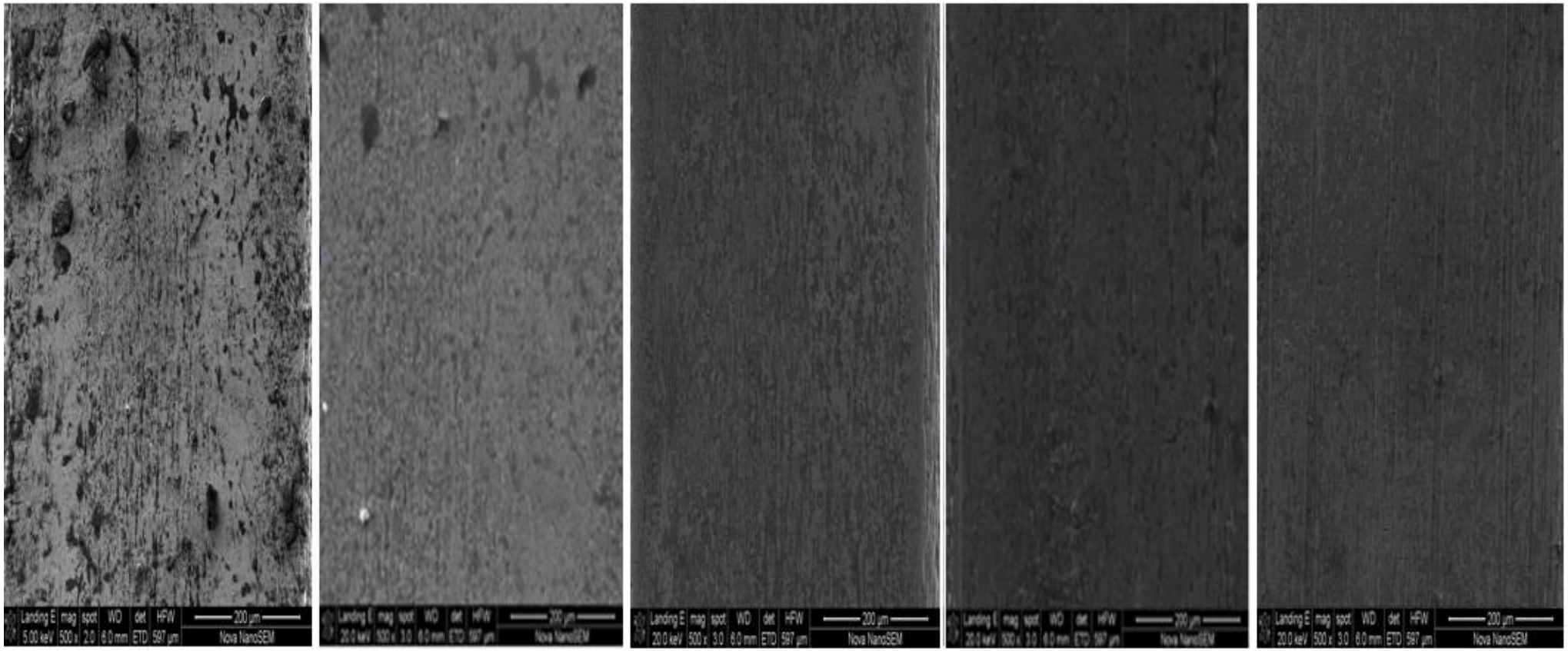

(a) (b) (c) (d) (e)

Figure 4.5: Surfaces analysis by SEM for (a) Uncoated β-Ti III archwire (b) Coated β-Ti III archwire with 5nm of Zr (c) Coated β-Ti III archwire with 10 nm of Zr (d)) Coated β-Ti III archwire with 25 nm of Zr (e)) Coated β-Ti III archwire with 50 nm of Zr at (500 ×) magnification

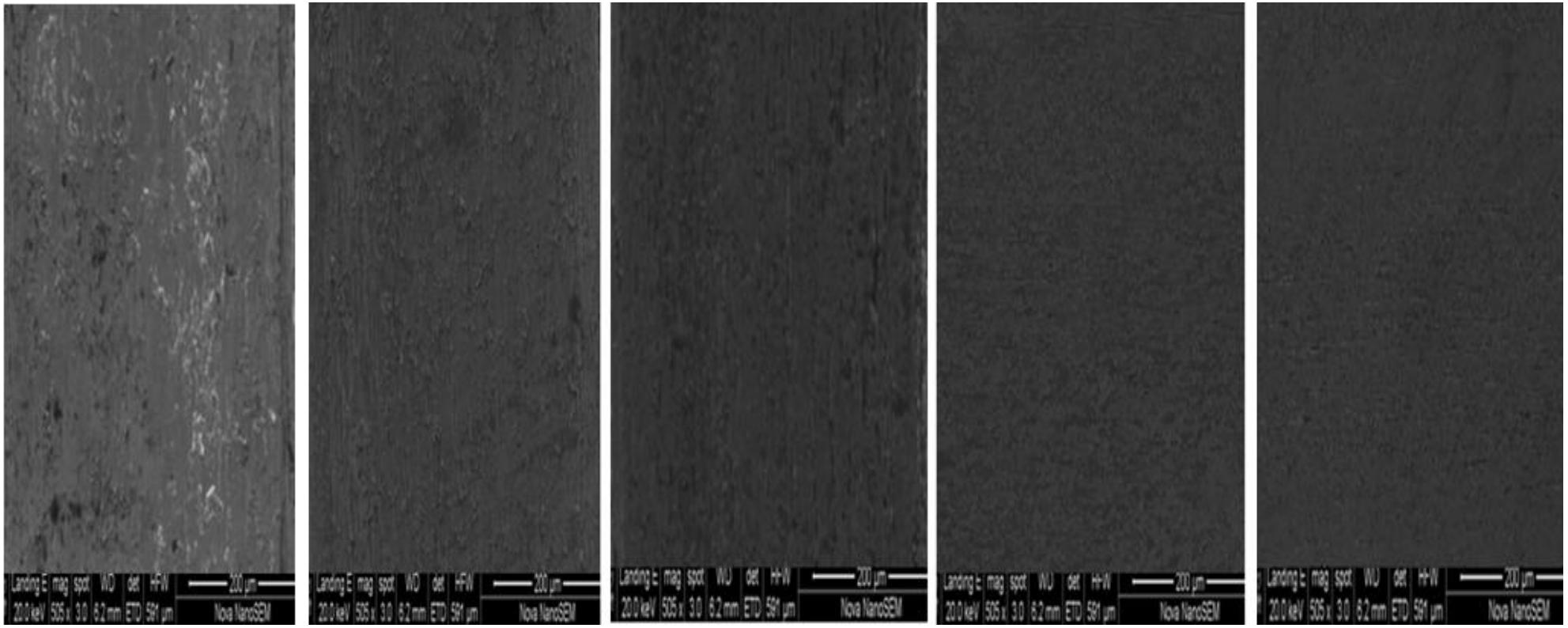

(a) (b) (c) (d) (e)

Figure 4.6: Surfaces analysis by SEM for (a) Uncoated TIM archwire (b) Coated β-Ti TIM archwire with 5nm of Zr (c) Coated TIM archwire with 10nm of Zr (d)) Coated TIM archwire with 25 nm of Zr (e) Coated TIM archwire with 50 nm of Zr at (500×) magnification

Elemental analysis results of β-Ti III orthodontic archwires are shown in **Figure 4.7** and composition analysis results of both uncoated β-Ti III / TIM archwires shown in **Table 4.2.**

Table 4.3: Composition analysis of uncoated β-Ti III / timolium archwires, determined by SEM

Archwire	Composition (wt.%)								Manufacturer
	Ti	Mo	Zr	Sn	Al	V	Mn	Cr	
β-Ti III	76.80	11.84	6.55	4.81	<0.05	<0.05	<0.05	<0.05	3M Unitek, Monrovia, USA
TIM	91.17	<0.05	<0.05	<0.05	5.73	3.10	<0.05	<0.05	TP Orthodontics, Lodi, USA

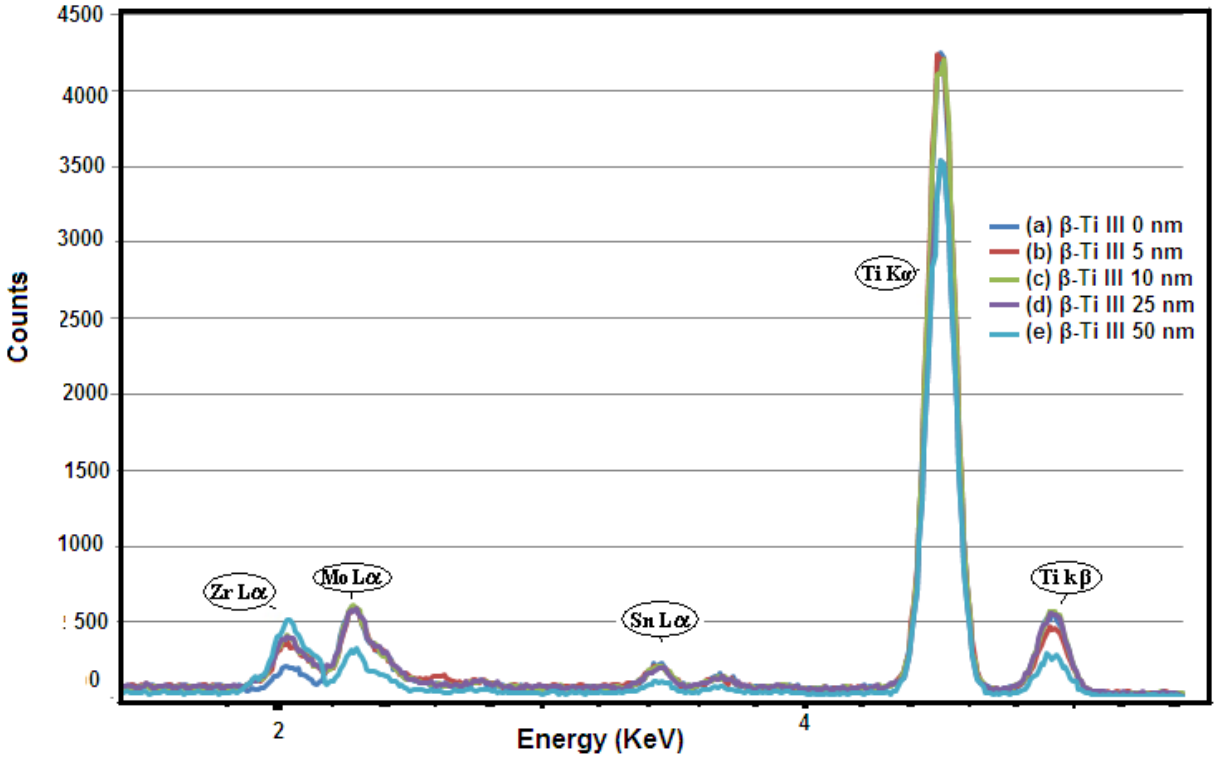

Figure 4.7: Elemental analysis by SEM of (a) uncoated β-Ti III archwire (b) coated β-Ti III archwire with 5 nm of Zr (c) coated β-Ti III archwire with 10 nm of Zr (d) coated β-Ti III archwire with 25 nm of Zr(e) coated β-Ti III archwire with 50 nm of Zr

The results of the elemental analysis by SEM of uncoated β-Ti III archwire and coated β-Ti III archwires with 5, 10, 25 and 50 nm of Zr are given in **Figure 4.7**. Coated β-Ti III archwires with 5, 10, 25 and 50 nm of Zr showed significant differences in height of rate of the Zr. β-Ti III archwires with 5, 10, 25 and 50 nm of Zr also showed significant differences in

declining of rate of Mo, Sn and Ti. The results of the elemental analysis by SEM of uncoated TIM archwire and coated TIM archwires with 5, 10, 25 and 50 nm of Zr are given in **Figure 4.8**. Coated TIM archwires with 5, 10, 25 and 50 nm of Zr showed significant differences in height of rate of the Zr and significant differences in declining of rate of Al, V and Ti. The coated and uncoated β-Ti III archwires had more Ti than TIM archwires and in addition Ti is contented Zr and Sn. Uncoated TIM archwire is contented TI, Al and V but did not content Zr. Coated TIM archwires are contented TI, Al, V and Zr.

Elemental analysis results of TIM orthodontic archwires are shown in **Figure 4.8:**

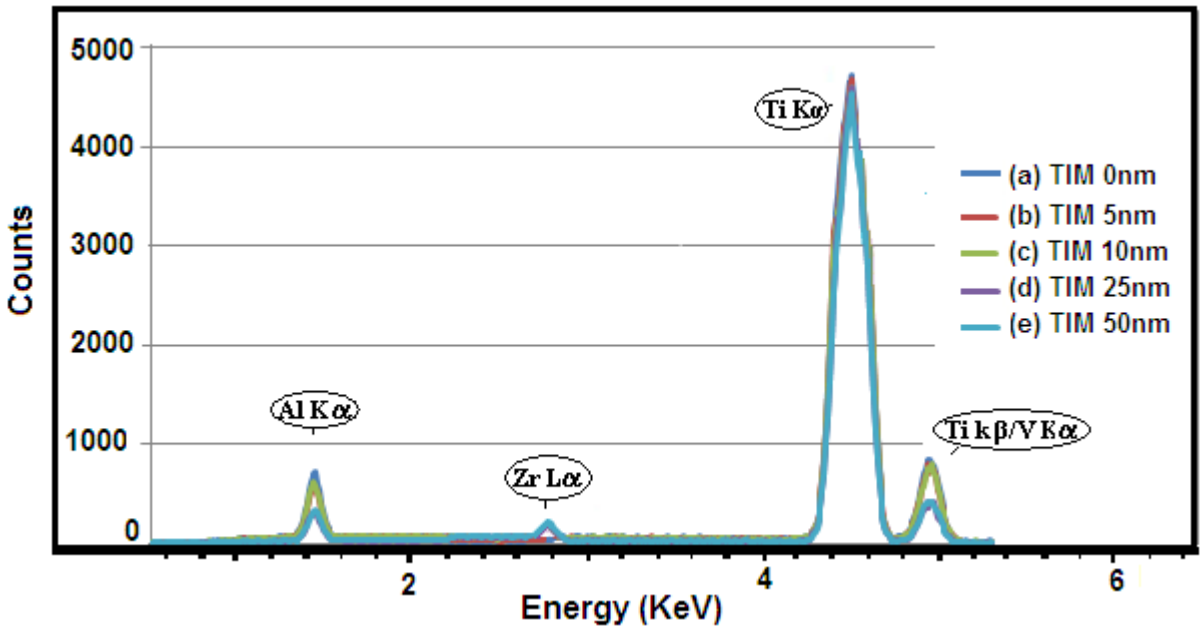

Figure 4.8: Elemental analysis by SEM of (a) uncoated TIM archwire (b) coated TIM archwire with 5 nm of Zr (c) coated TIM archwire with 10 nm of Zr (d) coated TIM archwire with 25 nm of Zr (e) coated TIM archwire with 50 nm of Zr

4.2 Discussion

The main aim of this study was to compare the performance of two orthodontic archwires namely, β-Ti and TIM archwires. Forthermore the study was designed to retain the strength of the archwires and improve condition of surface roughness.

In order to assess further the improvment of each archwire, it is recommended that three-point bend results are more reliable than four-point tests since the variances were lower. To ensure that a wire is tested within the range of its metallurgical properties, a deflection of no greater than 5% of span length is recommended. For the present study this would suggest a maximum deflection of 2 mm. However, in the mouth wire, deflections of between 2 and 4 mm are the norm and these values were therefore used in the present study.

Currently, a large variety of alloys is used to produce orthodontic archwires. Each type of archwire demonstrates certain properties which sometimes vary significantly between manufacturers. Different alloy properties combined with the variety in sizes and geometries and finishing of surface roughness make the selection of the proper archwire for a specific clinical case a demanding process. Knowledge of the mechanical and physical properties of archwires, which, to some extent, determine their clinical behaviour, is required to achieve a satisfactory and predictable outcome. Generally, as treatment progresses, archwires with gradually increasing stiffness, should be chosen. However, since the ideal archwire has not yet been discovered, each archwire may be an appropriate selection or not, depending on the treatment stage and the desired clinical result. The choice and sequence of archwires should neither be made irrationally nor be determined in advance for all patients. Instead, it should rely on current scientific evidence and the clinical requirements of each case.

Advances in the field of biomaterials have provided encouraging results with regard to the creation of aesthetic archwires with satisfactory properties. The performance of an archwire in sliding depends on the archwire material, cross-sectional geometry and surface roughness. Smaller archwires are chosen to ensure lower force at the initial stage of fixed appliance mechanotherapy but this results in inadequate control of tooth movement since there would be too much play between the archwire and the bracket.

The deposition of Zr on titanium-based archwires makes it possible to use larger archwires. Therefore, with β-Ti III and TIM, there would be less variation with the expected force delivery, thereby ensuring greater predictability of tooth movement.

Surface roughness influences friction more direct when dry, unlubricated sliding occurs. Very rough surfaces can cause considerable friction because of the contact between and interlocking of archwire and bracket. Frictional force is considered a major factor in

orthodontic mechanotherapy and studies have clearly shown that each force used for the retraction of a tooth must be higher than frictional forces. Frictional losses in orthodontic force are reported to be the lowest when TIM archwires are used. Inhomogeneous surfaces with different surface irregularities can be attributed to the manufacturing process. Therefore, the surface characteristics of the TIM archwires with deeper pits may be the result of their complex manufacturing processes and their proprietary surface treatments.

Surface roughness is the most important characteristic in the archwires. It is associated with the esthetics of dental products, as well as their corrosion behavior, biocompatibility and sliding movement. The extreme variability in the surface roughness of orthodontic β-Ti archwires suggests that some manufacturers do not pay sufficient attention to the quality of their products. This study showed that the surface roughness of two types of β-Ti archwires varied considerably, irrespective of the reputation of their brands.

It has shown from results in this study that the surface treatment of archwires does improve surface roughness towards enhance sliding of the bracket along the archwire. At best, the surface treatment can reduce the friction by 46% which is confirmed in the literature. Literature findings also confirm that the frictional properties of archwires were improved if a surface treatment was applied, for example, Teflon, polyethylene or ion implantation. The β-Ti archwires treated with ion implantation showed enhancment in the coefficient of friction, which supports findings in this study. These values only apply to new unused archwires. In contrast, in this study when the coated archwires were exposed to the artificial saliva to simulate the oral environment for a week, a normal interval for appointments in fixed appliance cases, the surface of coated archwires showed a high resistance to corrosion.

In the present study, topographic surface characteristics of orthodontic as-received archwires were evaluated by AFM. The AFM is considered a promising technique for the evaluation of surface qualities of dental materials, where the roughness of the material can affect the aesthetics of the appliance and the sliding mechanics caused by the influence of the coefficient of friction due to increased roughnesses of the archwires and bracket surfaces. However, this study has mainly focused on the mechanical properties of archwires. Since the determination of the roughness value depends on the measurement technique, the investigation protocol for surface roughness is important. Therefore, AFM is recommended for the quantitative analysis of surfaces with nano-scale irregularities. From the results of AFM measurements, coated β-Ti III archwires had more smooth surfaces than uncoated β-Ti III archwires of approximately 25 nm, whereas coated TIM archwires had more smooth surfaces than uncoated TIM archwires of approximately 17 nm. It seemed that although the uncoated β-Ti III archwires experienced higher frictional resistance than in the uncoated TIM

archwires experienced. Coated β-Ti III archwires and coated TIM archwires experienced showed significant decrease in surface roughness.

In this study the results showed that the least rough archwire was the TIM archwire. It has been demonstrated that TIM shows the lowest frictional coefficient and the lowest sliding resistance, when used in passive configuration because of its combination of low roughness, high hardness and high strength. The β-Ti III archwires were the roughest, which could be associated with the great friction generated by this material. Application of deposition of Zr on archwires should decrease the surface roughness of the materials and should improve the sliding of the archwire.

Application of ion implantation on orthodontic archwires decreased archwire strength, increased archwire hardness, reduced flexibility and improved surface finish. To obtain the maximum reduction on frictional force, ion implantation should be used on brackets and on archwires repeatedly, because it effected the archwire strength.

An important factor that influences the surface topography of orthodontic archwires is, therefore, the production technique. This hypothesis is confirmed by the fact that the roughness measured for various products from the same batch was homogeneous. Opposite opinions exist about the influence of surface quality of archwires and bracket slots on the production of friction. Frictional force between archwires and brackets is considered a harmful factor that influences the normal movement of the teeth during sliding mechanics.

Among the selected alloys, β-Ti III generally exhibits maximum frictional force, probably as a result of the high reactivity of the archwire's surface. The TIM archwire, on the other hand, creates lower friction than do the β-Ti III archwires. In fact, its force improves the performance of the archwire. The manufacturers of orthodontic archwires generally do not find the exact composition and manufacturing process of the archwires. The speed of tooth movement depends on several factors, including the surface quality of the archwire.

The surface roughness of orthodontic archwires may be measured using several methods, including AFM and SEM. The results of archwires showed an inhomogeneous surface with different patterns of surface irregularities, which may be attributable to the manufacturing process. The surface structure of archwires depends on the complex manufacturing processes, the surface finish treatments and the alloy used.

In this study, SEM showed differences in the patterns of irregularities on the β-Ti III archwires and TIM archwires produced by the different manufacturers. However, the patterns observed on the β-Ti III archwires and TIM made in USA were different to each other, with deep scratches parallel to the long axis of the archwires. In contrast, the β-Ti III archwire lacked

such clear horizontal and vertical grooves and had shallow dimples. A point of consideration in this regard is that the high magnification of SEM limited the investigation and interpretation of the surface roughness of a smaller area of the archwires. SEM showed that the elemental composition of the uncoated β-Ti III archwires was similar to that of the coated β-Ti III archwires with Zr and elemental composition of the uncoated TIM archwires was similar to that of the coated TIM archwires with Zr.

SEM micrographs obtained in this study showed more porosities, scratches and defects on the β-Ti III archwires than on the TIM archwires and the difference was significant. Although results in this study indicate the overall superior smoothness of the TIM archwires, the difference observed in this study was statistically significant. This can be attributed to the increase in the differences between the surface roughness of β-Ti III archwires wires and TIM archwires because of the very high variation observed between the different samples of the different types of β-Ti archwire. This study showed that the TIM archwires was smoother than β-Ti archwires.

Although β-Ti III and TIM were expected to appear quite similar, the α-β alloy (TIM) was distinct from the β-Ti III archwires because there were layers or sheets of drawn-out material with visible steps or fissures. The SEM analyses confirmed the compositions of coated β-Ti III archwires: Ti (78.24%-78.03%), Mo (11.89%-11.09%), Zr (5.28%-5.57%) and Sn (4.56%-43.0%). This favorably compares with the β-III alloy having a composition of 78% Ti, 11.5% Mo, 6.0% Zr and 4.5% Sn, but without substantial amounts of α-formers (for example, Al) or β-eutectoid formers (for example, Cr). The Material Safety Data Sheet from one of the suppliers (Ultimate Archwire forms) confirms these ranges of composition: Ti (70%-80%), Mo (10%-20%), Zr (5%-10%) and Sn (4%-8%).

In contrast, the TIM archwire, contained Ti (91.87%-90.65%), Al (5.68%-5.41%), V (3.45%-2.91%) and Zr (0.64%-1.03%). This confirms that this product was a mixture of α and β phases. Absent was Mo, which is essential to stabilise a β phase. Also absent were sufficient quantities of the strengthening elements, Zr and Sn, which are present in the β-Ti III alloys. The space closure mechanics in orthodontic treatment can be carried out either as frictional or sliding mechanics. The archwires used in frictional mechanics should be able to slide through the brackets easily and should exhibit low load deflection properties for optimal force application. The newly developed PVD coated archwires were significant in its corrosion resistance against saliva attack, showing low load deflection characteristics upon three-point bending test and were biocompatible upon cytotoxic evaluation. The coating process of 5, 10, 25 and 50 nm of Zr crossed the melting range of the beta titanium alloy and was found to affect the mechanical properties of the archwires, in order to be clinically applicable.

These orthodontic archwires were consistently showing lower load deflection characteristics than its uncoated forms, which was statistically significant. This might be the result of change in its load deflection properties while coating is performed over archwire blanks. However, orthodontic archwires deflection involves complex deflection processes with high chances of archwire fracture due to incorporation of stress-generating areas. Both coated archwires withstood the load deflection rates exhibited were also comparable with each other.

Increasing the vertical or horizontal dimension of the archwire increases its length incorporated into the archwire, which lowers the load deflection rate, assisted the application of low as well as consistent orthodontic forces. At the same time, archwire should be stiff enough for the stabilization of arches preventing untoward tooth movements. The load deflection rate evaluation with coated archwires showed high force application. Both β-Ti III and TIM coated archwires exhibited low load deflection characteristics in comparison with uncoated forms, making them ideal for space closure during frictionless mechanics. A low load/deflection ratio of both β-Ti III and TIM orthodontic coated archwires provide desirable force and good control of force magnitude. The fact that β-Ti III archwires possess those characteristics, among others, has made their use almost general.

Deposition of films of Zr, 5,10, 25 and 50 nm thick, on β-Ti orthodontic archwires using EB-PVD should lead to a decrease in the surface roughness of the archwires and improve the sliding between orthodontic archwires and brackets with no effect on the archwires strength.

AFM and SEM were considered a promising technique for the evaluation of surface qualities of dental materials. In the present study, topographic surface roughness of uncoated β-Ti III archwires and coated β-Ti III archwires with 5, 10, 25 and 50 nm Zr and uncoated TIM archwire and coated β-Ti TIM archwires with 5, 10, 25 and 50 nm Zr were evaluated by AFM and SEM. AFM results showed that the coated β-Ti III and TIM archwires had less surface roughness than the uncoated β-Ti III and TIM archwires. It has been demonstrated that deposition of 5, 10, 25 and 50 nm of Zr on both β-Ti III and TIM archwires resulted in the reduction of the surface roughness of these archwires.

Results of load deflection tests of 1 mm showed similar forces for both uncoated β-Ti III archwires and those coated with 5 nm Zr was 250g. The value for β-Ti III archwires coated with 10, 25 and 50 nm Zr, was up to 261g. Therefore the deposition of 5 nm Zr on β-Ti III archwires have not exhibited reduction in a archwires strength while deposit of 10, 25 and 50 nm Zr have exhibited increases in archwires deflection force. β-Ti III archwires contain strong elements such as Mo and Zr and deposition of 5, 10, 25 and 50 nm Zr contributed to improve the deflection force for these archwires.

Results of load deflection tests of 1mm showed that for uncoated β-Ti TIM archwires was 164g. These coated with 5nm Zr the load was 170g; with 10nm Zr the load was 172g; 25nm Zr 173g and 50 nm Zr, 176g. The value for coated β-Ti III archwires coated with 5, 10, 25 and 50 nm Zr was up to 176g. It can be concluded that the deposition of Zr on β-Ti TIM archwires improves the archwire deflection force. The β-Ti TIM archwires do not contain elements such as Mo and Zr and contain insufficient elements of V. These elements are considered strengthening the archwires. Deposition of Zr on TIM archwires improved their deflection force.

The newly developed Zr PVD coated β-Ti orthodontic archwires might be useful during the space closure stage of orthodontic mechanics, be it sliding or frictionless mechanics. Values of surface roughness of uncoated β-Ti III archwires indicate greater surface roughness compared with the coated β-Ti III archwires. The finding appeared to be consistent with those from the SEM and AFM analysis. After deflection tests with dead weights of 500g was done, the least force was observed with TIM archwires. β-Ti III archwires can be considered superior to TIM archwires but inferior to TIM archwires coated with 5, 10, 25 and 50 nm Zr. Clinically, this means that the net force required for transfer of movement will be lower for β-Ti III archwires and higher for TIM archwires. Surface evaluation of an archwire alloy is important because of its influence on the working characteristics.

SEM analysis of surface characteristics revealed a smooth surface with little surface irregularity for uncoated TIM archwires. Coated β-Ti TIM, coated with 5 nm Zr had a smooth surface with small concentration of mixed titanium and carbon which may be attributed to interaction inside the EB-PVD chamber. Coated TIM with 50 nm Zr showed the smoothest surface in all tested archwires. Uncoated β-Ti III archwires exhibited oriented cracks, vertical wire drawing lines and a very rough surface. It also clearly showed that the treatment with a 5 nm Zr coating on β-Ti III archwires improved their quality of surface roughness. Also observed was the improvement on the surface roughness of coated β-Ti archwires with 5, 10, 25 and 50 nm. Elemental analysis of β-Ti III archwires using SEM revealed titanium as the major constituent of the archwires, for all coated and uncoated β-Ti III archwires.

CHAPTER FIVE

CONCLUSIONS AND RECOMMENDATIONS

5.1 Conclusions

The main objective of this study was to improve the strength and surface roughness of the β-Ti archwires. Zirconium films was successfully deposited on the 0.43×0.64 mm β-Ti III and 0.040×0.64 mm TIM orthodontic archwires by EB-PVD, with a relatively smooth surface morphology and good strength.

This laboratory study showed that there are significant differences in the force that exist during deactivation among of the two types of coated and uncoated β-Ti archwires tested.

Deposition of Zr, thicknesses 5, 10, 25 and 50 nm, on 0.43×0.64 mm β-Ti III and 0.040×0.64 mm TIM orthodontic archwires significantly decreased the surface roughness. Surface roughness was much better than the corresponding uncoated wires, for both β-Ti archwires tested.

There was extensive variability in the surface roughness of the tested archwires: treated β-Ti III and TIM archwires were the least rough. The EB-PVD technique was useful for β-Ti archwires. Both β-Ti III and TIM orthodontic archwires exhibited qualitative surface topography changes following the deposition of 5, 10,25 and 50 nm Zr.

After deposition of 5, 10, 25 and 50 nm Zr, the β-Ti III orthodontic archwires exhibited significant similar force in load deflection tests and improve the force in β-Ti TIM orthodontic archwires. These the improvements may be clinically relevant to teeth movement.

Clinically, the use of coated β-Ti III and TIM orthodontic archwires with 5, 10, 25 and 50 nm Zr can be a factor in achieving reduced orthodontic treatment times.

This study revealed that β-Ti III and TIM archwires showed differ significantly in terms of their surface roughness. Further, the β-Ti III wire made by 3M Unitek, Monrovia, USA and the TIM archwires made by TP Orthodontics, Lodi, USA showed the greatest number porosities and defects. The findings in this study indicate that manufacturers need to pay more attention to reducing the surface roughness of their products in order to improve the surface roughness and quality of orthodontic treatment.

In conclusion, this investigation demonstrated the potential use of an AFM for the study of surface properties of orthodontic materials. In particular, the AFM has advantages, such as the production of topographical three-dimensional images in space. The samples do not

need any special treatment, such as metallization and the AFM can provide quantitative values for the investigated parameters. The most important AFM drawback is the small scan size, which, in association with the slow velocity of scanning, often impedes a complete analysis of the sample. Therefore, there might be some unselected regions with surface defects and thus with much larger roughness, that would be of clinical importance.

The composition of β-Ti III and TIM archwires were different, with TIM archwires having less Zr but more Ti. This could be a reason for the decreased stiffness when compared with β-Ti III archwires. TIM arc.hwires coated with 50 nm Zr had the smoothest surface in all tested archwires. The surface roughness levels showed an increased value for β-Ti III archwires compared with TIM archwires.

5.2 Recommendations for future research

The use of β-Ti III and TIM archwires coated with 5, 10, 25 and 50 nm Zr is recommended for use on all orthodontic archwires where significant developments in force and surface roughness These treated archwires may be more suitable in any stage of orthodontic treatment that needs bends or loops, or drawing the posterior teeth (molars), where these archwires had enough a strength and a smoothness as well.

Recommending depositing different thicknesses of pure Zr, by EB-PVD, on other orthodontic archwires, such as Ti- Ni archwires, SS or Cr-Co archwires might be effective to further improve their surface roughness and strength.

Future work should also include investigations deposition of different thicknesses of pure Zr by other techniques.

REFERENCES

Alavi, S. & Sinaee, N. 2013. Effect of dry heat and steam sterilization on load defl ection characteristics of β-titanium wires: An in vitro study. *Dental Research Journal*, vol. 9 (5), pp. 541-548.

Albrektsson, T., Zarb, G., Worthington, P., & Eriksson, A. R. 1986. The long-term efficacy of currently used dental implants: a review and proposed criteria of success. *Intentional Journal Oral Maxillofacial Implants*, vol. 1 (1), pp. 11-25.

Al-Waheidi, E. M. 1995. Allergic reaction to nickel orthodontic wires: a case report. *Quintessence International,* vol. 26 (6), pp. 385-387.

Amini, F., Rakhshan, V., Pousti, M., Rahimi, H., Shariati, M. & Aghamohamadi, B. 2012. Variations in surface roughness of seven orthodontic archwires: an SEM-profilometry study. *The Korean Journal of Orthodontics*, vol. 42 (3), pp. 129-137.

Anandkumar, B., & Maruthamuthu, S. 2008. Molecular identification and corrosion behaviour of manganese oxidizers on orthodontic wires. *Current Science Bangalore*, vol. 94 (7), pp. 891-896.

Andreasen, G. F., & Hilleman, T. B. 1971. An evaluation of 55 cobalt substituted Nitinol wire for use in orthodontics. *The Journal of the American Dental Association*,vol 82 (6), pp. 1373-1375.

Angolkar, P.V., Kapila, S., Duncanson , M. & Nanda, R. 1990. Evaluation of friction between ceramic brackets and orthodontic wires of four alloys. *American Journal of Orthodontics and Dentofacial Orthopaedics,* vol. 98 (6), pp. 499-506.

Ankem, S. & Greene, C. 1999. Recent developments in microstructure/property relationships of beta titanium alloys. *Materials Science and Engineering*: A, vol. 263 (2), pp. 127-131.

Arango, S., Peláez-Vargas, A. & García, C. 2012. Coating and surface treatments on orthodontic metallic materials. *Coatings*, vol. 3 (1), pp. 1-15.

Bania, P. J. 1994. Beta titanium alloys and their role in the titanium industry. Journal of Operations Management, vol. 46 (7), pp. 16-19.

Barrett, R.D., Bishara, S.E. & Quinn, J.K. 1993. Biodegradation of orthodontic appliances. Part I. Biodegradation of nickel and chromium in vitro. *American Journal of Orthodontics and Dentofacial Orthopaedics*, vol. 103 (1), pp. 8-14.

Binnig, G., Quate, C.F. & Gerber, C. 1986. Atomic force microscope. *Physical Review Letters*, vol. 56 (9), pp. 930-933.

Bogner, A., Jouneau, P.H., Thollet, G., Basset, D. & Gauthier, C. 2007. A history of scanning electron microscopy developments: towards “wet-STEM” imaging. *Micron*, vol. 38 (4), pp. 390-401.

Borges, C., Magne, P., Pfender, E. & Heberlein, J. 1999. Dental diamond burs made with a new technology. *The Journal of Prosthetic Dentistry*, vol. 82 (1), pp. 73-79.

Bourauel, C., Fries, T., Drescher, D. & Plietsch, R. 1998. Surface roughness of orthodontic wires via atomic force microscope, laser specular reflectance and profilometry. *The European Journal of Orthodontics*, vol. 20 (1), pp. 79-92.

Braga, P.C. & Ricci, D. 2004. Atomic force microscopy: biomedical methods and applications. Humana Press, New Jersey. ISBN: 1-58829-094-8.

Brandon, D. & Kaplan, W.D. 2008. Microstructural characterization of materials. 2nd Edition. Wiley, London. ISBN: 978-0-470-02785-1.

Brantley, W.A. & Eliades, T. 2000. Orthodontic materials: scientific and clinical aspects. 1st Edition. George Thieme Verlag, Stuttgant. ISBN: 978-0865779297.

Burrow, S. J. 2009. Friction and resistance to sliding in orthodontics: a critical review. *American Journal of Orthodontics and Dentofacial Orthopedics*, 135 (4), pp. 442-447.

Burstone, C. J., & Goldberg, A. J. 1980. Orthodontic appliance of titanium alloy. USA Patent No. 4,197,643.

Burstone, C.J. & Goldberg, A.J. 1980. Beta titanium: a new orthodontic alloy. *American Journal of Orthodontics*, vol. 77 (2), pp. 121-132.

Burstone, C.J. 1981. Variable-modulus orthodontics. *American Journal of Orthodontics*, vol. 80 (1), pp. 1-16.

Burstone, C.J. & Farzin-Nia, F. 1995. Production of low-friction and colored TMA by ion implantation. *Journal of Clinical Orthodontics*, vol. 29 (7), pp. 453-461.

Cacciafesta, V., Sfondrini, M.F., Scribante, A., Klersy, C. & Auricchio, F. 2003. Evaluation of friction of conventional and metal-insert ceramic brackets in various bracket-archwire combinations. *American Journal of Orthodontics and Dentofacial Orthopedics*, vol. 124 (4), pp. 395-408.

Campbell, F. C. 2008. Elements of metallurgy and engineering alloys. International serves materials professionals. Ohio, USA. ISBN: 978-0871708670.

Cao, G. & Wang, Y. 2004. Nanostructures and nanomaterials: Synthesis, properties and applications, Imperial College Press, London, UK. ISBN:1-86094-480-9.

Cash, A., Curtis, R., Garrigia-Majo, D., & McDonald, F. 2004. A comparative study of the static and kinetic frictional resistance of titanium molybdenum alloy archwires in stainless steel brackets. *The European Journal of Orthodontics*, 26 (1), 105-111.

Cheng, Y., Wei, C., Gan, K. & Zhao, L. 2004. Surface modification of Ti-Ni-Ti-Ni-Ni alloy through tantalum immersion ion implantation. *Surface and Coatings Technology*, vol. 176 (2), pp. 261-265.

Cheng, Y., Cai, W., Li, H. T., & Zheng, Y. F. 2006. Surface modification of NiTi alloy with tantalum to improve its biocompatibility and radiopacity. *Journal of materials science*, vol 41 (15), pp. 4961-4964.

Chu, P. K. 2007. Enhancement of surface properties of biomaterials using plasma-based technologies. *Surface and Coatings Technology*, vol 201(19), pp. 8076-8082.

Cohen, D. M. 1994. Low resistance implantable electrical leads. USA Patent No. 5,330,521.

Collings, E. 1994. In Materials properties handbook: titanium alloys. American Society for Metals: International serves materials professionals. Ohio, USA. ISBN: 0-87170-481-1.

Costa, M. T., Lenza, M. A., Gosch, C. S., Costa, I., & Ribeiro-Dias, F. 2007. In vitro evaluation of corrosion and cytotoxicity of orthodontic brackets. *Journal of Dental Research*, 86 (5), pp. 441-445.

Cunha, A. C. D., Marquezan, M., Freitas, A. O. A. D., & Nojima, L. I. 2011. Frictional resistance of orthodontic wires tied with 3 types of elastomeric ligatures. *Brazilian Oral Research*, 25 (6), pp. 526-530.

D'Antò, V., Rongo, R., Ametrano, G., Spagnuolo, G., Manzo, P., Martina, R., Paduano, S. & Valletta, R. 2012. Evaluation of surface roughness of orthodontic wires by means of atomic force microscopy. *Angle Orthodontist*, vol. 52 (5), pp. 922-928.

De Franco, D.J., Spiller, R.E.,Jr & von Fraunhofer, J.A. 1995. Frictional resistances using Teflon-coated ligatures with various bracket-archwire combinations. *The Angle Orthodontist*, vol. 65 (1), pp. 63-72.

Donachie Jr, M. J. 2000. Titanium: a technical guide.International serves materials professionals. Ohio, USA. ISBN: 978-0871706867.

El-Zohairy, M. A., Mostafa, A., Amin, A., Abd, E. F. H., & Khalifa, S. 2009. Mandibular reconstruction using pectoralis major myocutaneous flap and titanium plates after ablative surgery for locally advanced tumors of the oral cavity. *Journal of the Egyptian National Cancer Institute*, vol. 21 (4), pp. 299-307.

Faria, A. C. L., Rodrigues, R. C. S., Claro, A. P. R. A., de Mattos, M. D. G. C. & Ribeiro, R. F. 2011. Wear resistance of experimental titanium alloys for dental applications. *Journal of the Mechanical Behavior of Biomedical Materials*, vol. 4 (8), pp. 1873-1879.

Ferreira, M. D. A., Luersen, M. A. & Borges, P. C. 2012. Nickel-titanium alloys: a systematic review. *Dental Press Journal of Orthodontics*, vol. 17 (3), pp. 71-82.

Fridman, A. 2008. Plasma chemistry. Cambridge University Press. New York, USA. ISBN:9780521847353.

Garner, L., Allai, W. & Moore, B. 1986. A comparison of frictional forces during simulated canine retraction of a continuous edgewise arch wire. *American Journal of Orthodontics and Dentofacial Orthopedics*, vol. 90 (3), pp. 199-203.

Geetha, M., Singh, A. K., Asokamani, R., & Gogia, A. K. 2009. Ti based biomaterials, the ultimate choice for orthopaedic implants A review. *Progress in Materials Science*, vol. 54 (3), pp. 397-425.

Gjerdet, N. R., Erichsen, E. S., Remlo, H. E. & Evjen, G. 1991. Nickel and iron in saliva of patients with fixed orthodontic appliances*. Acta Odontologica*, vol. 49 (2), pp. 73-78.

Goldberg, J. & Burstone, C.J. 1979. An evaluation of beta titanium alloys for use in orthodontic appliances. *Journal of Dental Research*, vol. 58 (2), pp. 593.

Grainger, S. & Blunt, J. 1998. Engineering Coatings. Design and Application; Plastics Design Library, Cambridge, UK. ISBN: 1-884207-68-5Y.

Guerrero, A. P., Guariza Filho, O., Tanaka, O., Camargo, E. S., & Vieira, S. 2010. Evaluation of frictional forces between ceramic brackets and archwires of different alloys compared with metal brackets. *Brazilian Oral Research*, 24 (1), pp. 40-45.

Gurgel, J.A., Kerr, S., Powers, J.M. & LeCrone, V. 2001. Force-deflection properties of superelastic nickel-titanium archwires. *American Journal of Orthodontics and Dentofacial Orthopedics*, vol. 120 (4), pp. 378-382.

Gurgel, J.A., RM Pinzan-Vercelino, C. & Powers, J.M. 2011. Mechanical properties of beta-titanium wires. *The Angle Orthodontist*, vol. 81 (3), pp. 478-483.

Hennig, R. G., Lenosky, T. J., Trinkle, D. R., Rudin, S. P., & Wilkins, J. W. 2008. Classical potential describes martensitic phase transformations between the α, β and ω titanium phases. *Physical Review* B, 78 (5), pp. 54121

Hilgers, J.J. & Farzin-Nia, F. 1992. Orthodontic archwire. US Patent 696,100(5131843).

House, K., Sernetz, F., Dymock, D., Sandy, J. R., & Ireland, A. J. 2008. Corrosion of orthodontic appliances-should we care?. *American Journal of Orthodontics and Dentofacial Orthopaedics*, 133 (4), pp. 584-592.

Jian-Hong, Y., Huang, H.L., Li-chun, W., Jui-ting, H., Chang, Y.Y., Huang, H.H. & Tsai, M.T. 2011. Friction of stainless steel, nickel-titanium alloy and beta-titanium alloy archwires in two commonly used orthodontic brackets. *Journal of Mechanics in Medicine and Biology*, vol. 11 (04), pp. 917-928.

Junker, R., Manders, P., Wolke, J., Borisov, Y., Braceras, I. & Jansen, J. 2010. Loaded microplasma-sprayed calcium phosphate ceramic-coated implants in vivo. *Journal of Dental Research,* vol. 89 (12), pp. 1489-1493.

Juvvadi, S.R., Kailasam, V., Padmanabhan, S. & Chitharanjan, A.B. 2010. Physical, mechanical and flexural properties of 3 orthodontic wires: An in-vitro study. *American Journal of Orthodontics and Dentofacial Orthopedics*, vol. 138 (5), pp. 623-630.

Kaneko, K., Yokoyama, K., Moriyama, K., Asaoka, K. & Sakai, J. 2004. Degradation in performance of orthodontic wires caused by hydrogen absorption during short-term immersion in 2.0% acidulated phosphate fluoride solution. *The Angle Orthodontist*, vol. 74 (4), pp. 487-495.

Kapila, S. & Sachdeva, R. 1989. Mechanical properties and clinical applications of orthodontic wires. *American Journal of Orthodontics and Dentofacial Orthopedics*, vol. 96 (2), pp. 100-109.

Kapila, S., Angolkar, P. V., Duncanson, M. G., & Nanda, R. S. 1990. Evaluation of friction between edgewise stainless steel brackets and orthodontic wires of four alloys. *American Journal of Orthodontics and Dentofacial Orthopaedics*, vol. 98 (2), pp. 117-126.

Knosel, M., Attin, R., Kubein-Meesenburg, D. & Sadat-Khonsari, R. 2007. Cephalometric Assessment of the Axial Inclination of Upper and Lower Incisors in Relation to the Thirdorder

Angle. *Journal of Orofacial Orthopedics/Fortschritte der Kieferorthopädie,* vol. 68 (3), pp. 199-209.

Kobayashi, S., Ohgoe, Y., Ozeki, K., Sato, K., Sumiya, T., Hirakuri, K. & Aoki, H. 2005. Diamond-like carbon coatings on orthodontic archwires*. Diamond and Related Materials*, vol. 14 (3), pp. 1094-1097.

Krishnan, V., Krishnan, A., Remya, R., Ravikumar, K., Nair, S.A., Shibli, S., Varma, H., Sukumaran, K. & Kumar, K.J. 2011. Development and evaluation of two PVD-coated β-titanium orthodontic archwires for fluoride-induced corrosion protection. *Acta Biomaterialia,* vol. 7 (4), pp. 1913-1927.

Krishnan, V., Ravikumar, K., Sukumaran, K. & Jyothindra Kumar, K. 2012. In *vitro* evaluation of physical vapor deposition coated beta titanium orthodontic archwires. *The Angle Orthodontist*, Vol. 82 (1), pp. 22-29.

Kula, K., Phillips, C., Gibilaro, A. & Proffit, W.R. 1998. Effect of ion implantation of TMA archwires on the rate of orthodontic sliding space closure. *American Journal of Orthodontics and Dentofacial Orthopedics,* vol. 114 (5), pp. 577-580.

Kusy, R. 1981. Comparison of nickel-titanium and beta titanium wire sizes to conventional orthodontic arch wire materials. *American Journal of Orthodontics*, vol. 79 (6), pp. 625-629.

Kusy, R.P., Whitley, J.Q., Mayhew, M.J. & Buckthal, J.E. 1988. Surface roughness of orthodontic archwires via laser spectroscopy. *The Angle Orthodontist*, vol. 58 (1), pp. 33-45.

Kusy, R. & Whitley, J.Q. 1990. Effects of surface roughness on the coefficients of friction in model orthodontic systems. *Journal of Biomechanics*, vol. 23 (9), pp. 913-925.

Kusy, R., Tobin, E., Whitley, J. & Sioshansi, P. 1992. Frictional coefficients of ion-implanted alumina against ion-implanted beta-titanium in the low load, low velocity, single pass regime. *Dental Materials*, vol. 8 (3), pp. 167-172.

Kusy, R. P., & Whitley, J. Q. 2003. Influence of fluid media on the frictional coefficients in orthodontic sliding*. In Seminars in Orthodontics* (Vol. 9, (4), pp. 281-289.

Kusy, R.P. & Whitley, J.Q. 2007. Thermal and mechanical characteristics of stainless steel, titanium-molybdenum and nickel-titanium archwires. *American Journal of Orthodontics and Dentofacial Orthopedics*, vol. 131 (2), pp. 229-237.

Kusy, R.P., Whitley, J.Q. & Gurgel, J.A. 2004. Comparisons of surface roughnesses and sliding resistances of 6 titanium-based or TMA-type archwires. *American Journal of Orthodontics and Dentofacial Orthopedics,* vol. 126 (5), pp. 589-603.

Laheurte, P., Eberhardt, A. & Philippe, M.J. 2005. Influence of the microstructure on the pseudoelasticity of a metastable beta titanium alloy. *Materials Science and Engineering*: A, vol. 396 (1-2), pp. 223-230.

Laheurte, P., Eberhardt, A., Philippe, M. & Deblock, L. 2007. Improvement of pseudoelasticity and ductility of beta III titanium alloy application to orthodontic wires. *The European Journal of Orthodontics,* vol. 29 (1), pp. 8.

Lee, G.J., Park, K.H., Park, Y.G. & Park, H.K. 2010. A quantitative AFM analysis of nano-scale surface roughness in various orthodontic brackets. *Micron*, vol. 41 (7), pp. 775-782.

Liu, X., Chu, P.K. & Ding, C. 2004. Surface modification of titanium, titanium alloys and related materials for biomedical applications. *Materials Science and Engineering*: R, vol. 47 (3-4), pp. 49-121.

Loftus, B.P., Ârtun, J., Nicholls, J.I., Alonzo, T.A. & Stoner, J.A. 1999. Evaluation of friction during sliding tooth movement in various bracket-arch wire combinations. *American Journal of Orthodontics and Dentofacial Orthopedics*, vol. 116 (3), pp. 336-345.

Luppanapornlarp, S., Kajii, T.S., Surarit, R. & Iida, J. 2010. Interleukin-1β levels, pain intensity and tooth movement using two different magnitudes of continuous orthodontic force. *The European Journal of Orthodontics,* vol. 32 (5), pp. 596.

Malinov, S. & Sha, W. 2004. Application of artificial neural networks for modelling correlations in titanium alloys*. Materials Science and Engineering*: A, vol. 365 (1–2), pp. 202-211.

Matos de Souza, R., & Macedo de Menezes, L. 2008. Nickel, chromium and iron levels in the saliva of patients with simulated fixed orthodontic appliances. *The Angle Orthodontist*, 78 (2), 345-350.

Mattox, D.M. 2010. Handbook of Physical Vapor Deposition Processing, Elsevier, Burlington, USA. ISBN: 978-0-8155-2037-5.

McKnight-Hanes, C. & Whitford, G.M. 1992. Fluoride release from three glass–ionomer materials and the effects of varnishing with or without finishing. *Caries Research*, vol, 26 (5), pp. 345-350.

Mikulewicz, M., Chojnacka, K., Woźniak, B., & Downarowicz, P. 2012. Release of metal ions from orthodontic appliances: an in vitro study. *Biological trace element research*, vol. 146 (2), pp. 272-280.

Palmquist, A., Omar, O. M., Esposito, M., Lausmaa, J., & Thomsen, P. 2010. Titanium oral implants: surface characteristics, interface biology and clinical outcome. *Journal of the Royal Society Interface,* vol. 7 (5), pp. 515-527.

Park, J.B., Kim, Y.K. 2000. Metallic Biomaterials. Chemical Rubber Company Press limited liability publishing company, Boca Raton, USA. ISBN:978-0-85709-244-1.

Park, J.H. & Sudarshan, T. 2001. Chemical vapor deposition. ASM International Materials Park. Ohio', USA. ISBN: 0-87170-731-4.

Parvizi, F., & Rock, W. P. 2003. The load/deflection characteristics of thermally activated orthodontic archwires. *The European Journal of Orthodontics*, vol. 25 (4), pp. 417-421.

Pereira, M. C., Pereira, M. L. & Sousa, J. P. 1999. Histological effects of iron accumulation on mice liver and spleen after administration of a metallic solution. *Biomaterials*, vol. 20 (22), pp. 2193-2198.

Proffit, W. & Fields, H. 1993. Contemporary orthodontics. Mosby Company. St, Louis, USA. ISBN: 9780323083171.

Prososki, R.R., Bagby, M.D. & Erickson, L.C. 1991. Static frictional force and surface roughness of nickel-titanium arch wires. *American Journal of Orthodontics and Dentofacial Orthopedics*, vol. 100 (4), pp. 341-348.

Qiu, D., Wang, A. & Yin, Y. 2010. Characterization and corrosion behavior of hydroxyapatite/zirconia composite coating on Ti-Ni fabricated by electrochemical deposition. *Applied Surface Science*, vol. 257 (5), pp. 1774-1778.

Redlich, M., Gorodnev, A., Feldman, Y., Kaplan-Ashiri, I., Tenne, R., Fleischer, N., Genut, M. & Feuerstein, N. 2008. Friction reduction and wear resistance of electro-co-deposited inorganic fullerene-like WS2 coating for improved stainless steel orthodontic wires. *Journal of Materials Research*, vol. 23 (11), pp. 2909-2915.

Reed, S.J.B. 2005. Electron microprobe analysis and scanning electron microscopy in geology. Cambridge University Press, New York, USA. ISBN: 978-0521142304.

Rodrigues, A. A., Baranauskas, V., Ceragioli, H. J., Peterlevitz, A. C., & Belangero, W. D. 2010. In vivo preliminary evaluation of bone-microcrystalline and bone-nanocrystalline diamond interfaces. *Diamond and Related Materials*, vol.19 (10), pp. 1300-1306.

Rossouw, P.E., Kamelchuk, L.S. & Kusy, R.P. 2003. A fundamental review of variables associated with low velocity frictional dynamics. *Seminars in Orthodontics*, vol. 9 (4), pp. 223-235.

Samorodnitzky-Naveh, G.R., Redlich, M., Rapoport, L., Feldman, Y. & Tenne, R. 2009. Inorganic fullerene-like tungsten disulfide nanocoating for friction reduction of nickel–titanium alloys. *Nanomedicine*, vol. 4 (8), pp. 943-950.

Sukumaran, K. & Kumar, K.J. 2011. Development and evaluation of two PVD-coated β-titanium orthodontic archwires for fluoride-induced corrosion protection. *Acta Biomaterialia*, vol. 7 (4), pp. 1913-1927.

Schmalz, G., & Bindslev, D. A. 2008. Biocompatibility of dental materials. Springer, Berlin, Germany. ISBN: 978-3-540-77781-6.

Semiatin, S. L., Seetharaman, V., & Weiss, I. 1997. The thermomechanical processing of alpha/beta titanium alloys. *Journal of the Minerals, Metals and Materials Society*, 49 (6), pp. 33-39.

Sfondrini, M. F., Cacciafesta, V., Maffia, E., Massironi, S., Scribante, A., Alberti, G. & Klersy, C. 2009. Chromium release from new stainless steel, recycled and nickel-free orthodontic brackets. *Angle Orthodontist*, vol. 79 (2), 361-367.

Sifakakis, I., Pandis, N., Makou, M., Eliades, T. & Bourauel, C. 2009. Forces and moments generated with various incisor intrusion systems on maxillary and mandibular anterior teeth. *The Angle Orthodontist,* vol. 79 (5), pp. 928-933.

Silva, M. M., Ueda, M., Pichon, L., Reuther, H., & Lepienski, C. M. 2007. Surface modification of Ti_6Al_4V alloy by PIII at high temperatures: Effects of plasma potential. Nuclear Instruments and Methods in Physics Research Section B: Beam Interactions with Materials and Atoms, vol. 257 (1), 722-726.

Singh, J. & Wolfe, D. 2005. Review Nano and macro-structured component fabrication by electron beam-physical vapor deposition. *Journal of Materials Science*, vol. 40 (1), pp. 1-26.

Szuhanek, C., Fleser, T. & Glavan, F. 2010. Mechanical Behavior of Orthodontic TMA Wires. World Scientific and Engineering *Academy and Society Transactions on Biology and Biomedicine*, vol 7 (3), pp. 277-286.

Tecco, S., Tetè, S. & Festa, F. 2009. Friction between archwires of different sizes, cross-section and alloy and brackets ligated with low-friction or conventional ligatures. *The Angle Orthodontist*, vol. 79 (1), pp. 111-116.

Thompson, S. A. 2000. An overview of nickel titanium alloys used in dentistry. *International Endodontic Journal*, vol. 33 (4), pp. 297-310.

Tripi, T.R., Bonaccorso, A. & Condorelli, G.G. 2003. Fabrication of hard coatings on Ti-Ni instruments. *Journal of Endodontics*, vol. 29 (2), pp. 132-134.

Ushiki, T., Hitomi, J., Ogura, S., Umemoto, T. & Shigeno, M. 1996. Atomic force microscopy in histology and cytology. *Archives of Histology and Cytology,* vol. 59 (5), pp. 421-432.

Velisavljevic, N., MacLeod, S., & Cynn, H. 2012. Titanium Alloys at Extreme Pressure Conditions. Intechopen books, New Mexico, USA. ISBN:978-953-51-0354-7.

Verstrynge, A., Van Humbeeck, J. & Willems, G. 2006. In-vitro evaluation of the material characteristics of stainless steel and beta-titanium orthodontic wires. *American Journal of Orthodontics and Dentofacial Orthopedics*, vol. 130 (4), pp. 460-470.

Vijayalakshmi, R., Nagachandran, K., Kummi, P. & Jayakumar, P. 2009. A comparative evaluation of metallurgical properties of stainless steel and TMA archwires with timolium and titanium niobium archwires-An in vitro study. *Indian Journal of Dental Research*, vol. 20 (4), pp. 448.

Walker, M.P., Ries, D., Kula, K., Ellis, M. & Fricke, B. 2007. Mechanical properties and surface characterization of beta titanium and stainless steel orthodontic wire following topical fluoride treatment. *The Angle Orthodontist*, vol. 77 (2), pp. 342-348.

Weiss, I. & Semiatin, S. 1998. Thermomechanical processing of beta titanium alloys an overview. *Materials Science and Engineering: A,* vol. 243 (1), pp. 46-65.

Widu, F., Drescher, D., Junker, R. & Bourauel, C. 1999. Corrosion and biocompatibility of orthodontic wires. *Journal of Materials Science*: *Materials in Medicine*, vol. 10 (5), pp. 275-281.

Williams, D., Wood, R. & Bartlett, E. 1972. Effect of composition on the properties of strain-transformable β titanium alloys. *Metallurgical and Materials Transactions B*:, vol. 3 (6), pp. 1529-1536.

Williams, D.F., Roaf, R. & Maisels, D. 1973. Implants in surgery. Saunders Limited. London. UK. ISBN 0721694470.

Wyllie, I., Arney, D.S., Thorstenson, G.A. & Gates, B.J. 2007. Orthodontic articles with zirconium oxide coating. USA Patent 20,070,134,610

Zein El Abedin, S., Welz-Biermann, U. & Endres, F. 2005. A study on the electrodeposition of tantalum on Ti-Ni alloy in an ionic liquid and corrosion behaviour of the coated alloy. *Electrochemistry Communications*, vol. 7 (9), pp. 941-946.

Zheng, Y., Liu, D., Liu, X. & Li, L. 2008. Enhanced corrosion resistance of Zr coating on biomedical Ti-Ni alloy prepared by plasma immersion ion implantation and deposition. *Applied Surface Science*, vol. 255 (2), pp. 512-514.